Form: PGR_Submission_200701

NOTICE OF SUBMISSION OF THESIS FORM:

POSTGRADUATE RESEARCH

APPENDIX 1:

Specimen layout for Thesis Summary and Declaration/Statements page to be included in a Thesis

DECLARATION

This work has not previously been accepted in substance for any degree and is not concurrently submitted in candidature for any degree.

Signed ..... (candidate) Date 18/08/11

STATEMENT 1

This thesis is being submitted in partial fulfillment of the requirements for the degree of .....(insert MCh, MD, MPhil, PhD etc, as appropriate)

Signed ..... (candidate) Date 18/08/11

STATEMENT 2

This thesis is the result of my own independent work/investigation, except where otherwise stated.

Other sources are acknowledged by explicit references.

Signed ..... (candidate) Date 18/08/11

STATEMENT 3

I hereby give consent for my thesis, if accepted, to be available for photocopying and for inter-library loan, and for the title and summary to be made available to outside organisations.

Signed ..... (candidate) Date 18/08/11

Proteoglycans as dynamic regulators of the organised collagen fibril architecture in the cornea: An electron tomography study of the mouse corneal stroma

Geraint Parfitt

Structural Biophysics Research Group
Cardiff School of Optometry and Vision Sciences
Cardiff University

Supervisors:

Dr. Carlo Knupp

Prof. Andrew Quantock

ProQuest LLC
789 East Eisenhower Parkway
P.O. Box 1346
Ann Arbor, MI 48106-1346

Abstract

The cornea is the primary refractive element of the eye and is also fundamental to the protection of the visual system. Collagen is the major constituent of the cornea, where it is organised in a lattice that enables corneal transparency. Proteoglycan macromolecules are thought to regulate the diameter and spatial order of collagen fibrils in the cornea, which are both pre-requisites for corneal transparency, although the mechanisms by which they organise fibrils are not fully elucidated. This investigation examined the morphology, morphometry and organisation of proteoglycans three-dimensionally, in both normal and genetically altered mouse corneas, to gain a greater understanding of proteoglycan structure-function relationships.

In summary, we found that proteoglycans are primarily responsible for the remarkable collagen organisation in the mouse cornea, which allows for corneal transparency. The self-association of proteoglycans into complexes is likely to result in a robust attachment of neighbouring fibrils and provides biomechanical strength, whilst sulphation patterns are seen to have a direct effect on the aggregation potential of proteoglycans. Removal of proteoglycans, particularly lumican, affects the regulation of both fibril size and spatial order, both required for corneal transparency.

List of Publications

Parfitt GJ, Pinali C, Young RD, Quantock AJ, Knupp C (2010) "Three-dimensional reconstruction of collagen-proteoglycan interactions in the mouse corneal stroma by electron tomography" **Journal of Structural Biology 170:392-7**

Parfitt GJ, Pinali C, Lewis PN, Young RD, Quantock AJ, Knupp C (2010) "Three-dimensional reconstruction of the cornea by electron tomography" **Microscopy and Analysis 24(2):17-19 (EU)**

Knupp C, Pinali C, Lewis PN, **Parfitt GJ**, Young RD, Meek KM, Quantock AJ (2010) "The architecture of the cornea and structural basis of its transparency" **Advances in Chemistry and Structural Biology 78:25-49**

Parfitt GJ, Pinali C, Akama TO, Young RD, Nishida K, Quantock AJ (2011) "Electron tomography reveals mutliple self-association of chondroitin sulphate/dermatan sulphate proteoglycans in the *Chst5*-null mouse corneas" **J. Struct. Biol.**, doi:10.1016/j.jsb.2011.03.015

Acknowledgements

I would like to thank my supervisors, Dr. Carlo Knupp and Prof. Andrew Quantock, for not only being approachable and honest, but for giving me a fascinating project and many excellent opportunities that I will not forget from my time in the Biophysics group. I am extremely grateful for the help, advice and expertise they have offered me throughout my Ph.D.

I would also like to extend my gratitude to the post-docs Dr. Rob Young and Dr. Christian Pinali for their time and efforts in teaching me all the protocols detailed in this thesis. I would also like to thank Prof. Keith Meek and everyone in the Structural Biophysics Group for advice and support throughout my time in Cardiff University. This work was made possible through a Doctoral Training Award funded by the BBSRC.

Without the specimens provided by Prof. Kohji Nishida and Dr. Shukti Chakravarti, this thesis would not have been possible, and so I thank them for their generosity and the opportunity to work with them.

Contents

List of tables and figures

Chapter One: Introduction

Fig. 4.3: Surface-rendered volumes of collagen and proteoglycans in the corneas of the *Chst5*-null mouse (a and b) anterior, (c and d) mid and (e and f) posterior corneal stroma shown as stereo-pairs of (a,c,e) longitudinal and (b,d,f) transverse sections of segmented tomograms.

Fig. 4.4: Scatter plot of proteoglycan dimensions in the *Chst5*-null mouse cornea stroma. Measurements were limited to those proteoglycans that exhibit complete morphologies in the three-dimensional reconstruction.

Fig. 4.5: (a and b) Schematic of proposed periodic aggregation of chondroitin sulphate/dermatan sulphate proteoglycans in the *Chst5*-null mouse corneal stroma and the disaccharide constituents, (a) orthogonal binding with protein cores and (b) without.

Chapter Five

Fig. 5.1: Electron micrograph of (a) wild-type mouse (C57BL/6) corneal stroma and (b) posterior stroma of lum -/- mouse cornea.

Fig. 5.2. (Top panels) Electron micrographs of collagen fibrils in transverse section in the posterior stroma of a lumican knockout mouse cornea.

Fig. 5.3: Electron micrographs of wild-type (left column) and homozygous lumican-null (right column) mouse corneal stromas showing Cuprolinic blue stained proteoglycans after incubation in buffer (a and b), chondroitinase ABC (c and d), keratanase II (e and f) and both keratanase and chondroitinase ABC (g and h).

Fig. 5.4: Tomograms of collagen (blue) and proteoglycans (yellow) in the C57BL/6 wild-type mouse corneal stroma.

Fig. 5.5: Frequency plots of collagen fibril diameters from (a) C57BL/6 wild-type mouse corneal stroma; (b) Anterior Lum -/- mouse corneal stroma; (c) Mid-stroma Lum -/- mouse corneal stroma; (d) Posterior Lum -/- mouse corneal stroma.

Fig. 5.6: Stereo-pairs of three-dimensional reconstructions of collagen (blue) and proteoglycans (yellow) in the lumican -/- mouse (a and b) anterior, (c and d) mid and (e and f) posterior corneal stroma.

Fig. 5.7: Three-dimensional reconstruction of an irregularly sized fibril in longitudinal section of the lumican-null mouse posterior corneal stroma. Three collagen fibrils fuse locally to give the appearance of an enlarged fibril.

Fig. 5.8: Schematic representation of the proposed role of lumican in regulating collagen fibril diameter, maintaining interfibrillar spacing and preventing fibrils from fusing.

Fig. 6.1: The role of proteoglycans in the regulation of corneal collagen fibril architecture and the effects of altered proteoglycan biosynthesis.

Chapter 1 - Introduction

1.1 Introduction

The cornea forms a transparent, dome-shaped cover of the eye that is optimally designed for the focus of entry and refraction of light. It is the principal refractive element of the eye and the structural organisation it maintains plays a pivotal role in achieving optical functionality. The cornea accounts for approximately 15% of the surface of the human eye's outermost layer; the remainder is the white opaque sclera which protects the internal structures of the eye, helps to maintain its shape and serves as a portal for the passage of nerves and blood vessels in and out of the eye (Oyster, 1999). Collagen is the major constituent of the cornea, where it forms fibrils that are highly organised with remarkably uniform diameters and regular interfibrillar spacing. The sclera, also made mainly of collagen fibrils, exhibits relatively disorganised collagen fibril arrangement, however (Komai and Ushiki, 1991). This disparity between collagen fibril organisations in both tissues is believed to be the fundamental reason for the observed difference in transparency.

The precise arrangement of collagen fibrils enables the corneal stroma to withstand tensile stress, whilst the hydrated gel formed by proteoglycans creates inflation forces that prevent the structure from being compressed (Scott, 1995). The interaction between proteoglycans and collagen develops and maintains structural integrity whilst enabling the cornea to achieve transparency and the refraction of light into the eye. The interwoven collagen fibrils in both cornea and sclera tissues also confer rigidity, resistance to penetration and protect the eye's inner layers. Macro-molecular organisation within the cornea is also essential for the correct formation of corneal curvature; any dysfunction can lead to disease states such as keratoconus and improper imaging by the eye (Meek et al., 2005). The specific collagen architecture and the regulation of corneal hydration, particularly in the anterior region, contribute to the correct curvature required for the cornea (Muller et al., 2001). This thesis aims to further our understanding as to how proteoglycans regulate the intricate collagen fibril assembly in the cornea.

1.2 Corneal Structure

The cornea is attached to the sclera via a transitional region known as the limbus. The limbus, centre and periphery of the cornea exhibit varying compositions of collagen and proteoglycans (Borcherding et al., 1975) and, as a result, a significant change in interfibrillar spacing is noticed from the central corneal region to the limbus (Boote et al., 2003). The central 'prepupillary' area of the cornea is deemed to be the principal optical zone and is considered to comprise 70% of the total focusing power of the eye (Waring, 1989). The peripheral area surrounding the central zone is less curved however and is a refractive surface primarily aiding peripheral vision. Only recently has the composition of the peripheral cornea been investigated and it is suggested that peripheral vision plays a far more important role in overall vision than was first considered.

The varying collagen composition in the different areas of the cornea is exemplified by the absence of the long variant collagen type XII in the limbus that is expressed transiently throughout the corneal stroma. Type XII collagen is thought to contribute to the differences in the basement membrane zones of the cornea and limbus (Wessel et al., 1997). The limbo-scleral region, which is more disorganised in collagen arrangement, is abundant in chondroitin sulphate/dermatan sulphate proteoglycans in mammals other than mice, as opposed to the greater extent of keratan sulphate proteoglycans witnessed in the central cornea, a region which exhibits the highest degree of collagen organisation (Borcherding et al., 1975). In terms of collagen direction, fibrils extend from limbus to limbus with a preferred alignment in both the vertical and horizontal directions up to within 1mm of the limbus. The limbal collagen fibrils adopt a circumferential alignment, which is structurally relevant for the mechanical properties of the tissue, including development of correct corneal curvature (Aghamohammadzadeh et al., 2004). Meek (2004) illustrated that a significant proportion of collagen fibrils that run across the cornea change direction at the limbus, fusing with the limbal collagen that is orientated circumferentially.

The difference in proteoglycan and collagen composition is believed to be instrumental in the differences in collagen fibril diameter and interfibrillar spacing between the corneal zones

and also the reason why the central area of the cornea is almost completely transparent whereas the sclera and limbus are not.

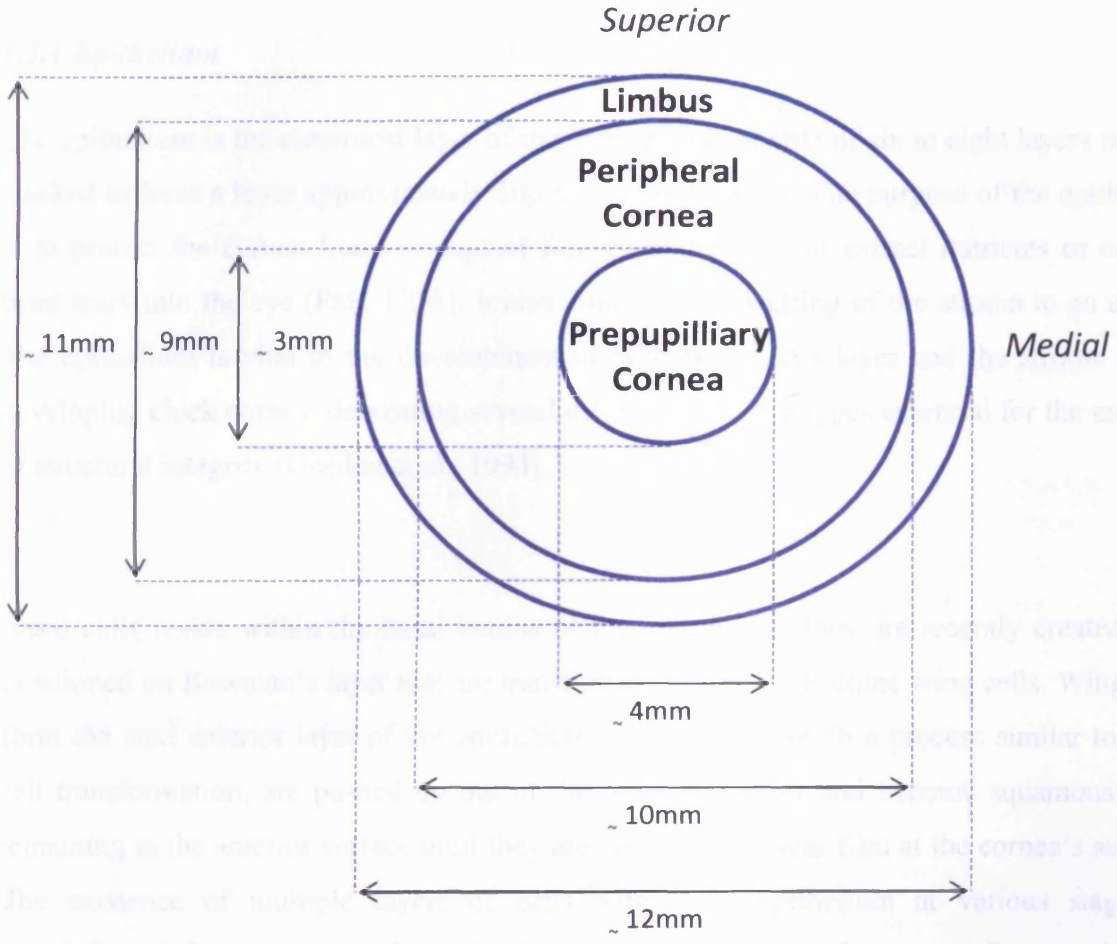

Fig. 1.1 Designation of anterior surface zones in human cornea, representing the different positions of the optical zones and positions with altered curvature within the cornea (Adapted from Boote et al., 2003, Waring, 1989).

1.3 Corneal Layers

The human cornea is segregated into five different layers that individually play an important role in the developing and mature corneal tissue. The largest domain of the cornea, the stroma, lies between the epithelium and endothelium and also contains two structurally distinct regions known as Bowman's layer and Descemet's membrane. The epithelium and endothelium are layers of cells that constitute the most anterior and posterior parts of the

cornea respectively. Bowman's layer separates the stroma from the epithelium whereas Descemet's membrane is situated between the stroma and the endothelium.

1.3.1 Epithelium

The epithelium is the outermost layer of the cornea and consists of six to eight layers of cells stacked to form a layer approximately 50μm thick in humans. The purpose of the epithelium is to protect the cornea from passage of foreign bodies and to extract nutrients or oxygen from tears into the eye (Fatt, 1978). It also controls the swelling of the stroma to an extent. The epithelium is vital to the development of both Bowman's layer and the stroma of the developing chick cornea, depositing several different collagen types essential for the creation of structural integrity (Gordon et al., 1994).

Basal cells reside within the basal lamina of the epithelium; they are recently created cells positioned on Bowman's layer that are transformed in time to become wing cells. Wing cells form the next anterior layer of the epithelium. The wing cells, in a process similar to basal cell transformation, are pushed up out of the wing cell layer and become squamous cells, remaining at the anterior surface until they are shed into the tear film at the cornea's surface. The existence of multiple layers of cells within the epithelium at various stages of morphology helps create a barrier to the free movement of water from tears. Compared to the endothelium, the epithelium is a highly selective barrier for osmotically active molecules (Oyster, 1999).

1.3.2 Bowman's Layer

Bowman's layer is situated in-between the epithelial basal lamina and the anterior region of the stroma. In humans, it is composed of collagen fibrils approximately 20 – 25nm in diameter individually running in varying directions (Komai and Ushiki, 1991). The developing corneal epithelium is believed to play a pivotal role in the formation of Bowman's layer; contributing type V collagen fibrils in early chick corneal development (Gordon et al., 1994). Also, It has been hypothesised that chemotactic influences regulated by cytokines

from the epithelium are paramount for the normal development and maintenance of Bowman's layer (Wilson and Hong, 2000).

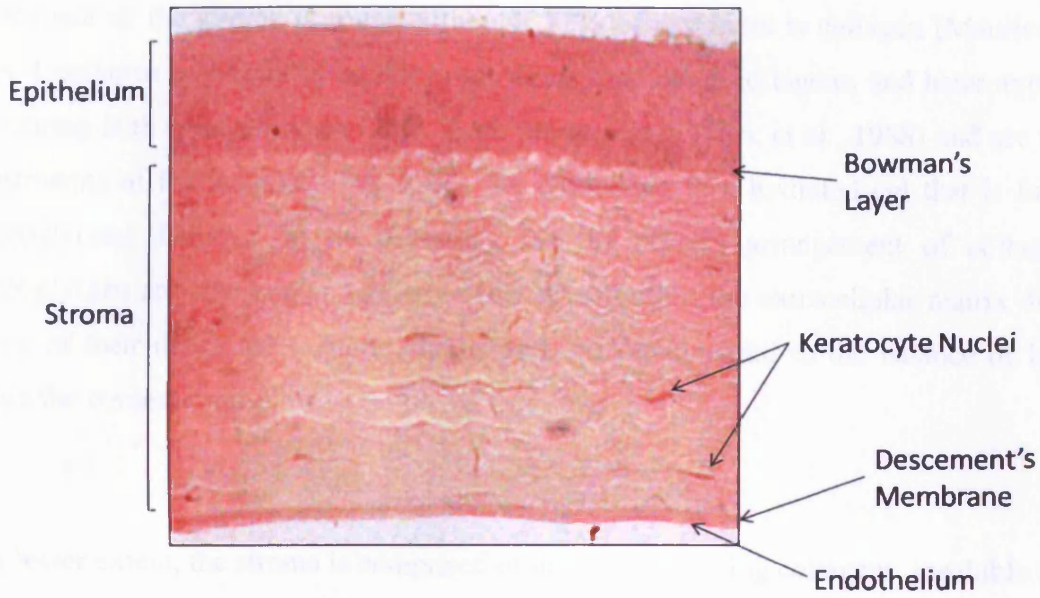

Fig 1.2 Cross-section of mouse corneal tissue illustrating the sub-layers (own image).

The arrangement of collagen within Bowman's layer differs significantly to that of the stroma. Collagen fibrils form relatively disorganised, densely woven felt-like sheets with individual fibrils that are comparatively thinner than fibrils of the stroma. There have been several attempts to deduce the function of Bowman's layer, including its potential for serving as a corneal ligament that maintains corneal structure, or even as a pathological barrier for viruses due to its acellular nature. Although, no evidence has been suggested to support these hypotheses and the fact that there are many species devoid of Bowman's layer indicates a less than critical role (Wilson and Hong, 2000).

1.3.3 Stroma

In humans, the corneal stroma accounts for 90% of the overall corneal depth (Oyster, 1999) and contains a highly organised network of collagen fibrils stacked into over 200 lamellae. X-ray diffraction studies have illustrated that most collagen fibrils in the stroma of the central

cornea adopt a preferred orientation in the inferior-superior and nasal-temporal directions (Aghamohammadzadeh et al., 2004). The stromal lamellae extend from limbus to limbus and are arranged at less than 90° to each other in the anterior stroma. However, lamellae in the posterior stroma exhibit near orthogonal conformations (Meek et al., 1987). The main constituent of the stroma is water, although 71% of dry mass is collagen (Maurice, 1957). Type I collagen is present in higher proportions than other collagens, and heterotypic fibrils containing both collagen types I and V are predominant (Birk et al., 1988) and are the main constituents of the lamellae. The fibrils are embedded in a hydrated gel that is formed by proteoglycans, believed to be necessary for the correct arrangement of collagen. The proteoglycans are also known to serve other roles within the extracellular matrix due to the nature of their dense electrostatic charge and are fundamental to the balance of hydration within the corneal tissue.

To a lesser extent, the stroma is comprised of non-fibril forming collagens, insoluble salts and keratocytes; the cells responsible for the formation of new collagen and proteoglycans that often sit in-between lamellae (Komai and Ushiki, 1991). Keratocytes occupy 3 – 5 % of stromal volume (Beuerman and Pedroza, 1996) and their function is to maintain the ordered meshwork within the corneal stroma. Experiments with avians showed that corneal collagens such as type I, V and VI (Ruggiero et al., 1996, Linsenmayer et al., 1998) are produced by keratocytes, illustrating their importance. Also, their nuclei are a source of backscattered light in normal human corneas, affecting the light transmission properties of the cornea (Moller-Pedersen, 2004). Bowman's layer and Descemet's membrane are continuations of the stroma, the ends of stromal collagen intertwine within Bowman's layer and separate the epithelium from the anterior stromal region (Oyster, 1999).

Corneal transparency arises from the uniformity of collagen fibril diameters and interfibrillar spacing within the stroma, thought to be established by the interrelationships between several different types of collagen and specific proteoglycans. The stroma is our primary interest within this report as investigation into the association of stromal collagen and the different proteoglycans is directly relevant for a greater understanding of the establishment of corneal transparency.

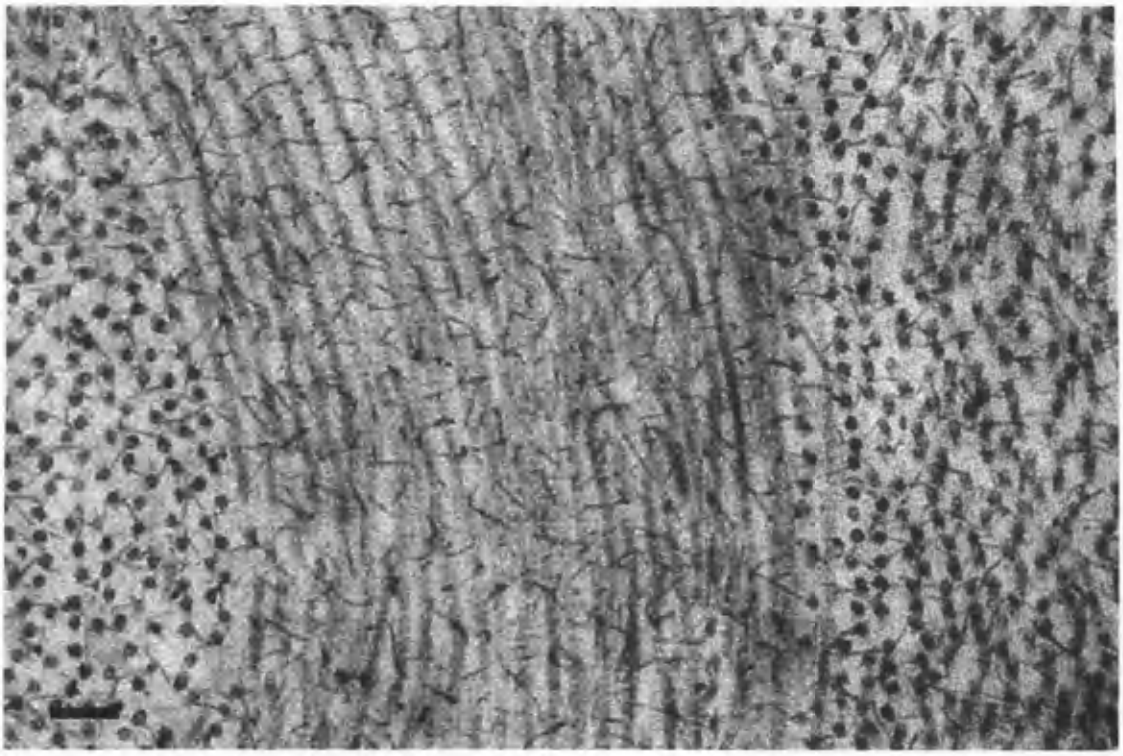

Fig. 1.3 Transmission electron micrograph illustrating the orthogonal arrangement of collagen fibrils in adjacent lamellae of the mouse corneal stroma. The consistent fibril diameter sizes and regular fibril spacing can be seen within the lamellae (own image). Scale bar = 100nm

1.3.4 Descemet's Membrane

Descemet's membrane is the layer situated between the posterior, mono-layered endothelium and the stroma. In humans, it is produced by the endothelium and may be distinguished at four months of gestation where it progressively thickens with age (Beuerman and Pedroza, 1996). Descemet's membrane has been described as a thick basal lamina secreted by the endothelium composed of an anterior banded portion and a posterior non-banded portion (Beuerman and Pedroza, 1996). Situated between Descemet's membrane and the stroma is a thin 0.5μm layer of irregularly arranged collagen fibrils (Komai and Ushiki, 1991).

1.3.5 Endothelium

The endothelial layer is approximately 4-6μm thick and mediates the transport of molecules and water from the aqueous humor into the stroma. It is a single layer of approximately

400,000 cells and is a less effective passive barrier than the epithelium. Executing a significant role in ion exchange, endothelial cells are considered the most metabolically active within the cornea due to the significant quantities of mitochondria and golgi witnessed (Beuerman and Pedroza, 1996). The endothelium is able to pump water out of the cornea in cases of increased stromal osmotic pressure and consequently it may control corneal swelling (Oyster, 1999).

1.3.6 Mouse Corneal Layers

The murine corneal stroma also exhibits regular interfibrillar spacing and collagen fibrils approximately 30-35nm in diameter (Quantock et al., 2001) that are slightly larger than human corneal collagen fibrils. Haustein (1983) illustrated that the total thickness of the mouse cornea is approximately 90μm, and is mainly constituted of a 25μm thick epithelium and a stroma measuring 60μm in size. This is supported by histological sections which report the same thickness (Hayashida et al., 2006). However, recent studies indicate that murine corneal thickness may depend on the strain and can range from 89 to 124μm (Lively et al., 2010). A rudimentary Bowman's layer can be seen in electron microscopy, which visualises a fibrous region posterior to the stroma but underneath the epithelium (Haustein, 1983).

Keratocytes in the mouse corneal stroma can be up to 30μm in diameter, displaying a thickness of 0.8-1.6μm. They lie adjacent to the lamella and their long axes are parallel to the surface of the cornea. The mouse corneal extra-cellular matrix is composed differently from other mammals; the thickness of the cornea is only 80-90μm which is much less than most other mammalian species and so the composition reflects this through a variation in proteoglycan content (Scott & Bosworth 1990)

1.4 Collagen

The collagen super-family accounts for approximately a quarter of all proteins in humans (Marshall et al., 1993) and are major components of tissues as diverse as the cornea, skin, cartilage and bone. Collagen is central to the structural integrity of connective tissues and

plays varying roles within their development and normal physiology. Extracellular matrices within connective tissues are composed of a variety of collagens and associated polysaccharides secreted locally to form an organised meshwork defining the physical characteristics of the respective tissues. The components of connective tissues have evolved to withstand the stresses of movement and the maintenance of shape (Scott, 1975). Currently, there are 29 known members in vertebrates (Soderhall et al., 2007), encoded by more than 40 genes, whereby type I is the most understood and predominately exists within most connective tissues. The different types of collagen display varying characteristics and functionality, although they retain structural homology and may also interact with each other. However, some collagen types, such as type XXVII, have functions yet to be elucidated (Pace et al., 2003).

Collagens exhibit a characteristic triple-chain helix with non-helical regions in varying amounts and are all common in this respect. Each collagen molecule shares a similar structure composed of three polypeptide chains, known as α chains, containing characteristic Glycine – X – Y repeats. X is commonly proline whereas Y is usually hydroxyproline. The individual α chain forms a left-handed helix; the three α chains wind around each other in a right-handed super-helix, where glycine, being the smallest amino acid with no side chain, plays a pivotal structural role within the core of the super-helix. The requirement of glycine in every third position is imperative for the structural integrity of the protein. If glycine is displaced by any other larger amino acid there is disruption of the helix (Piez and Reddi, 1984).

Fibrillar collagen molecules interact and stabilise through intermolecular bonds at their C and N terminals and aggregate to form micro-fibrillar structures. The inter-connected collagen molecules are known to aggregate in 'quarter-stagger' arrays in contact with approximately 75% of the neighbouring lateral molecule and reach about 300nm long, typically (Scott, 1988). The periodicity that arises as a result of the stagger gives rise to the characteristic collagen negative staining pattern. The cornea's transparency and mechanical resiliency is a result of the formation of an extra-cellular matrix consisting of narrow-diameter, heterotypic collagen fibrils displaying a remarkable degree of uniformity in their spatial organisation (Maurice, 1957). The fibrils are uniformly thick with an average diameter of 25-35nm in

humans (Komai and Ushiki, 1991) and have regular interfibrillar spacing of approximately 55nm (Meek and Leonard, 1993). Within the cornea, collagen forms as sheet-like structures known as lamellae, whereby each collagenous lamella is arranged near-orthogonal to its neighbour and to the path of light into the cornea (Maurice, 1957).

Fibril forming collagen type I and V are the predominant collagens within the corneal stroma. Other collagens, including micro-fibrillar, non-fibril forming and fibril associated collagen with interrupted triple helices (FACIT) collagens also pay important roles in the maintenance of corneal structure and function.

1.4.1 Collagen Biosynthesis

Collagen α chains are synthesised on membrane bound ribosomes where they are inserted into the rough endoplasmic reticulum (RER), primarily forming long proα chains as precursors to the α polypeptide chain. The α chain precursors contain signal sequences for transport of the nascent polypeptide to the RER which are subject to cleavage during transit, along with other amino acids termed propeptides at both the C and N terminus (Alberts et al., 2002). Different combinations of genes that encode collagen are expressed in different tissues. In theory, this could give rise to tens of thousands of different tropocollagen (mature collagen form consisting of three α polypeptide chains) molecules but only 29 are currently known to be produced. Type I collagen exists as a hetero-trimer containing two proα1(I) chains encoded by the gene COL1A1, and one proα2(I) chain translated from the gene COL1A2 (Michelacci, 2003). Type I collagen is the most extensively characterised and exists abundantly in most connective tissues. Several tissues, such as tendon, sclera and bone contain negligible amounts of any other collagen type (Scott 1988).

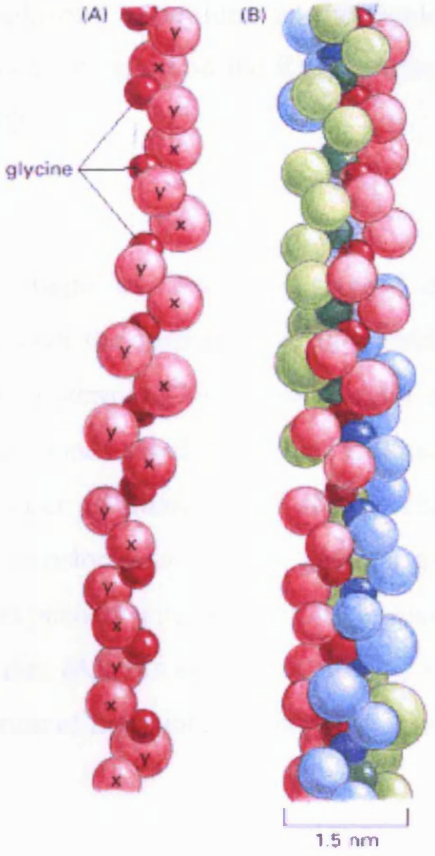

Fig 1.4 Collagen structure. (A) A single collagen α chain model illustrating the Gly-X-Y repeat. The chain is organised as a left-handed helix with glycine positioned every third amino acid. The α chain comprises of a series of Gly-X-Y sequences where X is commonly proline and Y is usually hydroxyproline. (B) Collagen molecule. The α chains are arranged to form a triple-stranded right-hand helix. Glycine is strategically positioned through the centre of the helix as it is the only amino acid small enough to do so. Normally, collagen molecules are 300nm in length (Taken from Alberts et al., 2002).

The proα chains may undergo post-translational modification within the RER which includes hydroxylation of lysine and proline residues as well as the glycosylation of the subsequently formed hydroxylysine or hydroxyproline (Alberts et al., 2002). However, the post-translational modification of proα chains varies in different collagen types. For example, the extent of hydroxylation of lyslyl and prolyl within type I and II collagen is more than 75% less than that of type IV (Michelacci, 2003). Hydroxylation of specific residues within the collagen helix is essential for the formation of inter-chain bonds that confer stability as well as potential substrates for glycosylation (Eyre et al., 1984). The hydroxylation of proline at position 4 is also a pre-requisite for thermal stability within the helix. Another addition to the

proα chain within the endoplasmic reticulum is the coalescence of asparagine-linked oligosaccharides which are also synthesised on the RER membrane and then processed within the golgi apparatus (Clark, 1982).

Once processing of the proα chains has occurred, three α chains align and the globular domains fold and stabilise through the formation of disulphide bonds. Subsequently, triple helix formation begins from the C-terminal to the N-terminal. Propagation of the triple-helix structure requires all the peptide bonds involving prolyl residues to be positioned in the *trans* form (Michelacci, 2003) in order to manufacture the procollagen molecule. Procollagen molecules are then subject to translocation into the golgi apparatus and exocytosis into the extracellular matrix. Upon expulsion into the ECM, procollagens undergo proteolytic cleavage by N and C-proteinases (Alberts et al., 2002). The triple-helical domain left after cleavage stabilises by the creation of more intermolecular bonds and becomes tropocollagen.

Tropocollagen molecules form aggregates that lead to the formation of micro-fibrils and collagen fibrils, precisely designed and orientated to fulfil their function within the ECM. Fibril formation is a non-enzymatic process and the size of aggregation differs in various connective tissues. It is thought that, in general, the regulation of collagen fibril diameters and the control of the rate of fibrillogenesis is due to the interaction of the collagen fibrils with proteoglycans. Control of fibrillogenesis is essential for limiting the diameters of collagen fibrils, achieved by the prevention of lateral self-assembly.

Evidence suggests that early fibrils present in developing tissues may be either bi-polar or uni-polar (Kadler et al., 1996). The aggregation and size of fibrils is considered to rely on the balance of polarities; the presence of anti-parallel fibrils may limit the rate of fusion of collagen fibrils (Scott and Parry, 1992). This also suggests that in the presence of parallel groups of fibrils, the probability of fusion is higher.

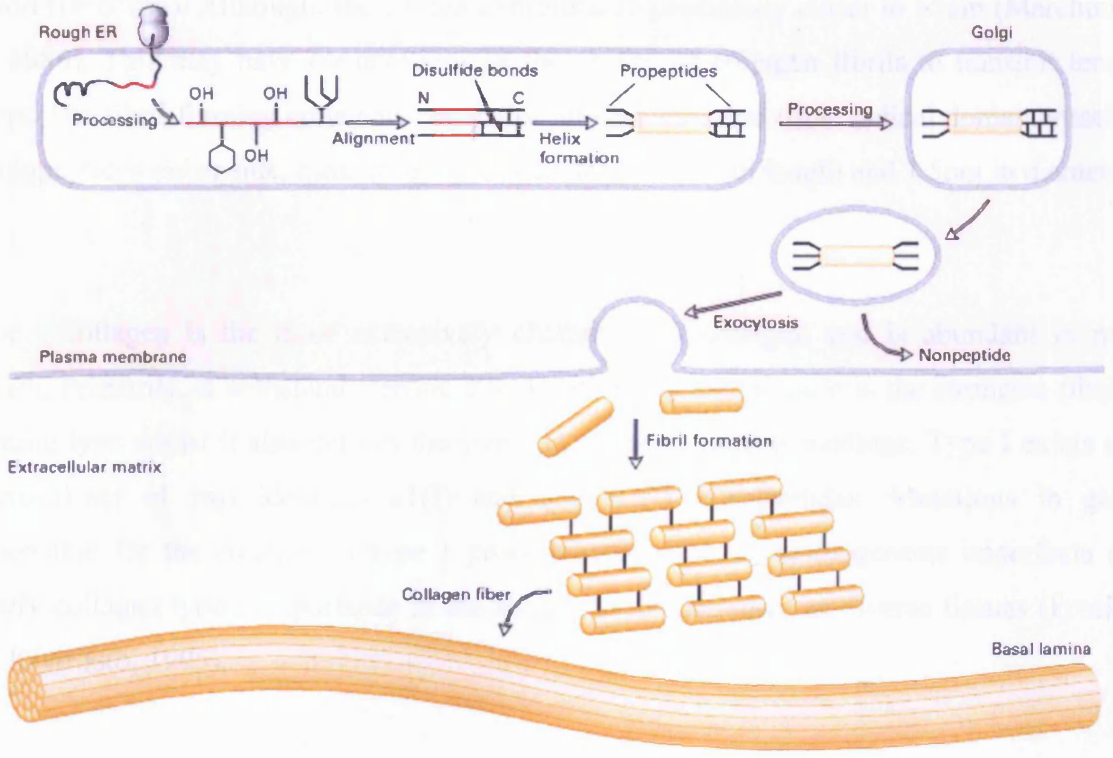

Fig 1.5 Schematic representation of collagen biosynthesis from translation of the α chain on ribosomes and injection into the RER to the subsequent post-translational modification and exocytosis (Taken from Lodish et al., 1999).

1.5 Collagen Types in the Cornea

Collagen exists in several different forms including: fibrillar forming, micro-fibrillar, FACIT (Fibril Associated Collagen with Interrupted Triple Helices) and non-fibril forming. Each form has an integral role in the formation of extracellular matrix structural integrity.

1.5.1 Fibril-forming

Within the corneal stroma, the fibril forming collagen types I and V are abundant, where they co-assemble to form heterotypic fibrils that are inextensible; resisting and transmitting tensile stress and ultimately defining the maximum size of the tissue (Scott, 1995). Collagen types I, II, III, V and XI are fibrillar-forming and all of them (excluding XI) may exist in the stroma at some stage in development and maturity of the cornea (Michelacci, 2003). Fibril forming collagens organize into the characteristic axial periodicity for collagen denoted as the D-

period (D=67nm). Although, the cornea exhibits a D-periodicity closer to 65nm (Marchini et al., 1986). This may have connotations in the ability of collagen fibrils to transmit tensile stress. The fibril-forming collagens consist of an uninterrupted triple helical domain attached to telopeptides either side, measuring approximately 300nm in length and 1.5nm in diameter.

Type I collagen is the most extensively characterised collagen and is abundant in most tissues. Primarily, it withstands tensile stress within the tissues as it is the strongest fibrillar forming type whilst it also defines the size and shape of its surroundings. Type I exists as a hetero-trimer of two identical α1(I) and one α2(I) polypeptides. Mutations in genes responsible for the creation of type 1 procollagens result in oesteogenesis imperfecta and signify collagen type I importance in the structural maintenance of diverse tissues (Prockop and Kivirikko, 1995).

Type II consists of three identical polypeptide chains, α1(II), which constitutes the triple helix structure. Type II collagen is primarily a cartilage collagen, although it is present in stromal development.

Type III has three identical polypeptides, α1(III) that constitute its triple helix. It has been found to attach to the stromal lamellae and also with the substratum of the epithelium. Collagen type III is believed to be involved with the structural maintenance and function of the epithelial tissue (Newsome et al., 1982). It is also considered to play a significant role in response to tissue damage, exerting its role in wound healing and inflammation.

Type V collagen co-assembles with type I within the stroma, where the resulting heterotypic fibril constitutes most of the collagen within the tissue. It is composed of three different polypeptide chains which are α1(V), α2(V) and α3(V). Birk (1990) illustrated that, *in vitro*, collagen fibrillogenesis is affected when collagen type V is displaced from the stroma, whereby fibril diameters increase; removal of type V collagen has implications in the development of heterotypic fibrils with narrow diameters.

Type XI is formed from α1(XI), α2(XI) and α3(XI) polypeptides in a 1:1:1 ratio (Morris and Bachinger, 1987). The α3(XI) chain however, is actually transcribed from the COL2A1 gene but results from a post-translational modification of an α1(II) polypeptide of collagen type II (Wu and Eyre, 1995).

Collagen Type	Group	Location	Functionality	Reference
I	Fibril Forming	Bowman's layer; Stroma (75% of collagen content in stroma)	• Fibril-forming; abundant in cornea • structural integrity and formation of transparency	(Michelacci, 2003, Birk et al., 1986)
III	Fibril Forming	Bowman's layer; Stroma	• Inflammation • wound healing	(Marshall et al., 1991, Michelacci, 2003)
V	Fibril Forming	Bowman's layer; Stroma (2% of collagen content in the stroma); Interfibrillar Matrix	• Forms heterotypic fibrils with type I • believed to regulate collagen fibril diameter	(Michelacci, 2003, Birk et al., 1986)

Table 1.1 The distribution of fibril forming collagen types throughout the cornea

1.5.2 FACIT

FACIT (Fibrillar-Associated Collagens with Interrupted Triple-Helices) collagens, as well as proteoglycans, are pivotal to the correct orientation of collagen fibrils within the extracellular matrix. Collagen types IX, XII, XIV, XVI, XIX, XX and XXI are all part of the FACIT collagens group (Gelse et al., 2003). FACITs are not fibril forming collagens, however, they

are known to co-aggregate with other collagens and extend from their surface, this enables collagen fibrils to form interactions with other matrix components or adjacent fibrils (Svensson et al., 2001). Each FACIT molecule has domains that lie along the fibril surface anchoring them to underlying fibrillar collagens, often by covalent interaction (Wu and Eyre, 1995). FACITs are common in the fact that they all share a non-helical sequence motif that interrupts the triple helical domain, as their name suggests.

FACITs are known to associate with the surface of collagen fibrils and alter their interactive properties. Type IX collagen is a hetero-trimer of α1(IX), α2(IX) and α3(IX) and co-distributes with collagen type II in cartilage (Gelse et al., 2003). Type XII collagen is localised within the corneal stroma and Bowman's layer. By comparison with type IX collagens, corneal FACITs XII and XIV may be expected to execute a similar role to type IX in cartilage. Therefore, the N-terminal domains of type XII and XIV may extend from the surface of collagen fibrils within the corneal stroma interacting with other proteins and polymers in the ECM.

1.5.3 Non-fibrillar/Filamentous

Collagen type IV is the most predominant collagen component of basement membranes; they form the anchoring plaques and the lamina densa. Type IV collagen molecules exhibit a long central collagenous domain with a non-helical domain at the C-terminal end (Linsenmayer et al., 1998). Type VIII and X collagens are known as short-chain collagens, existing in basement membranes and cartilage respectively.

Micro-fibrillar type VI collagens also exist within the stroma at different levels. Collagen type VII, which is also micro-fibrillar, acts as an anchoring fibril between the epithelium and its corresponding basement membrane (Linsenmayer et al., 1998). Collagen type XIII, a non-fibrillar collagen, has also been found bound to the cell membrane and within the posterior two thirds of the corneal stroma (Sandberg-Lall et al., 2000).

Collagen Type	Group	Location	Functionality	Reference
IV	Basement membrane	Descemet's membrane	• Adhesion of Descemet's membrane, stroma and endothelium	(Fitch et al., 1991, Linsenmayer et al., 1998)
VI	Micro-fibrillar	Stroma	• Forms thin filaments with a 100nm periodicity alongside collagen fibrils • Interact with proteoglycans to stabilise arrangement of collagen fibrils.	(Zimmermann et al., 1986, Linsenmayer et al., 1986, Nakamura et al., 1997, Nakamura et al., 1992)
VIII	Short chain	Anterior banded region of Descemet's membrane	• Homologous to type X although may have different functions. • Assembles as a hexagonal lattice in Descemet's membrane	(Sawada et al., 1990, Gelse et al., 2003)
XII	FACIT	Epithelium-basement; Bowman's layer, Stroma	• Involved in fibril organisation • Distribution indicates may play role in interactions in epithelial and stromal tissues	(Wessel et al., 1997, Akimoto et al., 2002) (Kato et al., 2000)
XVII	Membrane intercalated		• Hemidesmosomal attachment	(Linsenmayer et al., 1998, Gordon et al., 1997)

Table 1.2 The distribution of non-fibril forming collagen types throughout the cornea.

1.6 Collagen Fibrillogenesis

Collagen fibrillogenesis encompasses fibril assembly and the subsequent packing of collagen molecules according to the requirements of the tissue. Connective tissues are composed of various collagen types and the relative amounts of collagen types. How the collagen is ordered directly affects the physical properties of the respective tissues. Interestingly, collagen molecules incubated *in vitro* at physiological temperature and pH aggregate continuously to form insoluble fibrils of varying lengths and diameters (Kadler et al., 1996). Therefore, certain governing factors must exist that contribute to the specific organisation of collagen witnessed in the cornea.

Micro-fibrils within tendon are staggered longitudinally with an axial periodicity of 67nm, denoted as the D-periodicity, whereas, as mentioned earlier, the cornea exhibits a D-periodicity of 65nm (Marchini et al., 1986). The angular tilt patterns are believed to account for the noticeable difference in axial periodicity within different tissues (see below); corneal micro-fibrils tilt at an angle of 15 degrees (Holmes et al., 2001) whereas highly tensile fibrils run straighter at an angle of 5 degrees (Ottani et al., 2001). Fibril assembly in the cornea is governed by a multitude of factors that enable the formation of fibrils with regulated diameters and distribution. Studies have indicated that the diameter of human corneal heterotypic collagen fibrils is approximately 31nm and reaches up to 34nm with aging (Meek and Leonard, 1993). No evidence suggests that fibril diameters increase with respect to stromal depth (Freund et al., 1995).

Corneal collagen mainly consists of heterotypic fibrils that are composed of type I associated with type V collagen. The triple-helical domain of type V collagen is enclosed within the fibril and the N-terminus is exposed at the surface, protruding outwards through the gap regions. A short α helical region at the N-terminal domain acts as a flexible hinge-like region which allows the part of the polypeptide to extend from the molecule. This region is responsible for the regulation of the assembly of immature fibril intermediates. The N-terminal domain alters the cohesion of collagen molecules and lateral growth and therefore, inhibits the formation of insoluble fibrils with larger than normal diameters (Birk, 2001).

Average fibril diameters remain constant across the cornea before increasing at the limbus region (Borcherding et al., 1975).

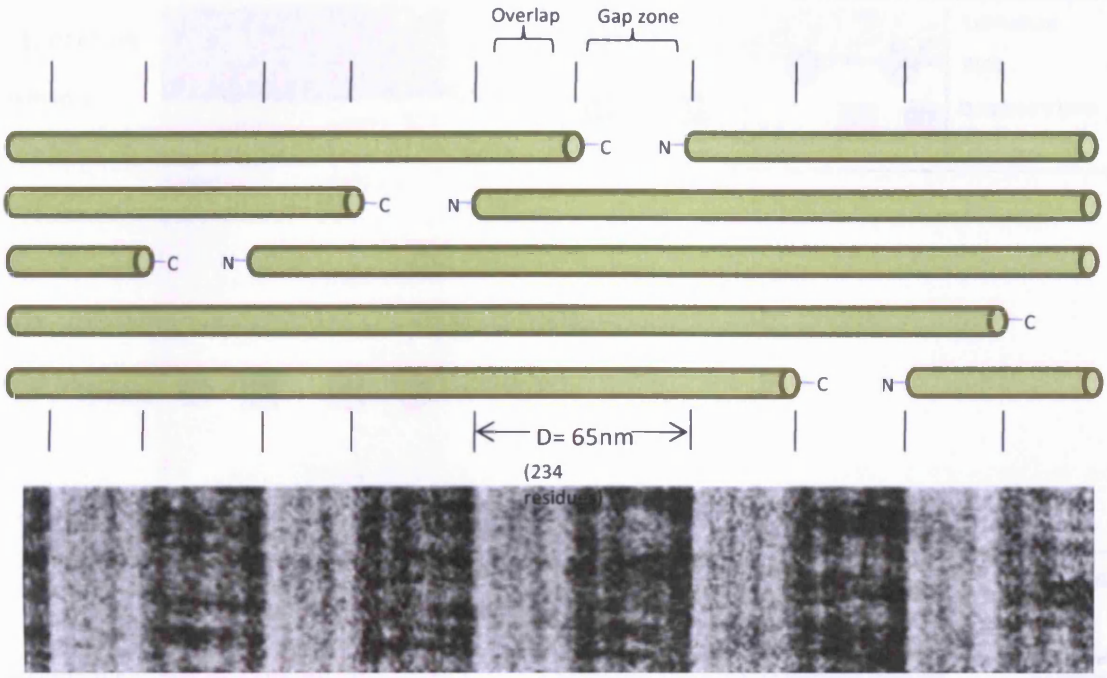

Fig. 1.6 Axial packing arrangement of triple-helical collagen molecules illustrating the characteristic 'quarter-stagger' and D-periodicity. Gap and overlap regions are indicated by negative staining, whereby staining is left over and therefore darker in regions where collagen presence is to a lesser extent, which is known as the 'gap' zone (Adapted from Kadler et al., 1996).

The fibrils are hydrated in a manner that results in a lateral distance between collagen molecules of 1.8nm (Malik et al., 1992). In the human cornea, collagen fibrils ~ 36nm in diameter are organised into micro-fibrils which are tilted by 15° to the fibril axis in a right handed helix (Holmes et al., 2001). Due to the 'quarter-staggered' nature of collagen fibril assembly, incomplete overlapping of collagen molecules results in a 'gap' zone that is clearly evident upon staining of collagen. The 'gap' zone is considered to be 0.6D (Meek and Quantock, 2001) and is the distance between the amino terminal of one collagen molecule and the next amino terminal to extend past it. 'Overlap' zones are deemed to be the areas where staining does not accumulate in negative staining methods and collagen molecules overlap one another. The D-period is further subdivided into 12 bands from a1 to e2 enabling

identification of axial position through the length of a collagen fibril (Hodge and Schmitt, 1960).

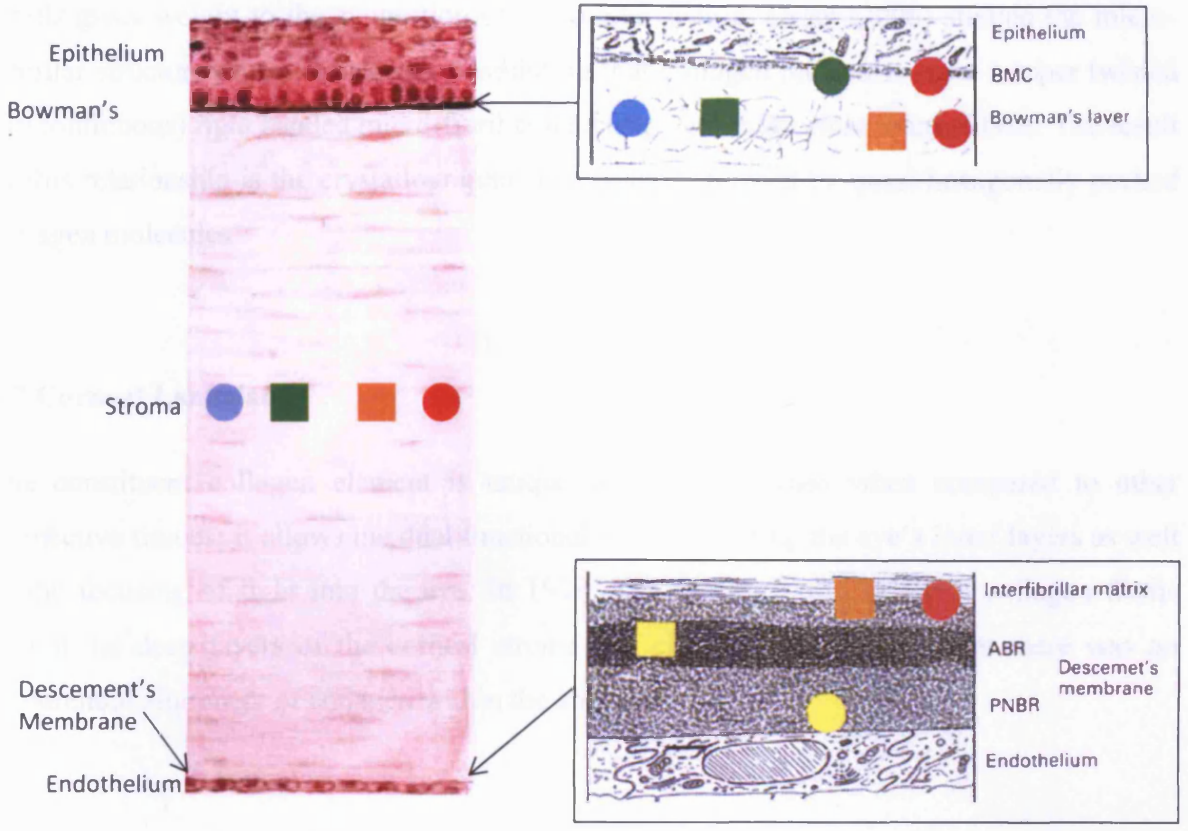

Fig. 1.7 Localisation of collagens type I-VIII in human cornea. Collagen I (blue circle), III (green square), V (brown square), and VI (red circle) are present within Bowman's layer and the stroma with only types V, VI being expressed within the interfacial matrix. Both types VI and VII (green circle) are present within the basal lamina situated in the sub-epithelium. Type IV collagen is abundant within Descemet's membrane. Type VIII collagen (yellow square is present within the anterior banded region (ABR) of Descemet's membrane. BMC – Basement membrane complex; ABR – Anterior Banded Region; PNBR; Posterior near-banded region (Adapted from Marshall et al., 1993)
Picture: http://education.vetmed.vt.edu/Curriculum/VM8054/EYE/CRNEADGM.JPG)

As stated previously, collagen fibrils are also considered to be directional because the collagen molecules that make up fibrils are orientated parallel to one another (Scott and Parry, 1992), although collagen molecules are also known to exists in anti-parallel conformations. Wess et al (1998) proposed that type I collagen fibrils are formed by five left-handed micro-fibrils. Micro-fibrils are considered to be interconnected covalently through

telopeptides at gap-overlap regions. It is also suggested that collagen fibrils are modular structures as opposed to the initial idea that they existed as quasi-crystalline aggregates (Scott and Parry, 1992). The regular appearance of proteoglycans that exist associated with collagen fibrils gives weight to the suggestion of a modular nature. Orgel (2006) studied the micro-fibrillar structure of type I collagen postulating that collagen molecules form a super twisted (discontinuous) right handed micro-fibril connecting with other close micro-fibrils. The result of this relationship is the crystallographic super-lattice formed by quasi-hexagonally packed collagen molecules.

1.7 Corneal Lamellae

The constituent collagen element is unique within the cornea when compared to other connective tissues; it allows the dual functionality of protecting the eye's inner layers as well as the focusing of light into the eye. In 1938, Kokott first postulated that collagen fibrils within the deep layers of the corneal stroma run circumferentially and that there was no preferential alignment of collagen within the anterior stroma.

Collagenous lamellae within the corneal stroma are indeed orientated differently in the anterior and posterior regions. Lamellae situated adjacently are positioned at varying angles to each other, except in the posterior region, where lamellae may be positioned orthogonally and a more tilted conformation is witnessed. This is illustrated by the total scattering cross-section of each region, where values for the posterior region were lower than the anterior portion, depicting a higher degree of order in the posterior stroma (Freund et al., 1995). Lamellae situated towards the anterior are thinner and exhibit a flat appearance (approx. 30μm wide an 1.2μm thick) when compared with the broader and thicker posterior lamellae (200μm wide and 2.5μm thick) (Komai and Ushiki, 1991).

Within the anterior stroma, lamellae appear to run in random directions and display a high degree of irregularity in their interweaving. There is an evident anterior to posterior lamellae interweave within the anterior stroma believed to help aid corneal curvature (Muller et al., 2001) and confers stability along with Bowman's layer (Bron, 2001). Central lamellae are

found to cross irregularly, forming interwoven networks. Posteriorly positioned lamellae run parallel to the corneal surface and are largely uninterrupted structures that extend from one region of the limbus to the other, which is believed to compound additional strength. The posterior region is hydrated to a greater extent at physiological conditions (Turss et al., 1970) and exhibits a lower refractive index (1.373) than the anterior stroma (1.380) (Patel et al., 1995). The hydration properties are, in part, a result of the glycosaminoglycan constituent of each region within the stroma. Due to keratan sulphate's greater affinity to water than Chondroitin sulphate, the posterior region, with a larger KS:CS ratio than the anterior stroma, exhibits a higher degree of hydration. This is also furthered by the proximity of the posterior stroma to the 'leaky' endothelium. Therefore, stromal swelling tendencies increase with respect to stromal depth (Castoro et al., 1988).

Fig 1.8 Scanning electron micrograph (SEM) of corneal lamellae in the mid-stroma region. The arrangement of the collagenous lamellae is depicted running at varying angles whilst also interweaving in some areas (short arrow). The angles between lamellae may be calculated by measuring the angle between the longitudinal axes of adjacent lamellae (large arrows). (Taken from Meek and Fullwood, 2001) Scale bar - 10µm

1.8 Proteoglycans

Proteoglycans are fundamental to the composition of the extracellular matrix in connective tissues, playing key roles in the maintenance of tissue shape and definition. Known for a variety of diverse biological functions; within the cornea they are compression-resistant, soluble polymers that interact with collagen and are primarily involved with the regulation of collagen fibril diameters and interfibrillar spacing (Scott, 1975). Ultimately, they are responsible for the uniform organisation of collagen fibrils through regulation of fibrillogenesis as well as the hydration of the corneal stroma (Hedbys, 1961). Proteoglycans swell in water occupying large volumes that press against the networking collagens and, in turn, resist compressive forces that would reduce the size of the tissue. This osmotic swelling mechanism is likely to play a key role in their regulatory functions, as discussed later. Proteoglycan diversity is reflected by the varying proteoglycan composition of tissues; tendon is designed to resist or transmit most types of tensile stress and therefore is more fibrillar in content, whereas cartilage, which is more elastic in nature, contains a considerably larger amount of soluble polymers than tendon (Scott, 1991). According to this concept, the cornea can be expected to also have a high degree of proteoglycan content when compared to tendon, which is indeed the case. Deficiency of proteoglycans has been shown to result in the aggregation of collagen fibrils and consequently corneal opacity (Hassell et al., 1980), depicting the necessity of proteoglycan presence in the maintenance of corneal transparency.

There are two major components of proteoglycans - a protein core covalently attached to one or more polysaccharide glycosaminoglycan side-chain(s). Within the corneal stroma, two major classes of proteoglycan exist according to their glycosaminoglycan component; keratan sulphate or a hybrid of chondroitin sulphate/dermatan sulphate (Iozzo, 1999). Glycosaminoglycans are negatively charged at physiological pH due to the high level of sulphation and confer this charge to the proteoglycan molecule, which stimulates interaction with counter-ions and other glycosaminoglycan chains. The electrostatic forces that exist due to the charge density of glycosaminoglycans enables the binding of cationic staining solutions such as Cupromeronic blue or Cuprolinic blue, which allows us to visualise proteoglycans under an electron microscope as electron-dense filamentous structures (Scott, 1980).

Proteoglycans can contain as much as 95% carbohydrate by weight, reaching $3x10^6$ Da in the case of the cartilage proteoglycan aggrecan (Alberts et al., 2002). However, within the cornea there exists a subsection of the family of proteoglycans known as the small leucine rich proteoglycans (SLRPs) that are considerably smaller than cartilage proteoglycans because of the respective glycosaminoglycan components, such as decorin, which has only a single glycosaminoglycan chain. SLRP protein constituents inhibit collagen fibrillogenesis in order to control the fibril diameter whereas the glycosaminoglycan chain extends to form interfibrillar bridges responsible for the development of regular fibril spacing. Proteodermatan and proteokeratan sulphate proteins exhibit horseshoe conformations, purposefully designed to aid interactions with collagen fibrils (Scott, 1996)

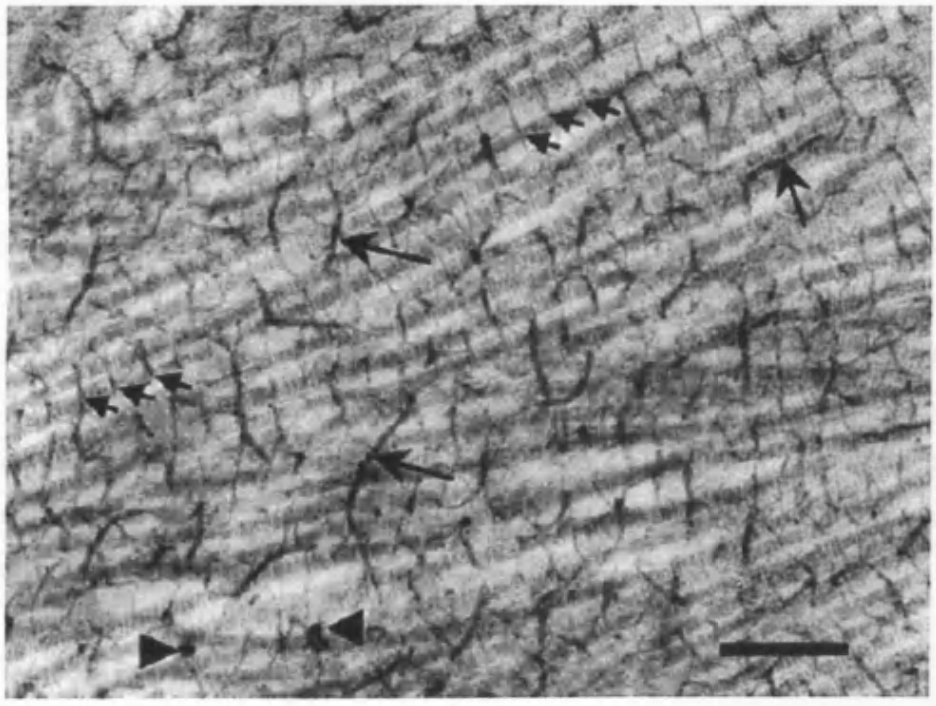

Fig 1.9 Transmission electron micrograph of mouse corneal stroma stained with Cupromeronic blue. Proteoglycan structures appear as electron-dense filaments and are found to be regularly associated with fibrils (short arrows) longitudinally, as well as appearing to be large, elongated structures running across several fibrils (long arrows). The large proteoglycan structures are illustrated as circular in transverse sections (arrow heads), reaching 20nm in diameter. Bar – 250nm (Taken from Young et al., 2005)

1.9 Glycosaminoglycans

Glycosaminoglycans are linear chains of repeating disaccharides. One of the sugars is an amino sugar whereas the second sugar is an uronic acid or galactose and either may be sulphated. Carboxyl (COO^-) and sulphate ester (SO_3^-) groups are present on specific sites of a glycosaminoglycan chain and confer a highly negative charge. The negative charges that exist through varying degrees of sulphation enable proteoglycans to interact with other molecules and other glycosaminoglycans. Anionic glycosaminoglycans are rigid chains that should display mutual repulsion, however they are known to aggregate (Fransson, 1976). They also attract counter-ions such as Na^+ which induces osmotic swelling or turgor. Glycosaminoglycans fill a large amount of space and exhibit strong swelling pressure at relatively low concentrations, forming hydrated gels that suck water into the matrix (Scott, 1995).

Keratan sulphate and chondroitin sulphate/dermatan sulphate are the predominant glycosaminoglycan chains that associate with SLRPs in the cornea (Iozzo, 1999) and attach to specific axial sites along collagen fibrils (*see 1.12)*. The subsequent hydrophilic property of glycosaminoglycans enables them to orientate into extended structures, although, it has been elucidated that glycosaminoglycans are in fact amphiphilic structures capable of hydrophobic interaction and hydrogen bonding. It is these interactions that enable the glycosaminoglycans to counteract the strong expected mutual repulsion and associate to form interfibrillar bridges (Scott, 2001).

1.9.1 Keratan Sulphate

Keratan sulphate is a sulphated glycosaminoglycan chain, first isolated by Karl Meyer (1953) in bovine cornea, that consists of the amino sugar N-acetylglucosamine (GlcNAc) and galactose repeated as disaccharide units. The glycosaminoglycan chain of keratan sulphate can contain a combination of non-sulphated, mono-sulphated and di-sulphated disaccharide units (Varki and Cummings, 2008). Keratan sulphate occurs as two different forms dependant on the linkage to its respective protein core. N-linked keratan sulphate molecules are termed keratan sulphate class I, whereas class II is defined as those linked to proteins through O-

linkage at Ser/Thr residues (Funderburgh, 2000). N-linked keratan sulphate exists primarily in the cornea and is therefore defined as corneal keratan sulphate. There is more than ten times the amount of keratan sulphate in cornea than in cartilage (Funderburgh et al., 1987). The principal glycosaminoglycan within the mammalian corneal stroma, keratan sulphate, is found attached to three different SLRPs; lumican, keratocan and mimecan (Funderburgh, 2000).

Keratan sulphate associated proteoglycans are known to attach at bands 'a' and 'c' of collagen fibrils (Meek et al., 1986) and the cornea is the only tissue known to have proteoglycan attachment sites at these loci (Scott, 1995). The sclera exhibits lower concentrations of keratan sulphate proteoglycans than the cornea and due to the differing fibril diameters inherent in each tissue, it is subsequently believed that keratan sulphate proteoglycans play important roles in the regulation of collagen fibril diameter (Borcherding et al., 1975), allowing light to be refracted through the cornea with minimal scattering (Varki and Cummings, 2008). This is evident when there is a failure to synthesize a mature keratan sulphate proteoglycan, which results in corneal opacity and even blindness (Hassell et al., 1980).

1.9.1.1 Keratan Sulphate Biosynthesis

Production of the keratan sulphate glycosaminoglycan chain occurs within the golgi apparatus and is subject to processing by glycosyltransferases and sulphotransferases. These two families of enzymes are responsible for chain elongation and the transfer of sulphate esters to the immature glycosaminoglycan, where upon maturation the keratan sulphate proteoglycan is secreted into the extracellular matrix. Elongation of the keratan sulphate chain is carried out by action of glycosyltransferases that alternately add galactose and GlcNAc to the elongating polymer (Funderburgh, 2000). The elongation of the immature glycosaminoglycan is processed by enzymes of two glycosyltransferase families, B1,3-N-acetylglucosaminyltransferase (B3Gnt) and B1,4-galactosyltransferase (B4GalT). When genes encoding B3GnT and B4GalT7 were suppressed in cultured human corneal cells, levels of sulphated keratan sulphate decreased, illustrating that these enzymes are necessary for elongation and the synthesis of normal keratan sulphate (Kitayama et al., 2007).

The enzymes responsible for the sulphation of the keratan sulphate glycosaminoglycan are keratan sulphate galactose 6-O sulphotransferase (KSG6ST) and corneal N-acetylglucosamine 6-O sulphotransferase (CGn6ST). CGn6ST only transfers sulphate to the non-reducing terminal GlcNAc but does not sulphate internal GlcNAc, suggesting that sulphation and elongation occur simultaneously (Kitayama et al., 2007).

Keratan Sulphate

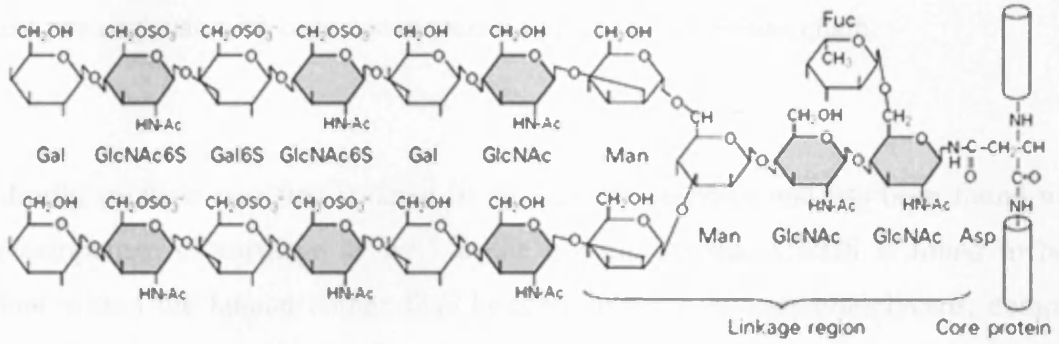

Chondroitin Sulphate/Dermatan Sulphate

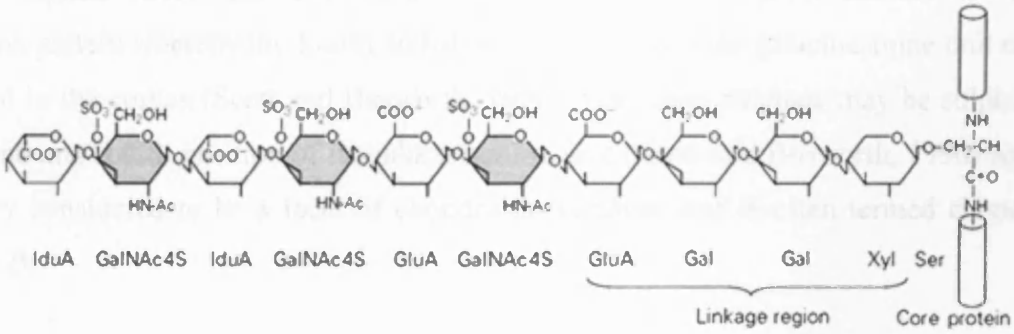

Fig 1.10 Structure of the main corneal stromal glycosaminoglycans. The glycosaminoglycan-protein linkage region is depicted as well as the main disaccharide sugars. Gal-Galactose; Fuc-Fructose; Man-Mannose; Xyl-Xylose; GluA-β-D-glucuronic acid; IduA-α-L-iduronic acid; GalNAc-N-acteylgalactosamine; GalNAc4S-N-acetylgalactosamine 4-sulphate; GlcNAc-N-acetylglucosamine; GlcNAc6s-N-acetylglucosamine 6-sulphate; Asp-Asparagine; Ser-Serine (Adapted from Michelacci, 2003).

1.9.2 Chondroitin Sulphate /Dermatan Sulphate

Chondroitin sulphate/dermatan sulphate (CS/DS) glycosaminoglycans contain N-acetylgalactosamine as its hexosamine constituent, with D-glucuronic and/or L-iduronic acid as its uronic acid within the repeating disaccharide. However, chondroitin sulphate contains no L-iduronic acid, which is commonly part of dermatan sulphate's disaccharide unit (Scott, 1988). Dermatan sulphate is a derivative of chondroitin sulphate, as it is formed by the epimerization of glucuronate C-5 upon creation of the glycan chain (Scott, 1988). Decorin is the main proteoglycan composed of hybrid CS/DS glycosaminoglycan chains; it is also the smallest proteoglycan with only one associated glycosaminoglycan chain.

Chondroitin sulphate was first isolated in the late 19th century and has been found to be a major component of cartilage as well as the corneal stroma. CS/DS is found to be less abundant within the human cornea than keratan sulphate glycosaminoglycans, comprising 20% of the total corneal glycosaminoglycan content (Scott and Bosworth, 1990). However, the opposite is true for the murine cornea; only 18% of total glycosaminoglycan content is keratan sulphate (Scott and Bosworth, 1990). Chondroitin sulphate exhibits a variable sulphation pattern whereby the fourth and sixth residue within the galactosamine unit may be sulphated in the cornea (Scott and Bosworth, 1990). Dermatan sulphate may be sulphated at the second and fourth position of its galactosamine unit (Scott and Bosworth, 1990) and was originally considered to be a form of chondroitin sulphate and is often termed chondroitin sulphate B.

1.9.2.1 Chondroitin Sulphate/Dermatan Sulphate Biosynthesis

CS/DS chains are attached to serine residues within core proteins through xylose. Xylotransferase (isoforms XT1 + XT2) utilises UDP-xylose as a donor to initiate the formation of the glycosaminoglycan chain (Varki and Cummings, 2008). Upon addition of xylose, a tetrasaccharide forms via the addition of two galactose subunits catalyzed by members of the glucuronosyltransferase family of enzymes. At this point in biosynthesis, the addition of α1-4 GlcNAc initiates the formation of Heparan sulphate or the addition B1-4GlcNAc begins development of the chondroitin sulphate chain. The sulphation of galactose is limited to chondroitin sulphate chains, however. Polymerisation of the chondroitin sulphate

chain is catalysed with chondroitin synthases that exhibit both B1-3 glucuronosyltransferase and B1-4 N-acetylgalactosaminyltransferase activities. The elongation of the polymer in chondroitin sulphate also requires the action of chondroitin polymerising factor, a protein that does not act independently but collaborates with the polymerases that transfer subunits. Sulphation occurs via the action of multiple sulphotransferases, conferring sulphation at 4-O and 6-O positions on N-acteylgalactosamine residues. Further enzymatic processing exists for the epimerisation of glucuronic acid to iduronic acid for dermatan sulphate production (Varki and Cummings, 2008).

1.10 SLRPs

The small leucine rich proteoglycan (SLRP) super-family consists of proteins within a range of diverse biological locations that are related both structurally and functionally. All SLRPs have one domain that is formed from the presence of tandem leucine rich repeats which adopts a curved solenoid fold (Hocking et al., 1998). The leucine rich repeat motifs within SLRPs are flanked on either side by cysteine-rich clusters, the presence of which are an integral part of the leucine rich repeat domain (Kobe and Kajava, 2001). Distribution of leucine rich repeat sequences within the protein structure and in different species illustrates the diversification of their roles, and this apparent retention throughout evolution indicates that the sequence provides an ideal conformation for binding to other proteins (Hocking et al., 1998).

SLRPs are classified into five distinct families according to protein and genetic homology and also the positioning of the N-terminal Cys-rich clusters (Iozzo and Schaefer, 2008). All SLRPs exhibit homologous sequences throughout their central domain of approx 10 fold repeats of a series of 24-amino acid leucine rich repeats (Iozzo, 1999). Leucine rich regions fold the protein into a series of beta-sheets forming a 3-D arch shape conformation that enables glycosaminoglycans to extend from the concave side of the arch (Iozzo, 1999). This conformation allows corneal proteoglycans to have bi-antennary functionality, attaching to collagen fibrils whilst protruding glycosaminoglycans that form interfibrillar bridges. The SLRPs are known to play a significant role in modulating collagen fibril diameter. Lumican and decorin have been show to inhibit the lateral aggregation of collagen fibrils (Rada et al.,

1993). Furthermore, studies indicate that the regulation of collagen fibrillogenesis is specific for certain proteoglycans. This is highlighted by the fact that biglycan and aggrecan display no effect on the rate of formation of collagen type I and II fibrils *in vitro* (Vogel et al., 1984).

SLRPs contain four regions that exhibit similar motifs in all members of the super-family (Iozzo, 1999). In the prototypic SLRP decorin, domain I consists of a signal peptide and propeptide; domain II comprises of four evenly spaced cysteine residues and the glycosaminoglycan attachment site; domain III, which contains the tandem LRR repeats and domain IV, a C-terminal domain of approx. 50 amino acids containing two conserved cysteine residues. The function of the propeptide is unidentified but the signal peptide dictates transit of the nascent peptide to the rough endoplasmic reticulum.

The crystal structure of a leucine rich repeat protein, pancreatic ribonuclease inhibitor, illustrated the nature of the repeats in the tertiary structure (Kobe and Deisenhofer, 1993). It is described as the characteristic leucine repeat fold. The significant number of tandem leucine rich repeat sequences in SLRPs forces the two parallel lines of α helices and beta-sheets into a curved shape homologous to the ribonuclease inhibitor (Kobe and Deisenhofer, 1993). The horseshoe conformation of SLRPs enables the attachment of SLRPs to collagen, as the diameter of space inside the horseshoe configuration (approx 2nm) is larger than the diameters of collagen micro-fibrils at (1.5nm) (Scott, 1996).

Corneal SLRPs have bi-functional character whereby the protein core binds the collagen fibrils at strategic areas and the attached glycosaminoglycan chain extends to regulate interfibrillar spacing. Each corneal SLRP has a unique core protein although they share 35% amino acid homology (Funderburgh et al., 1991).

1.11 Corneal Proteoglycans

The proteoglycans that exist within the cornea are all members of the SLRP super-family. The presence of the proteoglycans, differentiated by their glycosaminoglycan chain, varies

with respect to their position within the cornea. The proteoglycan differences co-ordinate the varying organisation of collagen that can be found from the centre of the cornea to the sclera. Specific interactions with respective fibrils hold down glycosaminoglycans but they orientate and maintain fibril organisation by forming interfibrillar bridges (Scott, 2001).

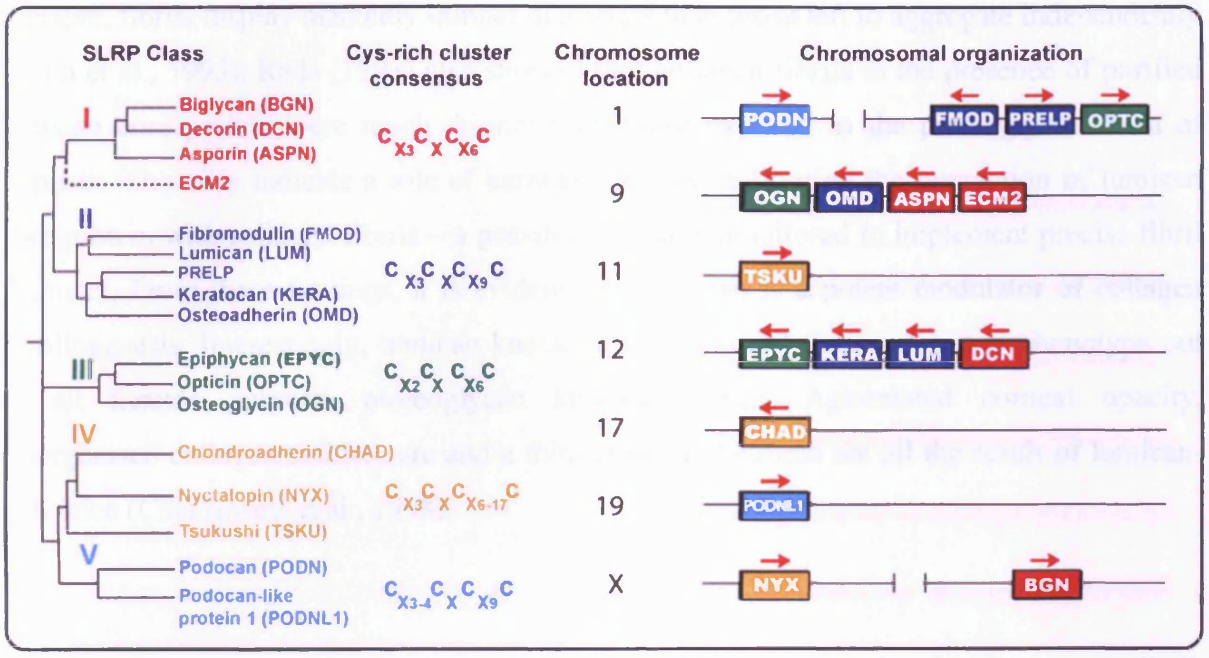

Fig. 1.11 Classification of SLRPs and consensus sequences of cysteine rich clusters (Taken from Iozzo and Schaefer, 2008).

1.11.1 Lumican

Lumican is a keratan sulphate proteoglycan and a member of the SLRP super-family. Originally isolated from a cDNA clone encoding chick cornea proteoglycan (Blochberger et al., 1992), lumican is similar to the other SLRPs; it contains the characteristic four domains and has a molecular weight of approximately 40kDa. Lumican plays an important role in the maintenance of corneal stroma architecture; lumican-null mouse corneas appear bright in confocal microscopy due to an increase in backscattered light, indicative of collagen fibril assembly disorder (Chakravarti et al., 2000). Lumican-deficient mice also displayed larger fibril diameters in the posterior of the stroma than that of wild type mice. In addition to the significant amount of large fibril diameters, lumican-null mice also exhibited irregular

interfibrillar spacing resulting from a disruption in lamellar organisation and abnormal fibril packing (Chakravarti et al., 2000).

Electron microscopy examination of fibrils formed *in vitro* illustrates that, in the presence of lumican, fibrils display markedly thinner diameters than those left to aggregate independently (Rada et al., 1993). Rada (1993) also showed that collagen fibrils in the presence of purified lumican core protein were much thinner than those exposed to the proteoglycan form of lumican. This may indicate a role of keratan sulphate in limiting the interaction of lumican core protein with collagen fibrils – a possible mechanism tailored to implement precise fibril diameter. From these findings, it is evident that lumican is a potent modulator of collagen fibrillogenesis. Interestingly, lumican knockout mice exhibit the most severe phenotype out of all keratan sulphate proteoglycan knockout mice. Age-related corneal opacity, disorganised collagen architecture and a thinner corneal stroma are all the result of lumican-null mice (Chakravarti et al., 1998).

Studies of keratocan-null mice and lumican-null mice indicate that lumican most likely prevents lateral fusion of collagen fibrils (Meek et al., 2003, Chakravarti et al., 1998). This is based on the fact that Keratocan deficient mice exhibit no large and irregularly shaped fibrils that are witnessed in lumican-null mice (Liu et al., 2003). It has also been postulated that lumican may in fact regulate the synthesis of keratocan. The modulation of keratocan has been measured via introsomal injection of a lumican mini-gene into the stroma of lumican-null mice (Carlson et al., 2005). SiRNA knockdown of lumican *in vitro* reduced keratocan, whereas increased keratocan translation was detected after insertion of a lumican mini-gene *in vivo* (Carlson et al., 2005). This evidence helps towards the understanding of why lumican-null mice display hazy corneas whilst keratocan-null mice retain corneal transparency.

Lumican, as well as keratocan, have sulphotyrosine residues situated at the N-terminal end of the core proteins (Funderburgh et al., 1995). Kao (2002) suggested that the sulphation of the tyrosine residues may affect interactions with cationic domains of extracellular matrix or cell surface proteins. In embryonic chick corneas, transparency increases in respect to the accumulation of lumican (Cornuet et al., 1994) and exerts its function early in collagen

fibrillogenesis (Ezura et al., 2000). It is clearly evident from current studies that the presence of lumican is imperative for the normal control of collagen fibrillogenesis within the cornea.

1.11.2 Keratocan

Keratocan is a 38kDa proteoglycan that is associated with 4-5 keratan sulphate glycosaminoglycan chains (Michelacci, 2003). Also part of the SLRP family, it is one of the major components of the corneal extracellular matrix. Keratocan exists abundantly within the cornea, expressed by keratocytes, but it is also found in skin and cartilage to a lesser extent. It is only subject to sulphation within the cornea, however. It has been postulated that keratocan and lumican display similar three-dimensional structures, also similar in arrangement to that of the porcine ribonuclease inhibitor (Dunlevy et al., 1998).

Keratocan-null mice exhibit clear corneas at early development compared to the hazy corneas that are seen from lumican null mice at the same stage (Kao and Liu, 2002). They display a thin corneal stroma at this stage, however. Later in development, collagen fibril spacing becomes abnormal when compared to that of wild type mice. However, fibrils appear to remain circular (Kao and Liu, 2002). Also, the expression of keratocan is specific to the adult corneal stroma in mice (Liu et al., 2003). In humans, mutations to the gene encoding keratocan results in the formation of cornea plana and ultimately, decreased vision acuity when corneal curvature is flattened and the refractive properties are altered (Pellegata et al., 2000). Investigations into the elucidation of keratocan's role suggest that along with other keratan sulphate proteoglycans it is a potent modulator of collagen fibrillogenesis.

1.11.3 Mimecan

Mimecan is a 25kDa keratan sulphate proteoglycan that is transcribed from the same gene that encodes osteoglycin and is synthesised via proteolytic splicing and/or mRNA alternative splicing (Funderburgh et al., 1997). Similar to keratocan, it is only sulphated within the cornea and is expressed to a lesser extent in other tissues. Mimecan contains a lower incidence of the tandem leucine repeat motifs, only six compared with the ten of the other

corneal SLRPs (Iozzo, 1997), and belongs to SLRP class III (Iozzo and Schaefer, 2008). On comparison with lumican and keratocan, a high level of sequence identity is not noticed. Structural domains within all three proteins are conserved, whereby each protein has one or more tyrosine residues situated next to acidic amino acids at their N-terminus (Funderburgh et al., 1997).

Collagen fibrils within the corneal stroma of mimecan-null mice are of a normal diameter and have regular interfibrillar spacing on average (Beecher et al., 2005). This evidence suggests that mimecan plays a role of lesser significance in the regulation of collagen fibrillogenesis than other keratan sulphate proteoglycans. However, Tasheva (2002) demonstrates that mimecan may modulate collagen fibrillogenesis and that in its absence, collagen fibril diameters increases in both skin and the cornea.

1.11.4 Decorin

Decorin was initially cloned from a human fibroblast cell line (Krusius and Ruoslahti, 1986) but has since been discovered localised in many other connective tissues. Like other SLRPs, it is a low molecular weight proteoglycan that contains a leucine rich 45kDa protein core and has a single glycosaminoglycan chain consisting of either chondroitin or dermatan sulphates. Decorin, unlike keratan sulphate proteoglycans, binds to the 'd' and 'e' loci of collagen fibrils (Scott, 1990) and was termed decorin due to its ability to 'decorate' collagen fibrils. It has been deduced that the sixth leucine motif within decorin is the major collagen type I binding site (Kresse et al., 1997) and recent evidence suggests that one molecule of decorin may interact with four to six collagen molecules (Orgel et al., 2009).

Decorin is proposed to be dimeric and each monomer folds into the curved solenoid characteristic of leucine rich domains with parallel β-sheets on the inside of the structure (Scott et al., 2004). Dimerisation occurs through the concave surfaces of the leucine rich repeat domains and the possible ligand-binding scenarios were reviewed by McEwan and colleagues (2006). Glycosaminoglycan attachment loci within decorin's structure is located at

a Ser residue in the N-terminal end situated proximal to the cysteine rich region (Iozzo, 1999).

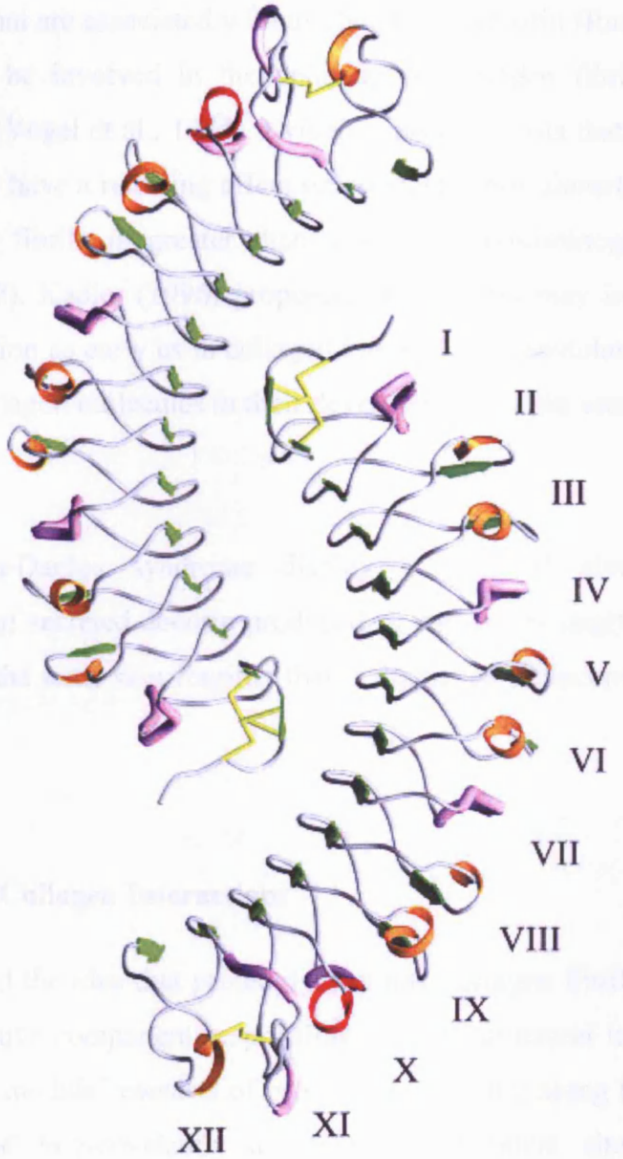

Fig. 1.12 Ribbon diagram of the dimeric leucine rich repeat domain of bovine decorin. Green arrows – β-strands, red ribbons – α-helical turns, pink tubes – polyproline II helix, orange ribbons – 3.10 helices and β-turns, yellow sticks – disulphide bonds (Taken from Scott et al., 2004).

Decorin is a multi-functional protein involved in diverse processes including the control of collagen fibril morphology (Danielson et al., 1997), cell adhesion and also the regulation of growth factors (Winnemoller et al., 1992, Yamaguchi et al., 1990). It has been established that in the absence of the decorin proteoglycan, collagen fibril diameters are increased when compared to fibrils that are associated with unglycanated decorin (Rada et al., 1993). Decorin has been shown to be involved in the delaying of collagen fibril lateral assembly and aggregation *in vitro* (Vogel et al., 1984). Evidence also suggests that the glycosaminoglycan chain of decorin may have a reducing affect on collagen fibril diameter, whilst the affinity of decorin to collagen fibrils is greater than that of glycosaminoglycan-deficient decorin (Ruhland et al., 2007). Kadler (1996) proposed that decorin may initiate the prevention of fibril lateral aggregation as early as in collagen biosynthesis, postulating that decorin may be secreted along procollagen molecules in their development within secretory vesicles.

Sufferers of Ehlers-Danlos syndrome display a lack of glycanated decorin, with approximately 50% of secreted decorin produced in patients is unglycanated. Ehlers-Danlos patients also exhibit the same skin-fragility that is displayed in decorin-null mice (Ruhland et al., 2007).

1.12 Proteoglycan – Collagen Interactions

Scott (1991) proposed the idea that proteoglycans and collagen fibrils form part of a 'shape module' that is a major component responsible for the structural integrity of extracellular matrices. The 'shape module' consists of proteoglycans lying along the length of a collagen fibril and are bound non-covalently at specific attachment sites, in addition to the glycosaminoglycan chains that extend outward and form interfibrillar bridges with adjacent proteoglycans. The SLRP is considered to inhibit lateral aggregation of collagen fibrils and therefore, exists as a regulator of collagen fibrillogenesis. SLRPs exist in a horseshoe conformation whereby their respective glycosaminoglycans chains extend from the convex side, leaving the protein free to bind to fibrils and consequently restrict the lateral aggregation of collagen. The result of which is the formation of narrow diameter collagen fibrils that are necessary for the low level of light scattering in the cornea. Projecting out from the leucine rich repeat protein is a bound, highly anionic glycosaminoglycan chain that interacts with

other protruding glycosaminoglycan chains facilitating the control of interfibrillar spacing. The interfibrillar anionic glycosaminoglycan bridges organise fibrils by 'tying' them together, bridging between and spanning fibrils, often several at a time (Scott and Thomlinson, 1998).

The SLRP core of a proteoglycan binds to certain axial locations of the collagen fibril, with one protein per binding site (Scott and Haigh, 1988a). Meek (1986) deduced that proteoglycans are situated at the 'a', 'c', 'd' and 'e' axial regions of collagen fibrils using x-ray diffraction methodology on bovine corneas. Scott (1991) expanded on the study; elucidating that keratan sulphate proteoglycans bind to the 'a' and 'c' regions whereas 'd' and 'e' bands accommodate CS/DS associated proteoglycans. Decorin therefore binds to 'd' and 'e' whereas lumican, keratocan and mimecan all bind to 'a' and 'c' sites due to the presence of their keratan sulphate glycosaminoglycan chain.

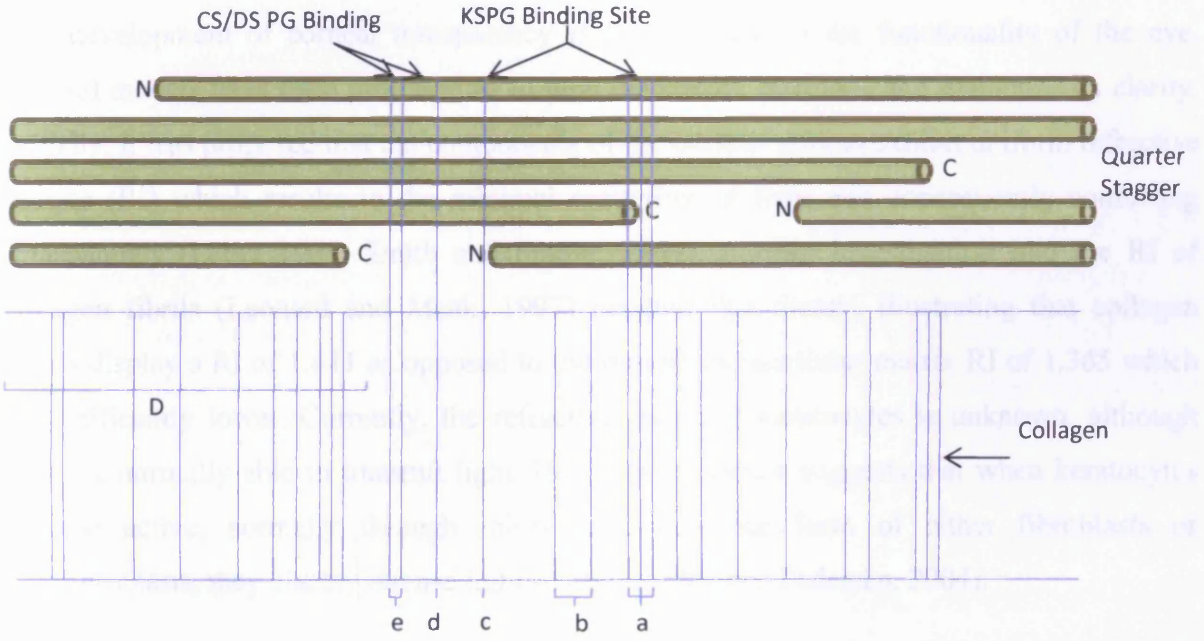

Fig 1.13 Representation of the proteoglycan-collagen binding sites. The quarter-stagger arrangement of collagen molecules is illustrated against the a-e banding pattern within the D-period. The proteoglycan locations are indicated across the quarter-stagger region, correlating with the a-e banding pattern. Keratan Sulphate proteoglycans are found positioned at the collagen bands 'a' and 'c' whereas Chondroitin Sulphate and Dermatan Sulphate are located at the 'd' and 'e' positions (Adapted from Scott and Haigh, 1988a).

Proteoglycans are also important for the balanced hydration of the corneal stroma. The highly anionic character of glycosaminoglycans means they have a high water binding capacity (Bettelheim and Plessy, 1975) and also attract counter-ions such as Na^+ into the stroma, necessary for the correct hydration of the tissue. Mice deficient in corneal glycosaminoglycans often exhibit noticeably thinner corneas as a result of dehydration and the imbalance of water intake into the stroma (Chakravarti et al., 2000, Liu et al., 2003). The apparent alteration of proteoglycan biosynthesis can also have differing effects on the development of the cornea. Disruption in normal matrix formation can lead to opaque tissue and blindness, as is the case in macular cornea dystrophy. Corneal scars that have reduced transparency display highly sulphated CS/DS and a reduction in keratan sulphate indicating that defects in processing have implications in the development of transparency and the ratio of different proteoglycans (Funderburgh, 2000).

1.13 Corneal Transparency

The development of corneal transparency is fundamental to the functionality of the eye. Several models have been proposed as to how the cornea develops and maintains its clarity. Initially, it was proposed that the components of the corneal stroma exhibit uniform refractive indices (RI) which results in the minimal scattering of light and consequently conferring transparency (Leber 1903, Smith and Frame, 1969). Further investigation into the RI of collagen fibrils (Leonard and Meek, 1997) negated this theory, illustrating that collagen fibrils display a RI of 1.411 as opposed to the overall extracellular matrix RI of 1.365 which is significantly lower. Currently, the refractive index of keratocytes is unknown, although they are normally able to transmit light. However, evidence suggests that when keratocytes become active, normally through injury, and take the form of either fibroblasts or myofibroblasts, they display intense light scattering (Moller-Pedersen, 2004).

Caspersson and Engstrom (1949) first developed the idea that transparency may be a result of the regular arrangement of collagen fibrils, whereby individual scattered waves cause destructive interference in all directions with the exception of the forward direction. In his now seminal work, Maurice (1957) compounded the idea of lattice theory and the notion that, as a result of regular interfibrillar spacing with a lower magnitude than the wavelength of

light, destructive interference of scattered light by individual fibrils occurs in all but the forward direction. The lattice theory proposes that the cornea appears transparent due to scattered light being projected only in the forward direction and therefore, light only enters through the primary visual axis (Maurice, 1957).

Maurice's theory (1957) was modified by Goldman and Benedek (1967) as the lattice theory could not explain the transparency of the dogfish cornea. Their findings centred on Bowman's layer, where a lack of fibril lattice-like arrangement scattered light less than the corneal stroma. It was deduced that transparency of Bowman's layer was a result of the regular interfibrillar spacing in distances that reached half the wavelength of light. As a result, it was elucidated that only a short-range order of collagen fibrils is a pre-requisite for the destructive interference of scattered light (Goldman and Benedek, 1967, Farrell and Hart, 1969).

Due to the nature of proteoglycan control of collagen fibrillogenesis, proteoglycans are fundamental to the development and maintenance of corneal transparency. Borcherding et al (1975) illustrated the differences between the concentrations of proteoglycans between the highly organised centre of the cornea and the opaque sclera. This finding is also compounded by the fact that an inability in humans to synthesize a mature keratan sulphate can result in the formation of corneal opacity (Hassell et al., 1980). Hassell et al (1980) also illustrated that keratan sulphate proteoglycans are uncommon in corneal scars, observing larger than normal interfibrillar spacing and a decrease in transparency that can be partially rectified by the re-introduction of keratan sulphate proteoglycans. Furthermore, it has also been indicated that stromal swelling can have a bearing on transparency due to the formation of water 'lakes' (Benedek, 1971), causing disruption in the regulation of collagen interfibrillar spacing (Goodfellow et al., 1978). Corneal opacity will occur if the 'lakes' containing no collagen reach or exceed half the wavelength of visible light (Benedek, 1971). As proteoglycans are involved in the attraction of counterions and the subsequent hydration of corneal tissue, any deficiency in proteoglycans can result in stromal hydration problems.

Both collagen fibril diameter and centre-to-centre fibril spacing are pivotal in the development of corneal transparency due to their scattering properties. Each collagen fibril, although they are the main scattering element within the cornea, is deemed to be ineffective at scattering light due to the narrow diameters they exhibit (McCally and Farrell, 1999). The size of the fibril diameter is much smaller than the wavelength of light (400-700nm) and if they were effective at scattering light the tissue would become opaque. At the early stages of development, both cornea and sclera are transparent and display relatively similar collagen diameters. Differences in fibril diameters between the tissues increases as the sclera tissue increasingly becomes more opaque (Smelser and Ozanics, 1959). The extent of fibrillar collagen within the cornea also requires destructive interference of scattered light in order to allow for transparency. Independent fibril scattering would result in a greater incidence of constructive interference (Freund et al., 1995) and subsequently defects in transparency. There is also the requirement to minimalise the size of the actual corneal tissue as the thickness dictates the amount of light scattering that occurs (Scott and Bosworth, 1990).

Farrell (1994) proposed a model which is currently the most widely accepted theory relating to corneal transparency. It states that corneal transparency at a given light incident wavelength, λ, relies on several factors that include fibril density packing, ρ, the diameter, a, of the collagen fibrils, the ratio, m, between the "ground substance", n_g, and collagen's refractive index, n_c, as well as the angle of scattered light, θ, and also the relative positions of fibrils to each other and the thickness of the cornea.

1.14 Stromal Hydration

The endothelial monolayer serves as a passage for nutrient uptake and waste removal in and out of the stroma whilst it also secretes fluid, counteracting the continuous leak of fluid into the stroma through ion transport (Bonanno, 2003). Maurice (1972) illustrated that the endothelium was responsible for 90% of the fluid transport into the rabbit cornea. Stromal polysaccharides, including keratan, dermatan and chondroitin sulphate, have several sulphate and carboxyl groups that are responsible for the binding of cations as well as hydration; the anionic glycosaminoglycan extensions are functionally important in stromal swelling due to their hydration properties (Hedbys et al., 1963). Enzymatic degradation of individual

glycosaminoglycans reduces the swelling pressure according to the glycosaminoglycan concentration (Maurice and Monroe, 1990).

Fluid uptake into the stroma occurs as a result of the ionic permeability of the endothelium as well as the presence of hydrophilic glycosaminoglycans responsible for the swelling pressure within the corneal stroma. Transendothelial transport results in the removal and uptake of ions to and from the aqueous humor. However, there is no net fluid intake into the stroma due to the active secretion and active counter-balance of fluid by action of the 'pump-leak' mechanism (Maurice and Giardini, 1951). The pump that forces fluid out of the stroma is also situated within the endothelium. The pump-leak mechanism, and essentially the endothelium, is therefore believed to modulate corneal hydration and the water balance between the aqueous humor and cornea.

Corneal thickness and transparency are both dependent on the regulation of corneal stroma hydration. A reduction in endothelial ion transport activity results in a loss of corneal transparency and impaired vision (Bonanno, 2003). Initially, it was postulated that the swelling pressure of the stroma was a result of the presence of excess ions in the aqueous humor (Maurice and Giardini, 1951). Maurice (1951) indicated that a difference in electrical potential, a result of excess ion transport across the endothelium, allows ions of the opposite charge (Na^+, K^+, Cl^- or HCO_3^-) to achieve electrochemical equilibrium across the endothelial cell layer. The epithelium is also involved in fluid transport through the cornea, absorbing nutrients from the tear fluid due to the avascular nature of the cornea. Klyce (1977) demonstrated that the epithelium can contribute to fluid transport when the Cl^- transport was stimulated by β-adrenergic agonists by way of increased cAMP.

1.14.1 Leak

Swelling pressure within a charged gel is created by ion imbalance, described by the Donnan effect. Hodson (1993) compounded earlier studies by establishing a relationship between the magnitude of the swelling pressure and charge density within the stroma over a range of hydration, a result of which was accounted for by the Donnan effect. The Donnan effect

describes the behaviour of charged particles which do not distribute evenly across a selectively permeable membrane. Hodson (1993) also found that the ratio of concentrations between Cl^- in the stromal tissue and the aqueous humor was different for Na^+ and added lactate, believed to be the result of an unknown ligand binding Cl^- transiently. The fixed charge density within stromal tissues can be attributed to the glycosaminoglycan chains of proteoglycans as well as the ion contribution. It has been found that glycosaminoglycan synthesis is according to the oxygen level within the tissue, a function of the thickness, varying from species to species (Scott and Bosworth, 1990).

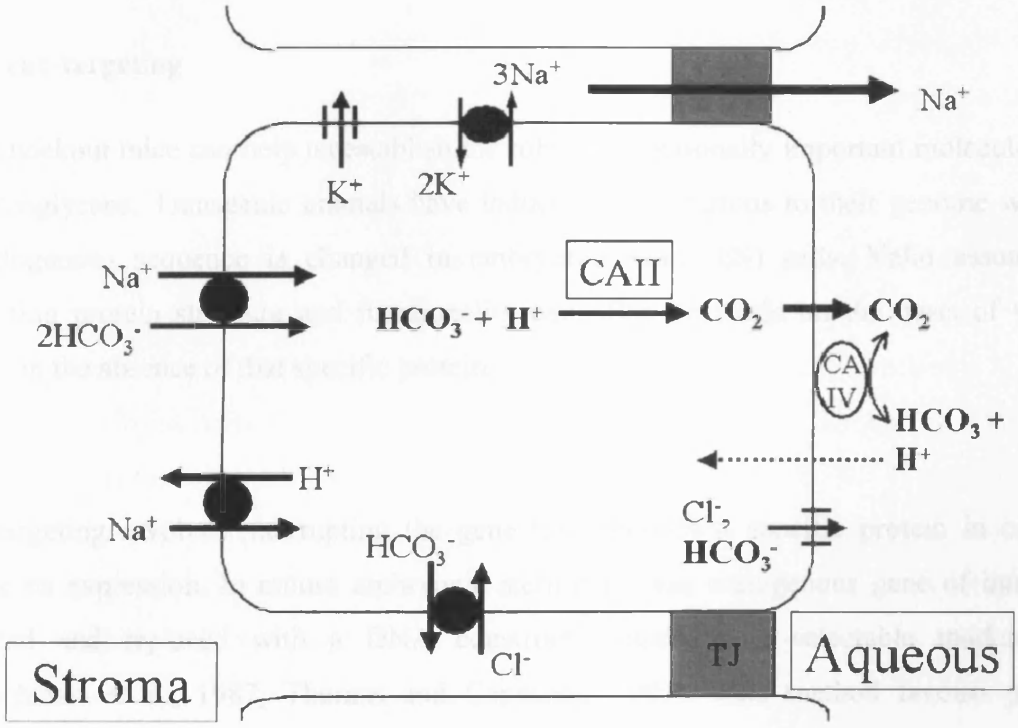

Fig 1.14 Schematic representation of transendothelial $HCO3^-$ transport (Taken from Bonanno, 2003).

1.14.2 Pump

Investigations into the endothelial pump have focused primarily on the role of the bicarbonate ion as the prime mover in fluid transport. Several studies (Doughty and Maurice, 1988, Kuang et al., 1990) measured the fluid transportation across endothelium - stromal preparations in the absence of high bicarbonate concentrations with significant results,

challenging the importance of the bicarbonate ion. However, Sanchez (2002) showed that fluid pumping is maintained by both bicarbonate transport and sodium recirculation through apical Na^+ channels. In order to control hydration and ultimately thickness of the tissue, it is believed that a set of receptors would be needed to control the active system, modulating endothelial pump activity and identifying the hydration levels of the tissue. No mechanism has been identified as of yet although several membrane proteins, such as adenosine and acetylcholine receptors (Walkenbach and Chao, 1985, Lind and Cavanagh, 1995) have been implicated in possible roles of cAMP regulation and stromal hydration control.

1.15 Gene-targeting

Gene knockout mice can help us establish the roles of functionally important molecules such as proteoglycans. Transgenic animals have induced modifications to their genome whereby an endogenous sequence is changed in embryonic stem (ES) cells. Valid assumptions concerning protein structure and functionality can often be made on the basis of what is evident in the absence of that specific protein.

Gene-targeting involves interrupting the gene that encodes a specific protein in order to remove its expression. In mouse embryonic stem cells, the endogenous gene of interest is disrupted and replaced with a DNA construct containing a selectable marker gene (Doetschman et al., 1987, Thomas and Capecchi, 1987). This method favours positive selection of transfected ES cells as the integrated gene is not transcribed.

DNA is introduced into ES cells by subjecting them to an electrical potential which disrupts the cell membrane – enabling exchange between cellular components and the culture that surrounds it. It is also necessary for the DNA construct to contain identical flanking target sequences as the endogenous gene so as to produce homologous recombination. The transfected cells are inserted into the uterus of a foster carrier and the offspring are mated in order to produce a homozygous breed of mouse.

1.15.1 Mice Proteoglycan Knockouts

Several studies have investigated the result of specific corneal proteoglycan-null mice, elucidating that collagen fibrillogenesis is affected with proteoglycan removal in most cases. Analysis into the collagen-proteoglycan association three-dimensionally in knockout mice may offer a valuable insight into the functionality of proteoglycans and whether any compensatory mechanisms occur in their absence. In the absence of components that form the 'shape module', induced by genetic manipulation, extracellular matrices do not form ordered tissue. Investigations into the organisation of corneal collagen in proteoglycan knockouts have been carried out extensively, although the interpretation of collagen order is mostly carried out via X-ray diffraction analysis. Using electron tomography as a visual tool we may be able to elucidate the role of proteoglycans in the collagen meshwork to a greater extent.

Chakravarti (1995) established the position of the gene encoding lumican and also developed lumican-deficient mice that exhibit a high degree of collagen disorder and corneal opacification as a direct result (1998). The 11kb gene encoding lumican localises to the same region as the decorin gene on distal mouse chromosome 10 (Iozzo and Murdoch, 1996) and so detection of decorin expression is necessary in order to evaluate whether or not the decorin gene has been disrupted in the process of lumican gene knockout. Lumican, similarly to keratocan, is encoded on a 6.5kb gene in mice whereby three exons are responsible for the transcription of the lumican mRNA.

Mimecan was initially isolated in truncated form from bovine bone (Madisen et al., 1990) and found to be part of the SLRP family of proteins. The single copy gene that encodes mimecan is situated on chromosome 9q22 in humans (Tasheva et al., 2002); transcription of the gene produces 8 mRNAs and its homology is conserved throughout mice, bovine and humans (Tasheva et al., 1997). The evolutionary conservation may serve as an indicator of mimecan's functional importance. Although it is currently unclear as to how mimecan exerts it biological function, it is suggested that mimecan plays a part in cellular growth control due to the ability for growth factors and cytokines to regulate its mRNA expression in corneal keratocytes (Long et al., 2000).

The gene encoding keratocan in mice spans 6.5kb of the genome and contains three exons and two introns (Liu et al., 1998). The second exon is responsible for encoding all ten of the leucine repeats. Keratocan has been found to be expressed more selectively than other SLRPs such as lumican, being transcribed almost solely within the cornea. Interestingly, keratocan mRNA can be found to be expressed within corneal keratocytes but not in sclera cells. Both keratocan and lumican genes found on the mouse distal chromosome 10 are deficient of a TATA box – an indication of how closely related they actually are (Ying et al., 1997).

The decorin gene exists at the 12q23 locus in humans. The high conservation of the decorin protein core when compared to homologous proteins in other species compounds the general assumption of the functional importance of this molecule. Decorin is found localised within many connective tissues other than the cornea and highly 'decorates' fibrils and is therefore seen as an important molecule for the order of the extracellular matrix. A mutation in the gene encoding decorin within humans, 12q22, causes congenital stromal dystrophies, indicative of decorin's role in stromal morphology (Bredrup et al., 2005).

1.16 Electron Tomography

The idea of using three-dimensional reconstructions for the elucidation of ultra-structural details at high-resolution was first described in 1968 (DeRosier and Klug, 1968). Electron tomography is a high resolution methodology for reconstructing the interior of an object from the two-dimensional projections collected at varying angles, rotated around a single or dual axis, using transmission electron microscopy. The electron beam within an electron microscope is fixed, and so the specimen holder is tilted around a single axis in order to create a tilt series. The projections are then collected from the specimen the micrograph images are then used to reconstruct the desired object in its entirety through a back-projection algorithm (Frank, 2006).

1.17 Aims and Objectives

The aim of this project is to achieve a greater understanding of the organisation of proteoglycans in the mouse corneal stroma and their role in collagen fibril assembly. A clearer comprehension of collagen-proteoglycan association and proteoglycan morphology will enable us to elucidate how proteoglycans regulate collagen fibril architecture in the corneal stroma extra-cellular matrix and therefore, understand more clearly how corneal transparency is achieved. Elucidating collagen-proteoglycan interactions in the wild-type mouse corneal stroma will provide a basis for interpreting the effects on collagen organisation in proteoglycan altered mouse corneas.

Specific aims:

- To visualise the organisation of proteoglycans in the wild-type mouse cornea three-dimensionally
- To understand the role of sulphation of proteoglycans and how it affects packing of proteoglycans
- To achieve a greater understanding of how proteoglycans regulate the uniform collagen architecture in the corneal stroma

Chapter 2 - Materials and Methods

2.1 Introduction

The methods detailed within this chapter were used to obtain three-dimensional reconstructions of collagen-proteoglycan associations in the mouse corneal stroma of wild-type and genetically manipulated mice. From the reconstructions, it is possible to ascertain proteoglycan dimensions as well as their three-dimensional conformations, allowing us to elucidate proteoglycan organisation in the mouse cornea. Digestion with specific glycosaminoglycan degrading enzymes reveals the identity of proteoglycans present in the different corneal specimens used. Utilising these techniques enabled a clear definition of specific proteoglycan organisation in the cornea, which provides a basis for the understanding of how proteoglycans regulate collagen fibril architecture. Image analysis was carried out using ImageJ, which allowed for the measurement of proteoglycan dimensions, fibril diameters and the calculation of radial distribution functions.

Both conventional electron microscopy and electron tomography was carried out on a JEOL 1010 transmission electron microscope operating at 80kV with a Gatan ORIUS SC1000 CCD camera attached.

The methodologies are subdivided into sample preparation and staining, enzyme digestion, transmission electron microscopy, image alignment and segmentation – the steps required for the generation of three-dimensional reconstructions.

2.2 Corneal Sample Collection and EM Preparation

Materials

0.05% Cuprolinic Blue (0.01g)
2.5% Glutaraldehyde (2ml)
25mM Sodium Acetate (20ml, pH5.7)
0.1M $MgCl_2$

Aq. 0.5% Sodium Tungstate
Ethanol (50%, 70%, 90%, 100%)

Mature, wild type (CD1 and C57BL/6) mice were obtained from Cardiff School of Biosciences, Cardiff University and their corneas were dissected in half to be fixed and stained accordingly. Eyes were removed within 5 minutes post-mortem after carbon dioxide anaesthesia and cervical dislocation. Animals were treated in accordance with the ARVO statement for the Use of Animals in Ophthalmic and Vision Research as well as local regulations at all times.

Chst5-null mice were bred and kindly provided by Professors Kohji Nishida (Osaka University) and Tomoya Akama (Sanford-Burnham Medical Research Institute). Lumican-null mice were collected from the lab of Dr. Shukti Chakravarti at Johns Hopkins School of Medicine, Baltimore and treated in exactly the same way as the wild-type mice detailed below.

In order to visualise the corneal proteoglycans, half mouse corneas were fixed for 24 hours in 2.5% glutaraldehyde in 25mM sodium acetate buffer (pH5.7) with 0.1M $MgCl_2$ and 0.05% Cuprolinic blue (Quinolinic phthalocyanate), a cationic dye for characterisation of proteoglycans (Scott and Haigh, 1988a). Glutaraldehyde was used to fix and preserve the tissue, helping to maintain the position and shape of the collagen and proteoglycan matrix. The samples were then rinsed three times with sodium acetate buffer (pH5.7) for ten minutes each and subjected to subsequent washes with aqueous 0.5% sodium tungstate, also for three ten minute periods. After rinsing, the samples were dehydrated using 50% ethanolic tungstate (0.5%) initially, followed by 15 minute washes in an incremental ethanol series (70%, 90%, 100%). Ethanolic tungstate was used to increase the electron density of Cuprolinic blue and, in turn, enhance the contrast of proteoglycan-dye complexes in electron microscopy.

Cuprolinic blue is an electron dense cationic dye which has a high affinity for the highly negative charge component of proteoglycans; the glycosaminoglycan side chain. The electron density of the stain is attributed to the presence of a Cu^+ ion. The corneal samples were

subject to a critical electrolyte concentration staining method (Scott and Haigh, 1988a) which allows us to visualise the proteoglycans as electron dense elongated, filament-like shapes. $MgCl_2$, a negatively charged salt, is also used to inhibit Cuprolinic blue staining on certain polyanions. The concentration we shall use is 0.1M $MgCl_2$, which is the concentration required for the prevention of Cuprolinic blue staining of a given polyanion, notably carboxylates (COO^-), phosphate esters (PO_4^-) and sulphate esters (SO_4^-) as they are prevalent within the cornea.

Cupromeronic blue, another cationic dye for staining of proteoglycans, was used in order to compare and contrast the two dyes performance and whether or not any proteoglycans were left unstained in either treatment. Initial analysis alluded to the fact that both dyes exert similar properties and stain glycosaminoglycan chains as effectively as each other; any differences were negligible. Although the critical electrolyte concentration ($MgCl_2$) was altered to 0.3M according to Scott (1988a).

2.2.1 Enzyme Digestion

Materials

Chondroitinase ABC (2.5U/ml)
Keratanase II (1U/ml)
1% Paraformaldehyde
Tris/sodium acetate buffer (pH 8)

To reveal the specific identity of proteoglycans in various corneal specimens, glycosaminoglycan-degrading enzymes were used; namely chondroitinase ABC (from *Proteus Vulgaris*) and keratanase II (isolated from *Bacillus sp.*). Chondroitinase ABC cleaves chondroitin sulphate/dermatan sulphate proteoglycans and, in mouse corneas, removes the majority of proteoglycans, whereas Keratanase II is responsible for targeting keratan sulphate associated proteoglycans (Young et al., 2005). Chondroitinase ABC cuts the β1-4 N-acetylhexosaminidic link to either D-glucuronic acid and L-iduronic acid, however keratanase II cleaves the β1-3 glucosaminidic linkages to galactose of keratan sulphate

glycosaminoglycans where the disaccharide sequence may be mono- or di-sulphated (Quantock et al., 2010).

As the proteoglycan population of the wild-type and *Chst5*-null mouse corneal stroma was deduced via enzyme digestion by Young and colleagues (2005) and Hayashida et al (2006) respectively, only lumican-null corneas required enzyme treatment to determine the nature of proteoglycans observed in electron microscopy. Excised corneas were dissected in quarters and prefixed with 1% paraformaldehyde to be washed with 1U/ml tris/sodium acetate buffer (pH 8), with one cornea to remain in the buffer as a control. Chondroitin sulphate/dermatan sulphate proteoglycans were removed initially, whereby one cornea was incubated in 2.5 U/ml chondroitinase ABC (Sigma Aldrich) for 4h at 37°C, whereas Keratan sulphate associated proteoglycans were degraded by treating another cornea with 1 U/ml keratanase, also for 4h at 37°C. To remove both types of proteoglycans, a combination of both enzymes was used and subject to the same temperature and duration. Samples were then fixed and proteoglycan-stained with Cuprolinic blue to be embedded for electron microscopy as detailed in *2.2.2*.

2.2.2 Resin Embedding

Materials

Propylene Oxide
Araldite Monomer CY212
DDSA Hardener
BDMA Accelerator

After the initial fixation and staining of glycosaminoglycan chains, the samples were exposed to a series of dehydration steps in 70%, 90% and 100% ethanol. An intermediate treatment of Propylene oxide (PO_2) and 100% ethanol for 15 minutes was used prior to two treatments of only PO_2 for 15 minute intervals to ensure dehydration. Samples were then put into a mixture of 50% araldite resin and PO_2 for an hour before a 100% araldite resin treatment, also for an hour period. The specimens were then transferred to another araldite resin treatment where

they were left for 12 hours being rotated gently. The araldite monomer and hardener are required to be pre-warmed in order to facilitate the easy, fluid measuring and pouring of araldite. The corneal samples were then inserted into moulds containing fresh araldite which was allowed to polymerise and form embedding moulds at 60°C for 48 hours. Polymerised blocks containing the half mouse corneas were then sufficiently hardened for glass knife sectioning.

2.2.3 Polyetherimide Support Films

Materials

Ethylene Dichloride (1,2 – Dicholoroethane) solution
Polyetherimide granules
Microscope Slides
Water Bath
Detergent
EM slot grids (2mm x 1mm)
Coplin Jar

Support films were made using 0.38% polyetherimide (PEI) in ethylene dichloride solution. 0.76g of PEI granules were dissolved in 200ml of ethylene dichloride and left to stand for approximately 72 hours. Microscope slides, wiped with detergent to ensure a clean side and also to coat a hydrophobic layer, were dipped into coplin jars containing PEI solution for approximately 20 seconds and then left to dry within the fume hood. After being left to dry in a desiccated area, the slides coated with PEI were scored along each edge with a razor-blade forming a rectangle and drawn off in a water bath. Grids (TAAB 2mm x 1mm slot) were placed shiny side up on the floating film which was then attached to another slide coated with PEI. The slides covered with grids were then left to dry for a few hours and lifted off gently with forceps.

2.3 Sectioning

Materials

Reichart-Jung Ultracut Microtome
Leica EMKMR2 Glass-cutter
Glass
De-ionised Water
Chloroform

Araldite resin embedded mouse corneal specimens were sectioned using glass knives on a Reichart-Jung Ultracut ultra-microtome and attached to the PEI film which was suspended in a 2mm x 1mm slot of a 3.05mm copper grid. Glass knives were obtained by using a Leica EMKMR2 glass cutter (Leica, Austria). Knives were tilted at 6° for cutting and sections were carefully cut using areas of the knife that did not appear to be serrated due to stress fracture occurrence when knives were created. Tape was carefully put from edge to edge at the top of the knife and sealed with wax to create a small water bath that allowed sections to be collected upon slicing with the knife. De-ionised water was pippetted into the bath and sections collected were placed onto the support film slot of the grids. Sections cut on the Reichart ultra-microtome approximately 90nm thick and gold in colour were lifted onto the PEI coated grids after being stretched out with chloroform. Initially, semi-thin (500nm) sections were obtained and transferred to a microscope slide using a single hair. The semi-thin sections were stained with toluidine blue which allowed us to check under the light microscope whether the tissue was adequate for visualisation using the electron microscope.

2.3.1 Section Staining and Gold Fiducial Markers

Materials

2% Uranyl Acetate
1% Phospho-tungstate Acid
10nm Colloidal Gold

For the contrast enhancement and definition of collagen fibrils within the sections cut, 2% uranyl acetate (UA) and phospho-tungstic acid (PTA) were used as negative stains. Gold fiducials work as markers for the plane in which the specimen is lying when applying the computer analysis part of electron tomography. Fiducials also enable the tracking of the specific region desired when proceeding with each individual tilt in the series. As we were expecting to work at magnifications of approximately x20k-x30k, 10nm diameter fiducials were the most appropriate gold markers to use.

To coat the grids with the staining solutions, droplets of UA, PTA and distilled water (x4 for each stain) were aligned on top of parafilm-covered distilled water, large enough for the grids to sit on top. Grids were placed face down and left for 2 minutes in PTA, 2 minutes each on four drops of distilled water, followed by 12 minutes in UA and a further 2 minutes each on four more droplets of distilled water.

After the staining treatments, grids were dipped into water approximately 30 times and then a steady flow of water was streamed onto the grid to wash any excess stain. The grids were then left to dry where they were then subject to gold fiducial staining in order to create the three-dimensional reconstructions. Similar to the UA, PTA staining technique, gold fiducial solution was pippetted into small (10μL) droplets onto water-covered parafilm. The grids were then placed face-down onto a single droplet for 20 seconds and then placed on a new droplet, face-up for a further 20 seconds. Once dried, the sections on the PEI support film grids were ready to be analysed using TEM.

2.4 Electron Microscopy and Electron Tomography

Transmission electron microscopy (TEM) is a powerful imaging tool that allows the user to visualise macromolecular organisation both inside and outside the cell, two-dimensionally. The first electron microscope was built in 1931 by Ernst Ruska and Max Knoll and although it was not capable of the high resolutions we can achieve today, it laid the foundations for the field of electron microscopy. Electron microscopy, as the name suggests, uses a highly charged beam of electrons to illustrate the composition of the specimen that is to be

investigated. The electron beam is focused onto the specimen and the resulting image is projected using a charge-coupled device (CCD) camera according to the scattering of electrons. Electrons are used as opposed to light as they are known to have a much shorter wavelength. The *de Broglie* wavelength of an electron is much smaller than that of a photon of light and this allows the electron microscope to achieve much higher resolutions than a light/confocal microscope.

The electron microscope is composed of magnetic lenses and metal apertures that are necessary for the focusing and restriction of the size of the beam. An electron source is used which creates a beam of monochromatic electrons that is accelerated by a positive electric potential. The electrons transmitted penetrate the specimen, illuminating a phosphorescent screen/CCD camera that depicts the content of the sample. However, TEM only permits two-dimensional illustration of a sample and so we must use the goniometer attached to the microscope to create a tilt series from a number of pictures taken at incremental degrees in order to create a three-dimensional reconstruction.

Electron tomography is a high resolution methodology for reconstructing the interior of an object from the projections collected using electron microscopy. The electron beam within an electron microscope is fixed, and so the specimen holder is tilted around a single axis, by one degree increments, in order to create a tilt series. The series of tilts is aligned into a stack and subjected to back-projection in order to generate a three-dimensional reconstruction (Frank, 2006). Electron tomography enables the assembly of a reconstruction of detailed three-dimensional structures whereby the electron microscope collects the initial two-dimensional data. The electron beam is passed through the sample at incremental degrees of rotation around the centre of the sample. The resolution of electron microscopes is at the nanoscopic scale and therefore, supra-molecular organisation and multi-protein structures, such as collagen, can be examined and reconstructed three-dimensionally.

2.4.1 Radial Distribution Functions

The extent of collagen fibril order in the corneal stroma may be calculated through examining radial distribution functions of their cross-sectional profiles in electron micrographs. Initially, a single reference fibril is selected and the interfibrillar distances of surrounding fibrils in a square region of interest are measured using ImageJ. Measurements are based on the pixel size of each image, which is 0.33nm per pixel for an image captured at 20kx magnification. A frequency plot of these interfibrillar distances with respect to the reference is determined through in-house software and is normalised to account for the number of fibrils that diminishes as the distance from the reference increases. Each fibril is then used as a reference and then all frequency plots are summed together in turn. The radial distribution function describes the order of lateral distribution of collagen fibrils and whether order exists past neighbouring fibrils and indicates what organisation of fibrils is required for corneal transparency. However, electron microscopy preparation, including fixation and staining, may affect the native fibril characteristics such as diameter and interfibrillar spacing. For more accurate measurements, x-ray diffraction offers precise insights into fibril organisation of the cornea.

Radial distribution functions for human (Freund et al., 1995), rabbit (Connon et al., 2003, Freund et al., 1995) and chick (Connon et al., 2004) corneas all suggest a short range ordering of collagen fibrils in the corneal stroma. Interfibrillar distances are maintained with considerable uniformity between neighbouring fibrils and so a prominent first peak is expected to indicate a distinct probability of two fibrils being in close proximity of between 40-60nm. Each distribution function appears to be defined by a second, less prominent peak suggesting that order exists, although, it does not appreciably extend past next-nearest neighbours at approximately 90nm. As a perfect lattice is not required, these radial distributions imply that short range ordering of fibrils in the stroma is enough to fulfill the requirements for the tissue's transparency

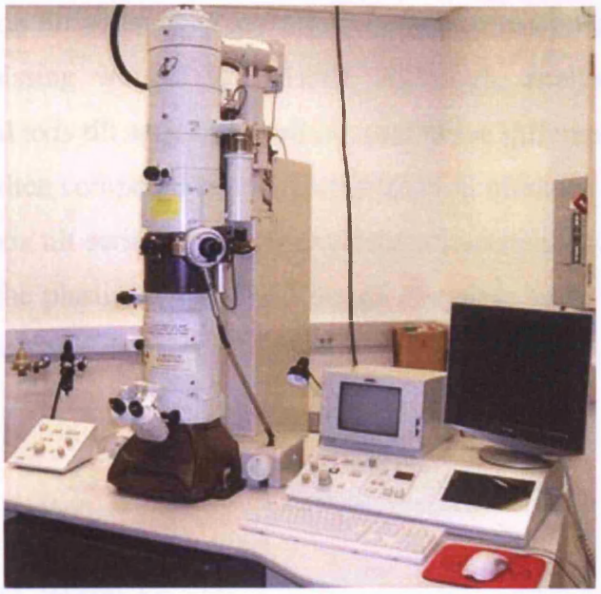

Fig 2.1 Jeol 1010 Electron Microscope

2.4.2 Tilt Series

Using the goniometer, we were able to create a tilt series of images from – 60° to + 60° rotation of the specimen. In order to be able to create the series, the axis of the sample is required to be aligned and centred so that the increments are at proportional degrees. Due to the fact that the electron beam is obstructed by the specimen holder after 60°, we are unable to reconstruct the full volume in its entirety. This experimental restriction is known as the 'missing wedge' and occurs as a direct result of not being able to tilt the specimen a full 180°. At every degree increment, we are required to return the image to the same position to that which is seen in the previous micrograph captured a degree before. This is achieved by marking a contour around a fiducial or group of fiducials that can be easily traced and returning the contour to its original position after every increment. Modern microscopes are capable of automated tomography, whereby tracking of the specimen and subsequent capturing of micrographs at each increment is completely automated; sections are preserved to a greater extent as they experience a lower dose of radiation due to the speed of automation.

Collection of a Dual axis tilt series data set offers improved resolution in the reconstruction as the size of the 'missing wedge' is reduced. Although, analysis of a reconstruction generated through a dual axis tilt series showed no qualitative differences in the ultrastructure of the corneal stroma when compared with a reconstruction obtained from a single axis data set. Therefore, single axis tilt series were collected for all specimens as there is significantly reduced irradiation of the plastic section, and image file sizes were also greatly minimised and much more manageable on desktop computer systems.

2.4.3 Alignment of Tilt Series

Once the 121 micrograph images are obtained, they are required to be converted from TIFF images into a .mrc file extension and also into an image stack with the file extension .st. The .st file extension is created as the eTOMO alignment program requires files of this type. The file conversions are carried out using the programs tif2mrc and newstack, respectively. Tif2mrc and newstack are programs within the IMOD software package. IMOD is a set of image processing, modelling and display programs that enable tomographic reconstruction of an object. IMOD is an open source program that is developed by the Boulder Laboratory for 3D electron microscopy of cells at Colorado University (Kremer et al., 1996). The end .st file is then inputted into the eTOMO program, a sub-program of IMOD.

The eTOMO program within IMOD enables the user to input their stack of images and through a series of alignment steps, a final tomogram is generated. The images are subject to coarse/fine alignment and tomogram positioning which results in the final tomogram that can also be post-processed within eTOMO. Alignment is computed through the tracking of fiducial markers and so the even distribution of fiducials in the specimen is paramount to acheiving a good alignment of images that is not skewed in any way. Once coarse alignment is calculated, fine alignment is computed through an iterative process and then tomogram positioning is processed by analysing sample tomograms. When the final stack is aligned, the eTOMO program generates a final tomogram which is a three-dimensional reconstruction of the initial two-dimensional micrograph. When creating the final tomogram, eTOMO uses back-projection to effectively 'smear' the aligned images onto each other to create a

reconstruction that allows the user to penetrate through the three-dimensional stack of images.

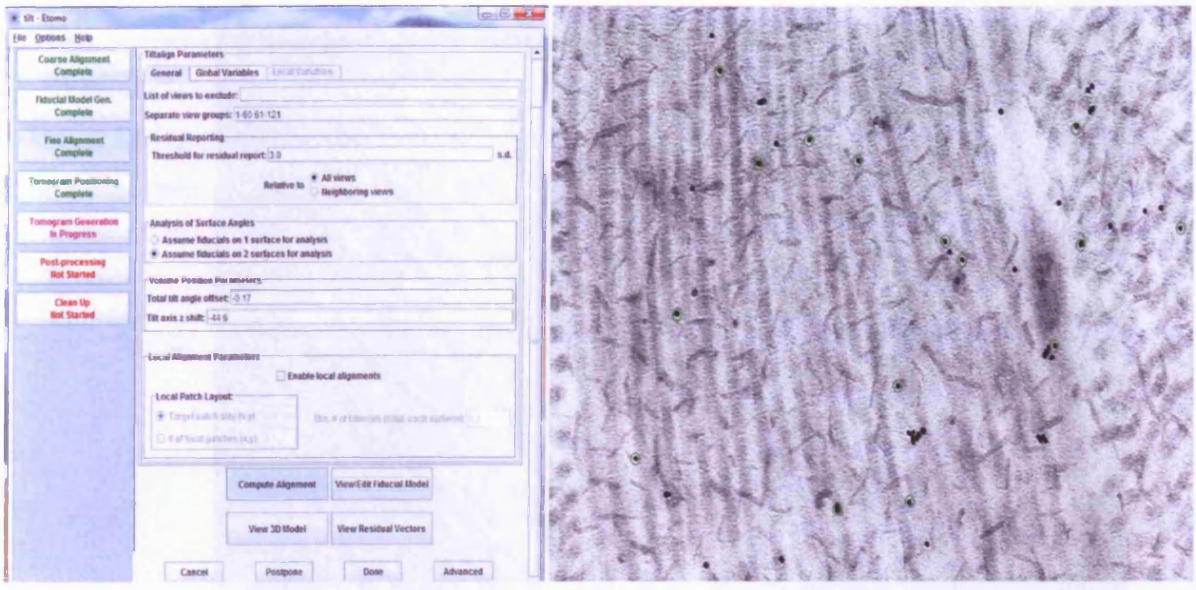

Fig 2.2. Screenshot of eTOMO program illustrating the fine alignment stage and the 0° micrograph with contours around fiducials for alignment.

2.4.4 Segmentation of Three-Dimensional Reconstruction

The final tomogram is a stack of images that represents the three-dimensional conformation of the object in question. The tomogram, similar to a micrograph, is greyscale format and by nature, it is difficult to interpret. In order to make the tomogram more meaningful and easier to analyse, we draw on each individual image in the stack in the segmentation process.

Segmentation of the wild type mouse cornea was carried out using EM3D, a software program for electron microscope tomography developed at Stanford University, USA (Ress et al., 2004). It is also possible to create a reconstruction in EM3D from the alignment calculated in eTOMO. The EM3D program requires contours to be selected around an object to be segmented manually. Once each image has been segmented, the image is rendered and a model of the object can be visualised in its entirety. Segmentation and modelling allows us to

analyse a much more meaningful image that can be interpreted and manipulated with greater ease than a two-dimensional greyscale image or tomogram.

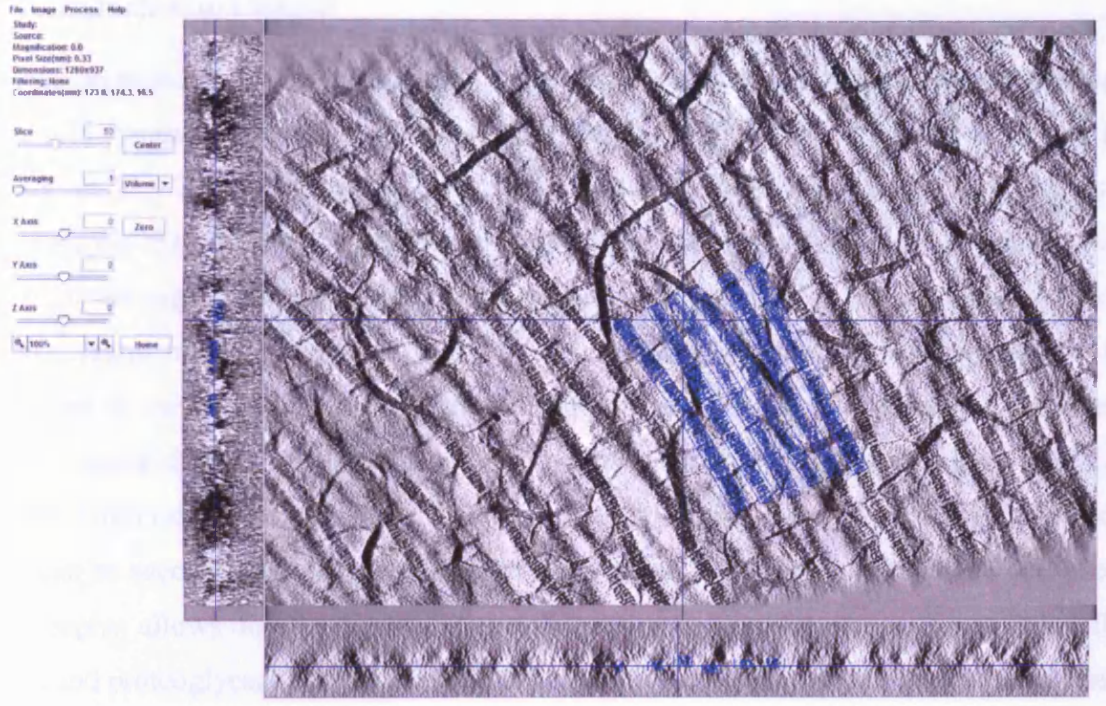

Fig 2.3. Screenshot of the EM3D program and the segmentation process. Three-dimensional reconstruction of the posterior region of the *Chst5*-null mouse corneal stroma.

2.4.5 Measurement of Proteoglycan Dimensions

Proteoglycan dimensions have previously been measured from conventional two-dimensional micrographs (Scott, 1992, Muller et al., 2004), which may be erroneous due to the fact that they may have been cropped or could be running obliquely through the section. It is possible to bypass these inaccuracies by consulting the three-dimensional reconstruction and determining which proteoglycans are wholly contained within the section and are suitable for measurement. Measurements are carried out using ImageJ after calibration using the characteristic collagen fibril D-period (approximately 65nm) and are based on an individual pixel size of 0.33nm from an image of 20kx magnification.

Chapter Three - Three-Dimensional Reconstruction of Collagen-Proteoglycan Interactions in the Mouse Corneal Stromal by Electron Tomography

3.1 Introduction to Chapter

Models proposed to describe the precise arrangement of proteoglycans in the cornea suggest a six-fold symmetrical order around collagen fibrils (Maurice, 1962, Farrell and Hart, 1969, Muller et al., 2004). Structural observations made from conventional two-dimensional micrographs may be misleading however, as they do not offer a true representation of proteoglycan organisation in three-dimensions. Moreover, recent evidence has suggested that proteoglycans in the mouse cornea vary in morphology and are undersulphated when compared to other mammalian corneas (Young et al., 2005). It is therefore necessary to obtain a more detailed understanding of proteoglycan morphology and organisation in the wild-type mouse corneas, so that observations made when studying proteoglycan-knockout mice can be successfully interpreted, and in some cases, related to a human disorder. Electron tomography allows for the internal three-dimensional reconstruction of corneal collagen fibrils and proteoglycans at a high resolution, offering potential new insights into the complex matrix assembly of the corneal stroma. Therefore, three-dimensional reconstructions of the anterior, mid and posterior mouse corneal stroma were obtained to re-evaluate the proteoglycan arrangement in the wild-type mouse cornea. Image analysis from electron micrographs verified with three-dimensional reconstruction data also enables the evaluation of proteoglycan and collagen fibril characteristics in the mouse corneal stroma.

In this chapter, methods used to obtain three-dimensional reconstructions of collagen-proteoglycan interactions in the cornea are detailed and used as a platform to suggest potential mechanisms of fibril control exerted by the proteoglycans.

3.2 Introduction

The relatively small diameters of collagen fibrils and their uniform interfibrillar spacing in the stroma are essential to the physical basis of corneal transparency. This is exemplified by the remarkable regularity of corneal collagen fibril diameter across a wide range of species

(Craig and Parry, 1981, Craig et al., 1986). As discussed in Chapter One, type V collagen limits lateral aggregation of collagen (Birk et al., 1990) and can therefore govern fibril diameter, as can proteoglycans with or without their glycosaminoglycan chains (Rada et al., 1993). However, how proteoglycans regulate the uniform interfibrillar spacing is less well understood. New evidence suggests that a systematic six-fold arrangement of proteoglycans is not present, and it is postulated that the proteoglycans govern interfibrillar spacing through a combination of thermal motion and a control of osmotic pressure instead (Lewis et al., 2010, Knupp et al., 2009). Elucidation of proteoglycan organisation in the mouse corneal stroma may help to compound these studies.

It is also possible to determine the spatial distribution of fibrils in the corneal stroma by calculating their radial distribution function from electron micrographs, as has been done for human (Connon et al., 2003) and rabbit corneas (Connon et al., 2000). Short-range order of neighbouring fibrils has been shown to correspond with the onset of transparency and proper formation of the developing avian cornea (Connon et al., 2004), and by determining the radial distribution function for fibrils in the mouse corneal stroma, it is possible to ascertain whether order extends beyond next-nearest neighbours.

The mouse corneal stroma extracellular matrix differs from other mammalian corneas as its proteoglycans are distinctly undersulphated, and a significant proportion of its chondroitin sulphate/dermatan sulphate is present as dermatan sulphate (~60% (Scott and Bosworth, 1990)). It also has the highest ratio of iduronate:glucuronate disaccharides within dermatan sulphate (Scott and Bosworth, 1990). Moreover, only 18% of the total glycosaminoglycan content within the mouse corneal stroma is present as keratan sulphate (Scott and Bosworth, 1990), significantly lower than in the thicker corneas of larger mammals, where keratan sulphate associated proteoglycans are the predominant type. In the mouse cornea, production of chondroitin sulphate/dermatan sulphate is likely to be preferentially facilitated by the availability of oxygen by diffusion from the atmosphere into the thin mouse corneal stroma (Stockwell and Scott, 1965).

For this investigation, we utilised three-dimensional reconstructions of the mouse cornea in order to gain a better understanding of collagen-proteoglycan organisation in the stroma. From structural information revealed through electron tomography we suggest mechanisms through which the organisation of collagen architecture and regulation of interfibrillar spacing by proteoglycans might be maintained.

3.3 Materials and Methods

3.3.1 Specimen Collection

Mature, wild type CD1 mice were obtained from breeding colonies at the School of Biosciences, Cardiff University, and eyes removed within 5 minutes post-mortem after carbon dioxide asphyxiation and cervical dislocation. Corneas were immediately excised for fixation and staining and animals were handled in accordance with the ARVO Statement for the Use of Animals in Ophthalmic and Vision Research and local regulations at all times.

3.3.2 Specimen Preparation

Corneas were cut into halves with a scalpel and fixed for 24 hours in 2.5% glutaraldehyde in 25mM sodium acetate buffer (pH5.7) with 0.1M $MgCl_2$ and 0.05% Cuprolinic blue (Quinolinic phthalocyanate), a cationic dye for characterisation of proteoglycans (Scott, 1972). Cuprolinic blue complexes with the glycosaminoglycan chains of proteoglycans owing to the presence of negatively charged sulphate and carboxylate residues. After fixation and staining, the samples were washed with sodium acetate buffer followed by aqueous, then 50% ethanolic, sodium tungstate at 0.5%. The samples were dehydrated using an incremental ethanol series and embedded in Araldite resin. 90nm sections (gold interference) were cut using glass knives and collected on copper slot grids coated with a support film made using 0.38% polyetherimide (PEI) in ethylene dichloride solution. Sections were contrasted with saturated aqueous uranyl acetate solution and 1% aqueous phosphotungstic acid. Finally, grids were exposed to a solution of 10nm colloidal gold (BBI, Cardiff, UK) to provide gold particles on each face of the slot grid as fiducial markers to be used in the image alignment process.

3.3.3 Electron Tomography

Collagen lamellae in each stromal region were imaged via a tilt series ranging from -60° to +60° captured at a magnification of x20k, in one degree increments, using a Gatan ORIUS SC1000 CCD camera linked to a JEOL 1010 transmission electron microscope operating at 80kV. The images captured were then aligned using the IMOD software package (Kremer et al., 1996). Once the images had been carefully aligned according to the positions of individual gold marker fiducials, back-projection and tomogram generation was carried out using the EM3D program (Ress et al., 2004). Segmentation of the three-dimensional reconstruction was also carried out using EM3D.

3.3.4 Radial Distribution Function

The spatial distribution of collagen fibrils in the mouse cornea was assessed by determining the radial distribution function of fibrils (n= 11201) throughout the stroma (Cox et al., 1970). A collagen fibril is selected as a reference and the center-to-center distances of the surrounding fibrils are measured using ImageJ (Abramoff, 2004). The frequency plot of the distances of neighbouring fibrils with respect to the reference fibril is then obtained using in-house software. This plot is normalised to account for the fact that the number of fibrils per unit area diminishes as the distance from the reference fibril increases. All fibrils are then utilised in turn, and all frequency plots are summed together in order to improve statistics. Because of the way it is constructed, the radial distribution function describes the lateral packing of collagen fibrils and indicates whether long and/or short-range order exists within a system (Eikenberry et al., 1982).

3.3.5 Measurement of Collagen Fibril and Proteoglycan Dimensions

Measurements of collagen fibril and proteoglycan dimensions were carried out using ImageJ software after internal calibration using the collagen D-period (~65nm in cornea). For the measurement of fibril diameters, 142 collagen fibrils were used. The measurement of proteoglycan length and thickness was limited to those proteoglycans entirely contained within a plastic section (n=50), as shown by their three-dimensional reconstruction.

3.4 Results

Electron micrographs of the central corneal region showed two prominent populations of Cuprolinic blue-positive proteoglycans and regular collagen fibril order in the anterior (fibril diameters: 30.8 ± 1.9nm), mid (fibril diameters: 32.0 ± 2.8nm) and posterior (fibril diameters: 28.9 ± 1.7nm) mouse corneal stroma (fig. 3.1). In between the collagen fibrils, small filament-like structures were numerous (arrows in fig. 3.1), as were larger, curved, electron-dense complexes (arrowheads in fig. 3.1). These results confirm what was seen in previous electron microscopy investigations of the mouse cornea in two dimensions (Scott and Haigh, 1988b, Young et al., 2005, Hayashida et al., 2006).

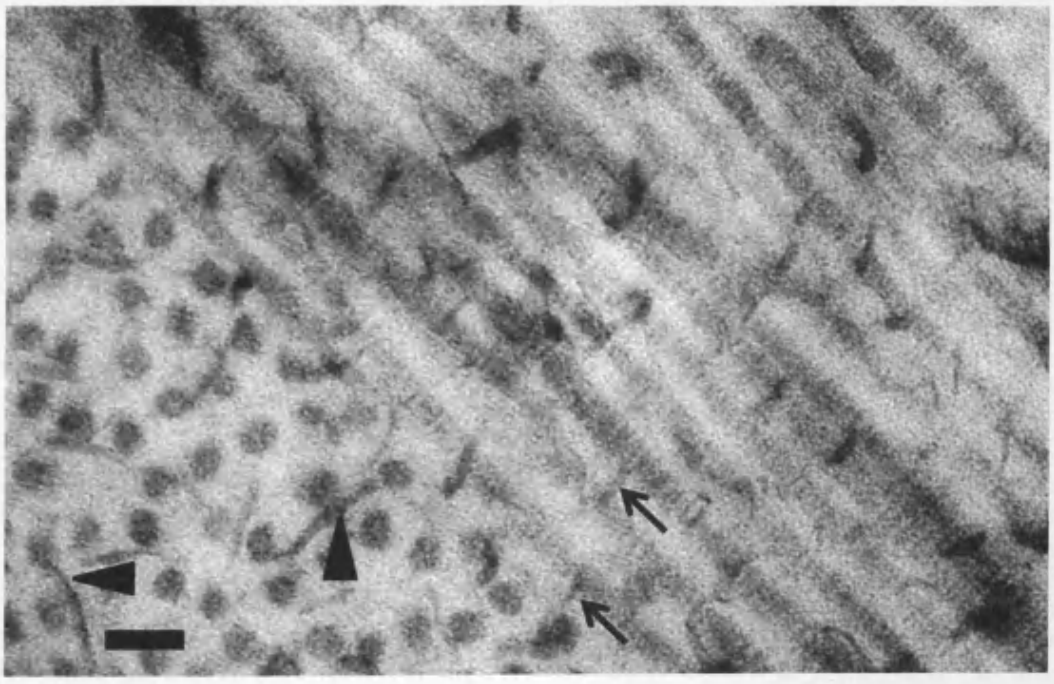

Figure 3.1. Ultrastructure of the mouse corneal stroma. Two proteoglycan populations are evident in the micrograph. Small, poorly contrasted proteoglycans (arrows) are frequently positioned orthogonally whereas the larger, electron-dense complexes (arrowheads) exhibit sinuous profiles. Scale bar = 100nm

Three-dimensional reconstructions of collagen fibrils and associated proteoglycans in longitudinal and transverse sections in the anterior, mid and posterior stroma in the central, prepupillary region of the wild-type mouse cornea were obtained (fig. 3.2). The reconstructions of each stromal region showed similar collagen fibril organisation, in which

fibrils were of a regular average diameter throughout the stroma and the interfibrillar spacing between fibrils was consistently uniform. No distinct structural differences in proteoglycan content, at the resolution obtained, were observed in the reconstructions of the anterior, mid, or posterior stroma and the distribution of proteoglycan types was also relatively similar.

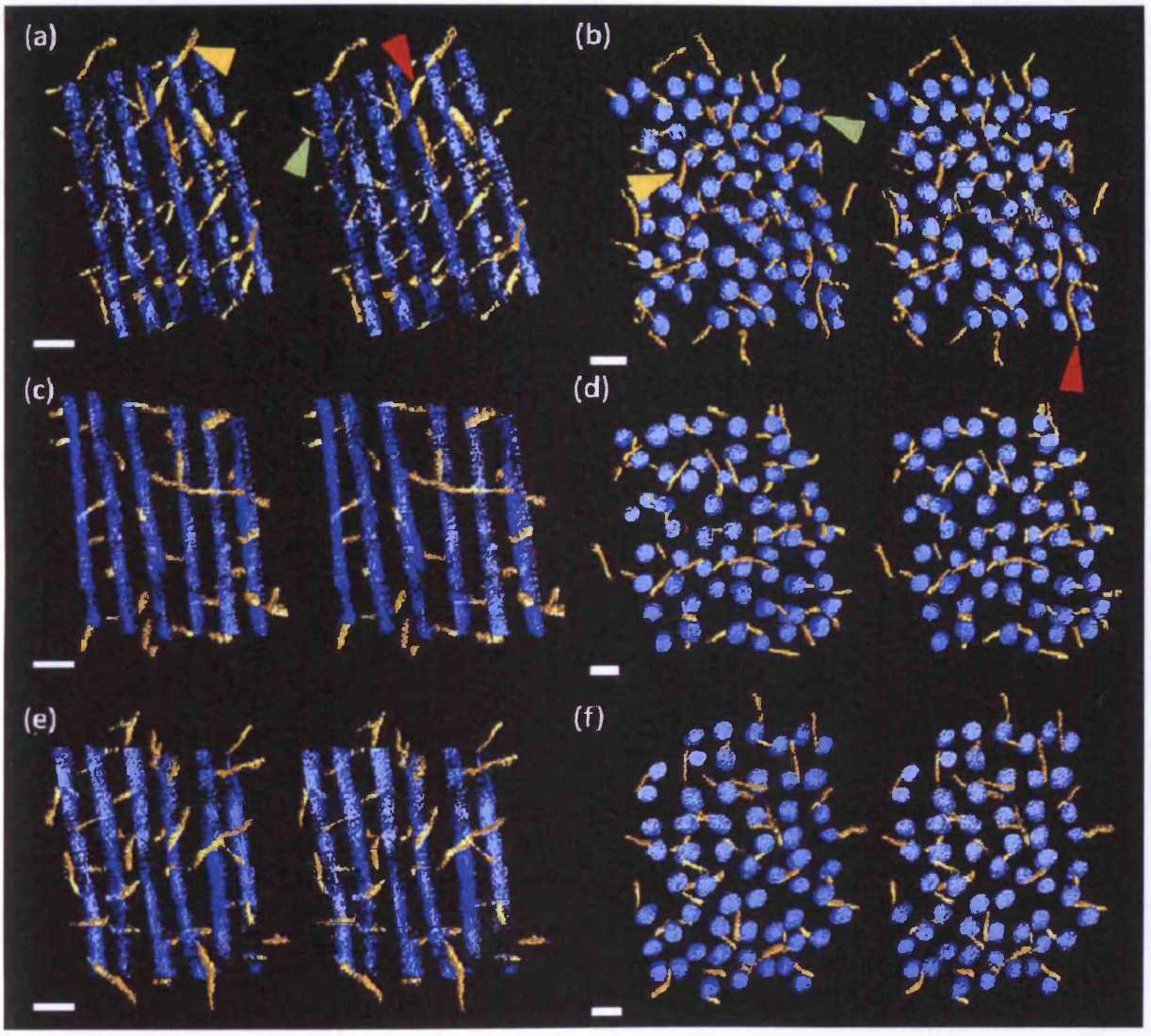

Figure 3.2. Three-dimensional reconstructions of proteoglycan and collagen fibril organisation within the anterior (a and b), mid (c and d) and posterior (e and f) stroma of the mouse cornea. Stereo-pairs of segmented tomographic reconstructions in both (a, c, e) longitudinal and (b, d, e) transverse views. Proteoglycans are yellow in colour and collagen fibrils are coloured blue. Small proteoglycans are depicted by green arrowheads; intermediate proteoglycans are pointed out by orange arrowheads whereas the largest proteoglycans are marked by red arrowheads. Scale bar = 50nm

A scatter plot of proteoglycan length versus thickness revealed three morphologically distinct populations throughout the corneal stroma (fig. 3.3). Small proteoglycans (31.4 ± 3.5nm in length measured over the three regions; green arrowheads in figs. 3.2(a) and 3.2(b)) were seen interconnecting only neighbouring fibrils, and were frequently positioned orthogonal to the fibril. Lengths were approximately equivalent to the surface separation of collagen fibrils. Larger proteoglycans varied in thickness, had sinuous profiles and were of two distinct lengths; intermediate sized proteoglycans (64.5 ± 3.9nm long; orange arrowheads in figs. 3.2(a) and 3.2(b)) usually interconnected two fibrils, but sometimes could be seen to run alongside a collagen fibril, whereas the largest proteoglycans linked three fibrils (122.5 ± 9.8nm long; red arrowheads in figs. 3.2(a) and 3.2(b)) and were seen less frequently than the other types.

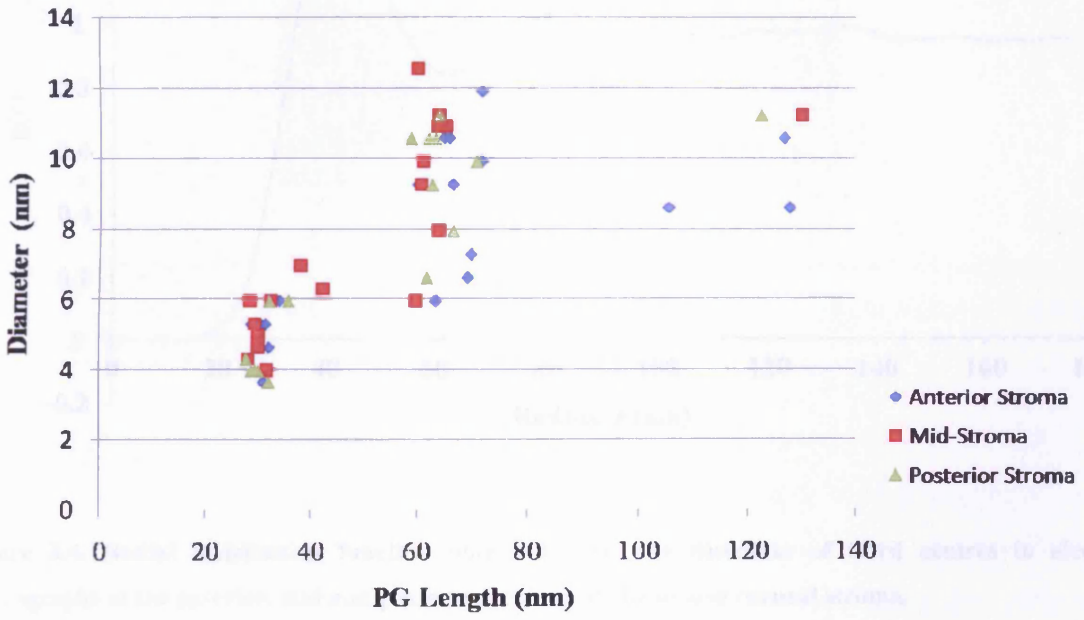

Figure 3.3. Scatter plot of proteoglycan length versus thickness in the anterior, mid and posterior stroma of the mouse cornea. Proteoglycan measurements are restricted to the proteoglycans that display a complete structure within the reconstruction. Small proteoglycans = 5.0 ± 1.0nm (thickness in diameter); 31.4 ± 3.5nm (length). Intermediate proteoglycans = 9.5 ± 1.9nm (thickness in diameter); 64.5 ± 3.9nm (length). Largest proteoglycans = 10.4 ± 1.3nm (thickness in diameter); 122.5 ± 9.8nm (length).

The radial distribution function in *figure 3.4* shows that localised, short-range order exists in the mouse corneal stroma, whereas long-range order beyond next-nearest neighbours is not apparent. The function g(r) indicates the probability of locating two fibril centres by a distance *r*. Nearest neighbour separation is illustrated by a prominent first peak at a ~44nm distance and a more diffuse, less prominent second peak at ~90nm suggests that next-nearest fibrils show some slight positional regularity. Beyond the second peak, there is little appreciable evidence of positional order between fibrils.

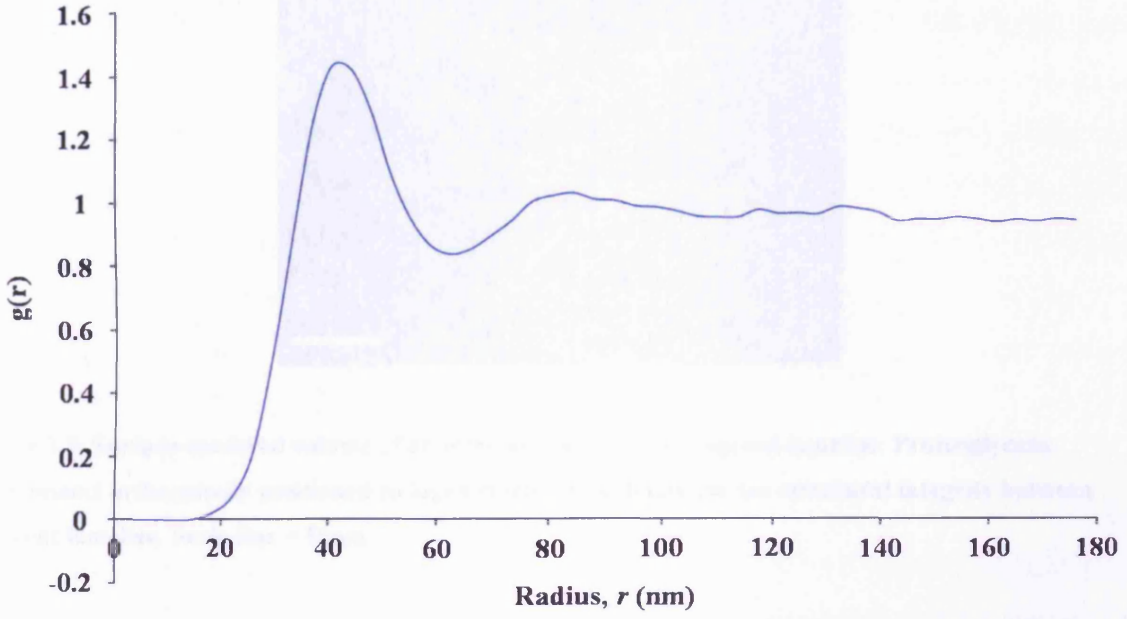

Figure 3.4. Radial distribution function obtained from the distances of fibril centres in electron-micrographs of the anterior, mid and posterior regions of the mouse corneal stroma.

Reconstruction of an interface between two orthogonal lamellae (Fig. 3.5) reveals the proteoglycan organisation at the junction between fibrils positioned perpendicular to each other in the mouse corneal stroma. Again, the proteoglycans appear to have no pre-defined orientation or symmetry in their organisation. Proteoglycans interconnect neighbouring orthogonally positioned fibrils, which is likely to provide a robust enough attachment to prevent slippage of lamella whilst allowing the transport of nutrients and water through the tissue.

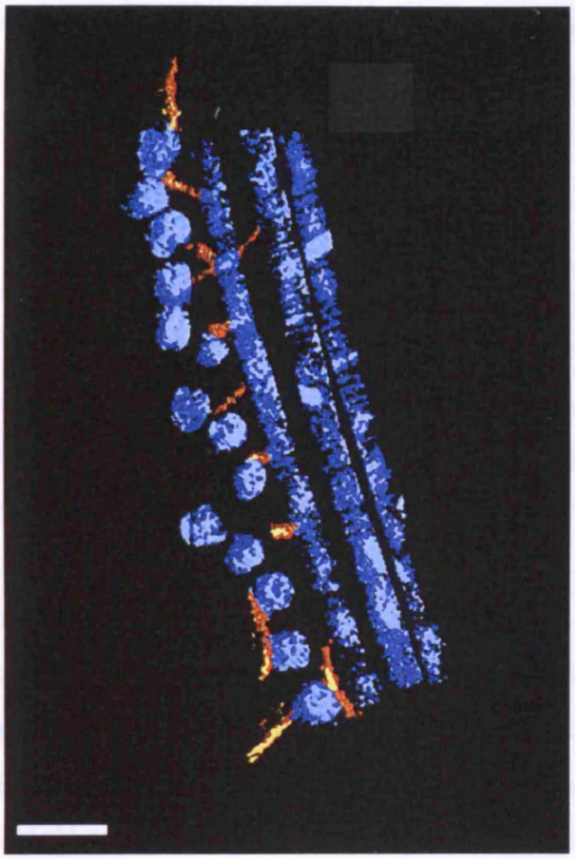

Figure 3.5. Surface-rendered volume of an interface between orthogonal lamellae. Proteoglycans interconnect orthogonally positioned collagen fibrils, most likely for the structural integrity between adjacent lamellae. Scale Bar = 50nm

In the reconstructions, proteoglycans showed no specific symmetrical arrangement around collagen fibrils, neither within lamellae or at the interface between two orthogonally positioned collagen fibrils (see figure 3.5). Neighbouring fibrils were frequently connected at near-regular axial distances, primarily by the small proteoglycans with up to three collagen fibrils often inter-connected by the largest proteoglycans.

3.5 Discussion

Our reconstructions provide an insight into the interactions between the structural components of the mouse corneal stroma, illustrating the highly organised collagen fibril architecture and the less well organised three-dimensional arrangement of proteoglycans. A complex, almost random relationship between proteoglycans and collagen is observed, in

which adjacent and next-nearest neighbour collagen fibrils are connected by proteoglycans which ultimately are likely to hold the fibril pseudo-lattice arrangement in a three-dimensional matrix.

When interpreting the results presented here, particular attention should be paid to the fact that mouse cornea contains considerable amounts of low-sulphated or unsulphated keratan sulphate (Scott and Bosworth, 1990, Young et al., 2005). Thus, not all keratan sulphate associated proteoglycans may be observed owing to the lower affinity of undersulphated proteoglycans for the cationic Cuprolinic blue dye. Chondroitinase ABC digestion of mouse cornea, which cleaves chondroitin sulphate/dermatan sulphate associated glycosaminoglycans, reveals a low population of small, poorly-contrasted filamentous structures considered to be keratan sulphate (Young et al., 2005, Hayashida et al., 2006). Keratan sulphate proteoglycans are observed bridging neighbouring fibrils at regular, frequently orthogonal intervals. Chondroitin sulphate/dermatan sulphate proteoglycans on the other hand interconnect neighbours and also next-nearest neighbours, and in some cases lie along the fibril axis.

To accurately determine the morphometry of proteoglycans in mouse cornea, the dimensions of proteoglycans which were wholly contained within the plastic section were measured. The variation in length of chondroitin sulphate/dermatan sulphate proteoglycans suggests a possible end-to-end aggregation (figs 3.5 and 3.6). There are numerous potential mechanisms that may make this possible, for example, hydrophobic attraction and hydrogen bonding could enable the highly anionic glycosaminoglycans to associate (Scott, 2001), whilst positive ions (i.e. Na^+, K^+) drawn into the stroma could screen negative charges and negate the chains' mutual repulsion. An increase in ionic strength has been shown to disrupt aggregation of proteoglycans (Roughley et al., 1995), thus ionic balance might be important for self-association. Ionic strength changes have also shown both changes in corneal stromal transparency and in the order of collagen fibrils (Regini et al., 2004) The observed differences in thickness of our stained proteoglycan filaments (fig. 4) could be accounted for by variations in sulphation, resulting in a greater accumulation of Cuprolinic blue stain. However, the relative size of Cuprolinic blue (<0.5nm) and tungstate ions used for staining of

proteoglycans is probably insufficient to account for the observed differences in glycan chain thicknesses (Scott, 1992). This gives rise to the possibility that in mouse corneas chondroitin sulphate/dermatan sulphate proteoglycans aggregate laterally in the form of tetramers or polymers. Lateral aggregation of proteoglycans may be facilitated by adjacent protein cores contributing their glycosaminoglycan chains to form complementary, anti-parallel multimers through the attractive forces described previously (fig. 3.6). The lateral association of several proteoglycans would confer enhanced structural integrity, and it is also possible that they may exist in helical conformations, similar to the structure of hyaluronan (Arnott et al., 1983). Multiple aggregations of this type would be able to account for the overall thickness of proteoglycans. The observed variation in proteoglycan thickness thus suggests a higher potential for self-association such that different phases of aggregation are evident. In addition, such a property could accommodate an ability of proteoglycans to readily dissociate and re-aggregate to enable fibril flexibility. This flexibility would allow for the passive movement of water and nutrients through the tissue. In addition to lateral associations of proteoglycans, it appears that end-to-end linear associations also occur, so that proteoglycans can bridge more than two adjacent fibrils. The proposed end-to-end accretion of chondroitin sulphate/dermatan sulphate may be facilitated by the dimerisation of decorin (Scott et al., 2004), the chondroitin sulphate/dermatan sulphate-containing protein core. Decorin dimerisation allows chondroitin sulphate/dermatan sulphate proteoglycans to have two opposing glycosaminoglycan extensions each of which may connect neighbouring fibrils by association of proteoglycans substituted with only a single glycosaminoglycan chain (fig. 3.6). Dimerisation of decorin could potentially result in an overlapping end-to-end system extending over many fibrils, although in mouse cornea bridges of only three fibrils were most frequent. The dimerisation of decorin in solution is not universally accepted, however (Goldoni et al., 2004).

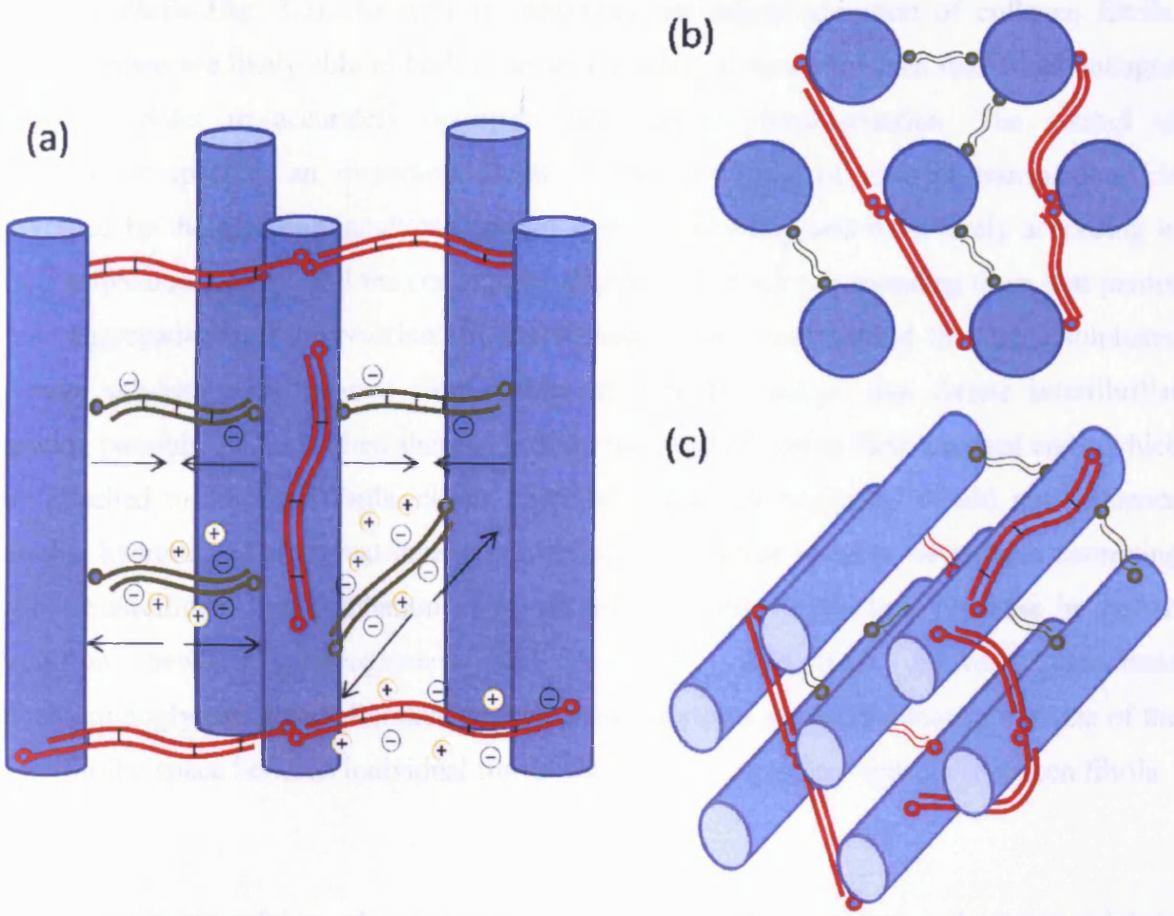

Figure 3.5. Models of proteoglycan and collagen fibril organisation in the mouse cornea. Keratan sulphate proteoglycans are illustrated in green and chondroitin/dermatan sulphate proteoglycans are represented in red. (a) Proteoglycans are shown exerting opposite forces to control the spatial characterisation of collagen fibrils according to the charges that surround them and their thermal motion. (b and c) The azimuthal disorder of proteoglycans is represented, reflecting the three-dimensional reconstructions. Proteoglycans interact with each other through hydrophobic and hydrogen bonding attraction with their respective glycosaminoglycan side-chains, countering the mutual repulsion created by sulphate and carboxylate residues that are positioned on the repeating disaccharides. Also, negative charges may be screened by positive ions limiting repulsive forces, or from salt bridges. Chondroitin/dermatan sulphate proteoglycans have longer glycosaminoglycan chains, aggregate further and occupy a larger volume of space than the smaller keratan sulphate proteoglycans.

To explain the uniformity of interfibrillar distances, we propose a three-dimensional model for the mouse corneal stroma, similar to that proposed for bovine cornea (Lewis et al., 2010, Knupp et al., 2009) in which two equal but opposite forces are exerted simultaneously on the

collagen fibrils (fig. 3.5). As well as inhibiting the lateral accretion of collagen fibrils, proteoglycans are likely able to both contract and expand space between individual collagen fibrils in order to accurately optimise their spatial characterisation. The control of interfibrillar spacing, an important factor in the formation of corneal transparency, is governed by the glycosaminoglycan components of proteoglycans most likely according to their sulphation patterns and the consequent electrostatic forces surrounding them that permit their aggregation and dissociation. In the mouse cornea, we contend that undersulphated keratan sulphate proteoglycans form stable interfibrillar bridges that dictate interfibrillar spacing possibly thanks to their thermal motion that tends to bring their terminal ends, which are attached to adjacent fibrils, closer together. These proteoglycans would not influence stromal hydration to any great extent, conferring mechanical stability whilst also restricting osmotic swelling. Undersulphation of glycosaminoglycans results in a decrease in mutual repulsion between proteoglycans and a stable interaction between associated glycosaminoglycans arises. Keratan sulphate proteoglycans are approximately the size of the interfibrillar space between individual fibrils and so they can act as 'spacers' between fibrils.

Large chondroitin sulphate glycosaminoglycans, where 60% is present as dermatan sulphate in mouse (Scott and Bosworth, 1990), may also control interfibrillar spacing through stabilising more than two adjacent fibrils, forming multimers and regulating the swelling pressure of the tissue through their sulphate residues. These proteoglycans, specifically in the mouse cornea, are likely to contribute to the expansion of interfibrillar spacing to a greater extent. In fact, chondroitin sulphate contains more disaccharide motifs than keratan sulphate (Plaas et al., 2001), and therefore has more potential sites for sulphation and a higher proportion of hydrophobic regions. We hypothesise that undersulphated proteoglycans, or proteoglycans with more hydrophobic regions 'pull in' fibrils to restrict, stabilise and tether interfibrillar spacing through their interactions. Conversely, highly sulphated proteoglycans capable of attracting counterions 'push out' fibrils through an influx of water because of the Donnan effect (Elliott and Hodson, , 1998) (Fig. 3.5). Thus, proteoglycans govern the intake of water and ions from outside the tissue to control interfibrillar spacing and the overall thickness of the tissue, and are interchangeable when oxygen may not be readily available.

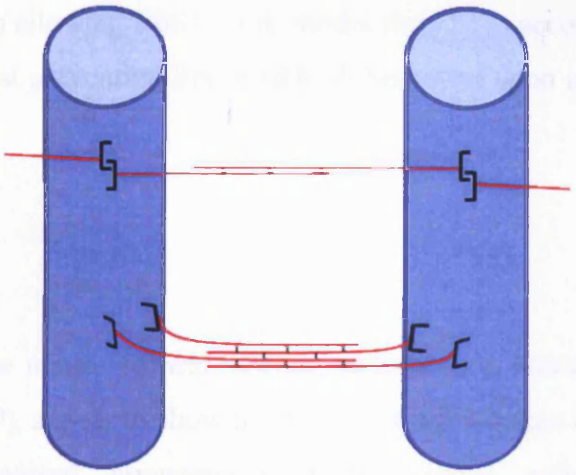

Figure 3.6. Proposed modes of aggregation of proteoglycans. The dimerisation of decorin (black) allows the end-to-end aggregation of chondroitin/dermatan sulphate (red) proteoglycans forming an elongated proteoglycan able to attach three fibrils. Also, proteoglycans may bind to adjacent binding sites and form multiple aggregates, possibly tetramers, with proteoglycans on a neighbouring fibril.

Collagen fibrils within the mouse cornea have a defined range of nearest neighbour separation as confirmed by the radial distribution function, although order does not appreciably extend beyond next-nearest neighbours (fig. 3.4). The regularity of collagen fibril diameter, coupled with the short-range order the fibrils exhibit, is essential for mutual interference of light entering the cornea (Cox et al., 1970). Light rays impinging on collagen fibrils are scattered in all directions and if the collagen fibrils in the cornea are of equal diameter, the scattered light from each fibril will have equal intensity and wavelength. If the separation between adjacent fibrils is less than half the wavelength of the light rays, the rays scattered from all fibrils will interfere destructively in all but the forward direction so that light entering the cornea will pass through unaffected (see Hart and Farrell, 1969, Cox et al., 1970 for a detailed explanation). However, if the collagen fibrils have different diameters, as is the case in the white sclera of the eye, this is no longer the case and the scattered rays will interfere destructively, making the cornea opaque. The degree of corneal opacity depends on the degree of collagen fibril inhomogeneity, where small variations will cause only a small degree of opacity. Proteoglycans do not show, and being weak scatterers do not need to show, the same co-ordinated arrangement as collagen fibrils in order to guarantee transparency. The cornea, we propose, is a flexible, adaptive system in which proteoglycans adopt different,

reversible conformations allowing fibrils to re-model slightly to accommodate the passage of water and nutrients whilst preventing irreversible deformation upon impact injury and loss of transparency.

3.6 Conclusion

Proteoglycans within the mouse corneal stroma, like those in bovine cornea (Lewis et al., 2010, Knupp et al., 2009), appear to show no specific order whereas collagen fibrils maintain a regular pseudo-hexagonal arrangement. Both keratan sulphate and chondroitin sulphate/dermatan sulphate are likely to utilise their electrostatic charges and self-aggregation as a means to govern and optimise the spatial distribution of collagen fibrils. We consider that proteoglycans possibly form tetramers and in some cases extend end-to-end which allows them to adopt different conformations and connect more than two fibrils. This arrangement of proteoglycans is likely to be paramount to the transparency, flexibility and resilience of the cornea. Ongoing studies of mouse strains with genetic alterations in proteoglycans and/or glycosaminoglycans will allow us to test these conclusions more fully.

Chapter Four - Electron Tomography reveals multiple packing of chondroitin sulphate/dermatan sulphate proteoglycans in Chst5-null mouse corneas.

4.1 Introduction to chapter

To gain a more precise understanding of proteoglycan function, their native structure, and how they are intricately assembled and packed in the corneal stroma, requires elucidation. Earlier investigation by Fransson and colleagues (Fransson, 1976, Fransson and Coster, 1979) showed, through affinity chromatography, that glycosaminoglycans are able to self-associate even though they are highly anionic in nature. Scott (2001) elaborated on this study, postulating that glycosaminoglycan self-aggregation was analogous to DNA, in that hydrophobic and hydrogen bonding counter-acts the expected mutual repulsion so that complexes may be formed. As indicated in the previous chapter, mouse corneal proteoglycans exhibit much larger thicknesses than which may be accounted for by the cationic stain coating and the width of an individual glycan chain, and so further analysis is required to determine how proteoglycans pack in the mouse cornea.

In order to understand more about the structure of proteoglycans and their aggregation mechanisms in the cornea, three-dimensional reconstructions of collagen-proteoglycan interactions in the anterior, mid and posterior stroma from a *Chst5* knockout mouse, which lacks a keratan sulphate sulphotransferase, were obtained. The disruption in transfer of sulphate groups to keratan sulphate appears to affect the morphology of proteoglycans and their significantly increased size is suggestive of increased self-association (Hayashida et al., 2006). Therefore, high resolution three-dimensional reconstruction of the proteoglycans inherent in the *Chst5*-null mouse may shed light on how proteoglycans aggregate and maintain the ordered fibril assembly in the cornea. From this, we suggest possible mechanisms as to how sulphation differences may lead to this increase in aggregation of proteoglycans in the *Chst5*-null mouse corneal stroma and how this relates to proteoglycan packing in healthy corneas.

4.2 Introduction

In humans, the gene *CHST6* is responsible for encoding the N-acetylglucosamine 6-O sulphotransferase enzyme, and its mutation has been implicated in macular corneal dystrophy - a disease which causes abnormal collagen fibril assembly and corneal opacity, coupled with oversulphation of chondroitin sulphate/dermatan sulphate proteoglycans (Nakazawa et al., 1984, Meek et al., 1989, Akama et al., 2000, Plaas et al., 2001). In mice, the N-acteylglucosamine 6-O sulphotransferase enzyme is encoded by the gene named *Chst5*. Mice with mutated *Chst5* exhibit no detectable sulphated keratan sulphate as well as altered chondroitin sulphate/dermatan sulphate proteoglycan morphology compared to the wild-type, even though corneal transparency remains unaffected (Hayashida et al., 2006).

From Chapter Three we have seen that chondroitin sulphate/dermatan sulphate proteoglycans interact with up to three adjacent fibrils in the mouse cornea and exhibit a variety of morphologies which suggest different modes of self-association. The aggregation of chondroitin sulphate/dermatan sulphate proteoglycans was initially demonstrated through gel chromatography (Fransson, 1976, Fransson and Coster, 1979) and then rotary-shadowing electron microscopy (Ward et al., 1987, Scott et al., 1992). Later evidence suggested that complementary, anti-parallel disaccharide chains may counter the expected mutual repulsion owing to sulphation and unbalanced charge distribution by hydrophobic and/or hydrogen bonding (Scott, 2001), as well as, possibly, through the formation of saline bonds via counter-ions present in the extra-cellular matrix. These aggregation mechanisms are likely to be influenced by the arrangement of disaccharides in the glycosaminoglycan chains; frequently alternating, iduronate-rich sequences being more prone to association (Fransson and Coster, 1979). Although corneal proteoglycan self-association *in situ* has been postulated, little is known about the influence sulphation has on glycosaminoglycan aggregation potential and the manner in which proteoglycans pack, as well as how this influences proteoglycan properties and the regulation of collagen fibril architecture in the corneal stroma.

This investigation utilised electron tomography techniques to visualise the interactions between collagen and proteoglycans in the cornea of *Chst5*-null mice. From the three-dimensional conformations of proteoglycans, we postulate mechanisms as to how

proteoglycans may aggregate and interact with each other in the *Chst5*-null mouse. It is hoped that this will help to throw light on how proteoglycans, in healthy corneas, associate and regulate fibril organisation and in turn, corneal transparency.

4.3 Materials and Methods

4.3.1 Specimen preparation

3-month old, wild-type C57BL/6 and homozygous *Chst5*-null mice were obtained and corneas were excised within 5 min post-mortem. Animals were handled in accordance with the ARVO Statement for the Use of Animals in Ophthalmic and Vision Research and local regulations at all times. Half corneas from a mouse of each genotype were fixed in 2.5% glutaraldehyde in 25 mM sodium acetate (pH 5.7) with 0.05% Cupromeronic blue dye (wt/vol). Cupromeronic blue stains sulphated proteoglycans owing to fixed anionic charges on both the sulphate and carboxylate residues present on the glycosaminoglycan extension (Scott, 1972). The dye was included in the glutaraldehyde fixative in a critical electrolyte concentration method, competing with $MgCl_2$ at either 0.1M or 0.3M. Qualitatively, no obvious difference was seen between these two preparative regimes. Corneal samples were then washed with sodium acetate buffer followed by immersion in sodium tungstate at 0.5% to increase the contrast of proteoglycan complexes. Dehydration was carried out by washes in an incremental ethanol series (70 - 100%) followed by embedding in Araldite resin.

4.3.2 Electron Tomography

Araldite-embedded corneal tissue was cut into 100 nanometre sections, gold in colour, which were then stained with 1% aqueous phosphotungstic acid and saturated uranyl acetate for 2 minutes and 12 minutes respectively, with washes in-between and after. Colloidal gold (10nm - BBI, Cardiff, UK) solution was then added to each face of the section, which was supported on a 0.38% polyetherimide film-coated grid. For electron tomography, a -60° to +60° single axis tilt series of collagen and proteoglycans was captured, in one degree increments, in the anterior, mid and posterior corneal stroma using a JEOL 1010 transmission electron microscope (80kv) attached to a Gatan ORIUS SC1000 CCD camera at 20k magnification. Both longitudinal and transverse sections, in each stromal zone, were reconstructed and

segmented for a full three-dimensional insight into proteoglycan-collagen interactions (n=6). These images, at a pixel size of 0.33nm, were then aligned according to the position of the gold fiducial markers on each image using the IMOD software package (Kremer et al., 1996). Backprojection of the aligned tilt series to generate the final tomograms, and their subsequent segmentation, was carried out using the EM3D program (Ress et al., 2004).

4.3.3 Measurement of Proteoglycan Dimensions

All measurements were made using ImageJ software after internal calibration with the diameter of gold fiducial markers (10nm). Proteoglycans were measured selectively according to their orientation; only those wholly contained within the three-dimensional reconstruction and lying in the plane of the plastic section were analysed (n=52). For calculation of the average distance between neighbouring quasi-orthogonal branches, n=15.

4.4 Results

Cupromeronic blue-enhanced electron microscopy of the *Chst5*-null mouse cornea discloses proteoglycans with altered morphologies with respect to the C57BL/6 wild-type mouse cornea. The proteoglycans in the mutant cornea appear variably elongated (Fig. 4.1(b), black arrow) and are more electron-dense than the proteoglycans apparent in the wild-type (Fig. 4.1(a), white and black arrowhead). Cross-section of an oversized *Chst5*-null proteoglycan reveals off-shoots around the periphery of the main proteoglycan body (Fig. 4.1(b), white arrow) and reconstructions also point to a spindle-like appearance (Fig 4.1(c)).

Segmented tomographic volumes of the wild-type C57BL/6 corneal stroma show organised collagen fibrils with uniform diameter and distribution, embedded in a matrix of interfibrillar proteoglycans (Fig. 4.2). A non-specific arrangement of proteoglycans is evident, and although fibrils are often interconnected at near regular axial distances, there appears to be no symmetrical order of proteoglycans around any collagen fibrils. Proteoglycans also appear to vary in morphology; small interfibrillar proteoglycans (Fig. 4.2(a and c), red arrowhead), as well as more sinuous types (Fig. 4.2(a and d), green arrowhead), are able to interconnect two

adjacent fibrils. Three fibrils may also be connected by elongated proteoglycans (Fig. 4.2(a and e), white arrowhead), although less frequently.

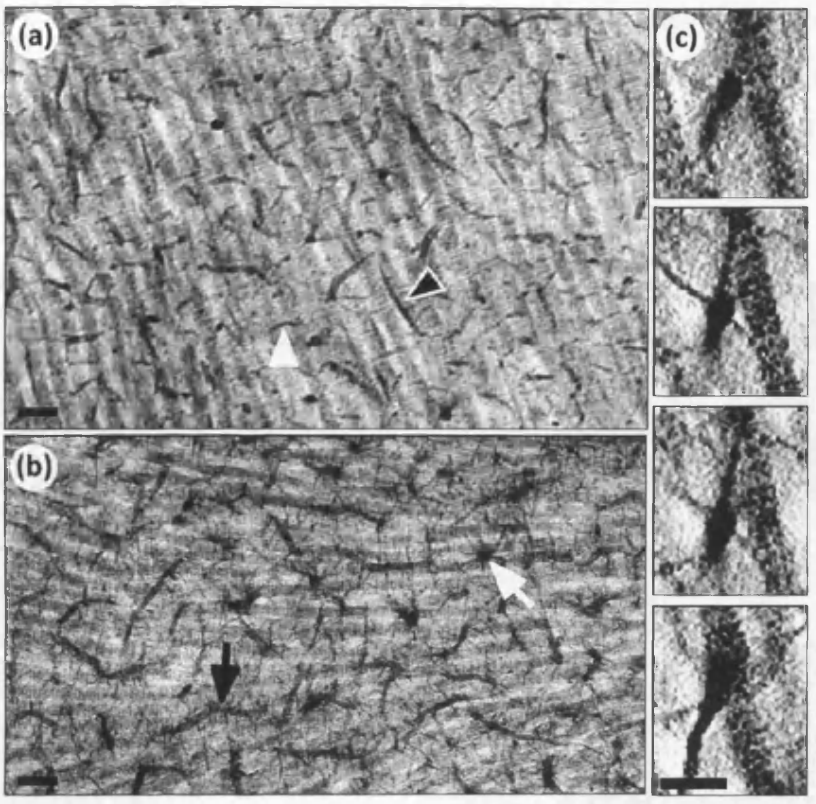

Fig. 4.1. Electron micrographs of the corneal stroma of (a) C57BL/6 and (b) *Chst*5-null mice with collagen fibrils running in longitudinal section. Large (black arrowhead) and small (white arrowhead) proteoglycan filaments are evident in wild-type sections (a). Previous enzyme digestion (Hayashida et al., 2006, Young et al., 2005) revealed that small collagen-associated filaments were keratan sulphate and the larger ones are of the chondroitin sulphate/dermatan sulphate type. In the *Chst*5 mutant (b), enlarged chondroitinase ABC-susceptible filaments are branched, giving them a "caterpillar-like" morphology in longitudinal section (black arrow) and a star-shaped appearance with proteoglycans around the circumference in both cross-section (white arrow), and successive slices through the reconstruction (c). Scale bars = 100nm ((a) and (b)); 50nm ((c)).

Previous investigation has shown that *Chst*5-null mouse corneas retain transparency despite a marginal decrease in interfibrillar spacing (Hayashida et al., 2006). When compared to the non-mutated mouse cornea, many proteoglycans in the *Chst*5-null mouse cornea appear grossly enlarged both in thickness and length, and near-periodic, orthogonal off-shoots are also evident, as shown by the three-dimensional reconstructions and segmented volumes (Fig.

4.3, purple arrowhead and Figs. 4.3(g - j), white arrowheads). These branched proteoglycans are significantly longer and thicker, to variable extents (up to 450nm in length, 29nm in thickness; Fig. 4.4), than both the unbranched types seen in the *Chst5*-null mouse cornea (71 ± 17nm (length), 9 ± 2nm (thickness); Fig. 4.4) and any of the proteoglycans prevalent in the wild-type mouse cornea (Parfitt et al., 2010 - (Chapter Three)). However, there are unbranched proteoglycans similar in morphology and dimensions to the largest proteoglycans observed in the wild-type corneas (Fig. 4.3(c), green arrowhead; Fig. 4.4).

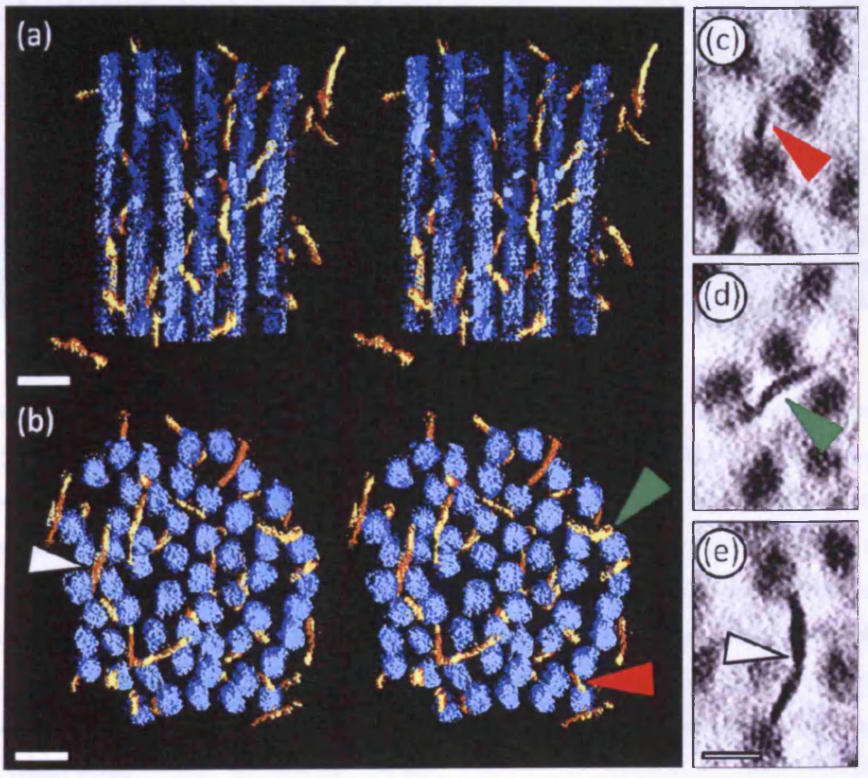

Fig. 4.2. Segmented reconstruction volumes of collagen and proteoglycans in the C57BL/6 wild-type mouse corneal stroma. Stereo-pairs of surface-rendered volume in (a) longitudinal and (b) transverse section whereby proteoglycans are coloured yellow and collagen fibrils are blue. In the segmented volumes (a and b) and reconstructions (c,d,e), proteoglycans adopt a non-symmetrical organisation and are able to connect neighbouring fibrils (red and green arrowheads) and, in some cases, next-nearest neighbours (white arrowheads). Scale bars = 50nm

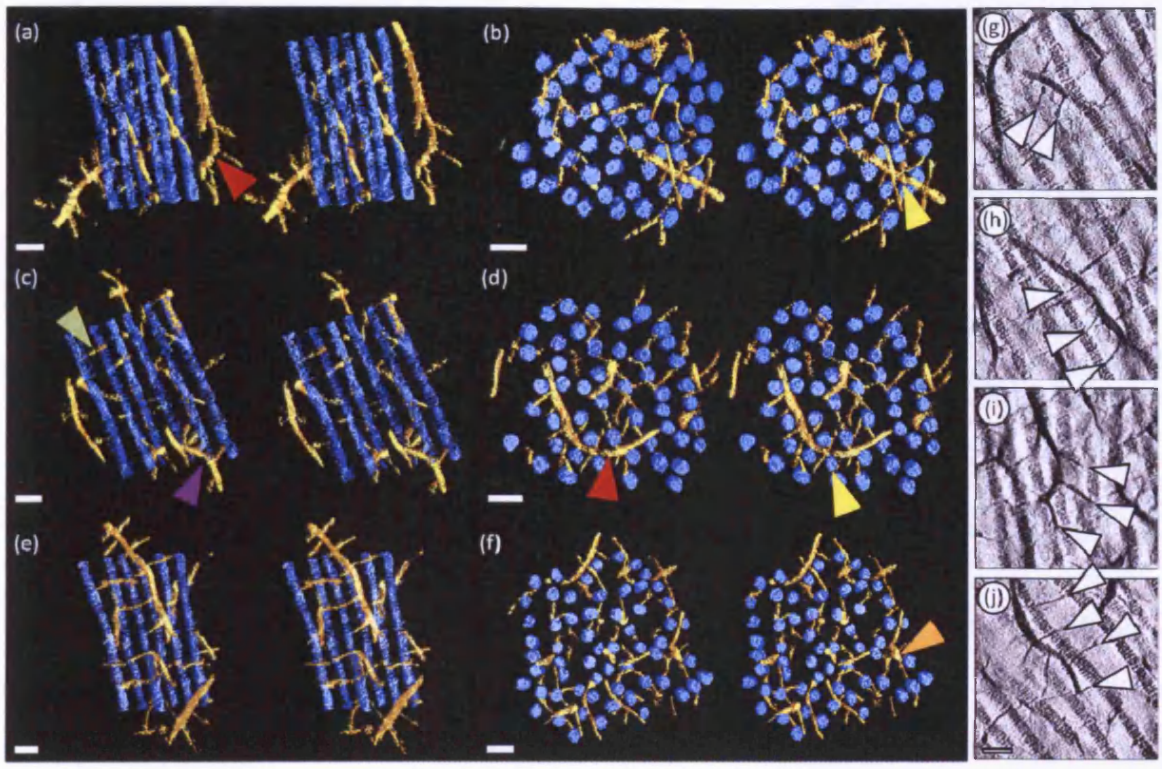

Fig. 4.3. Surface-rendered volumes of collagen and proteoglycans in the corneas of the *Chst5*-null mouse (a and b) anterior, (c and d) mid and (e and f) posterior corneal stroma shown as stereo-pairs of (a,c,e) longitudinal and (b,d,f) transverse sections of segmented tomograms. Proteoglycans are yellow in colour whereas collagen is depicted in blue. Red arrowheads highlight significant proteoglycan curvature and flexibility. Yellow arrowheads indicate tight packing of fibrils along glycosaminoglycan extension. The orange arrowhead shows a proteoglycan main body in cross-section whereas the green (unbranched) and purple (branched) arrowheads mark out the two prominent proteoglycan types observed. The near-periodic appearance of quasi-orthogonal off-shoots ((g-j), white arrowheads) are evident in the reconstructions (right hand panel). Scale bars = 50nm

The elongated proteoglycans in the *Chst5*-null cornea are able to span and connect many more fibrils than the largest proteoglycan type evident in wild-type corneas. More than 10 fibrils may be connected by the enlarged sinuous proteoglycan filaments which display remarkable flexibility, bending around fibrils in some cases (Fig. 4.3(a) and 4.3(d), red arrowheads). The chondroitinase ABC susceptible proteoglycans seen here (Hayashida et al., 2006) have diameters comparable to collagen fibrils when viewed in cross-section (Fig. 4.3(f), orange arrowhead), indicative of significantly increased thickness. Also, the proteoglycan off-shoots are markedly thinner than the proteoglycan body to which they are attached (Fig. 4.4.).

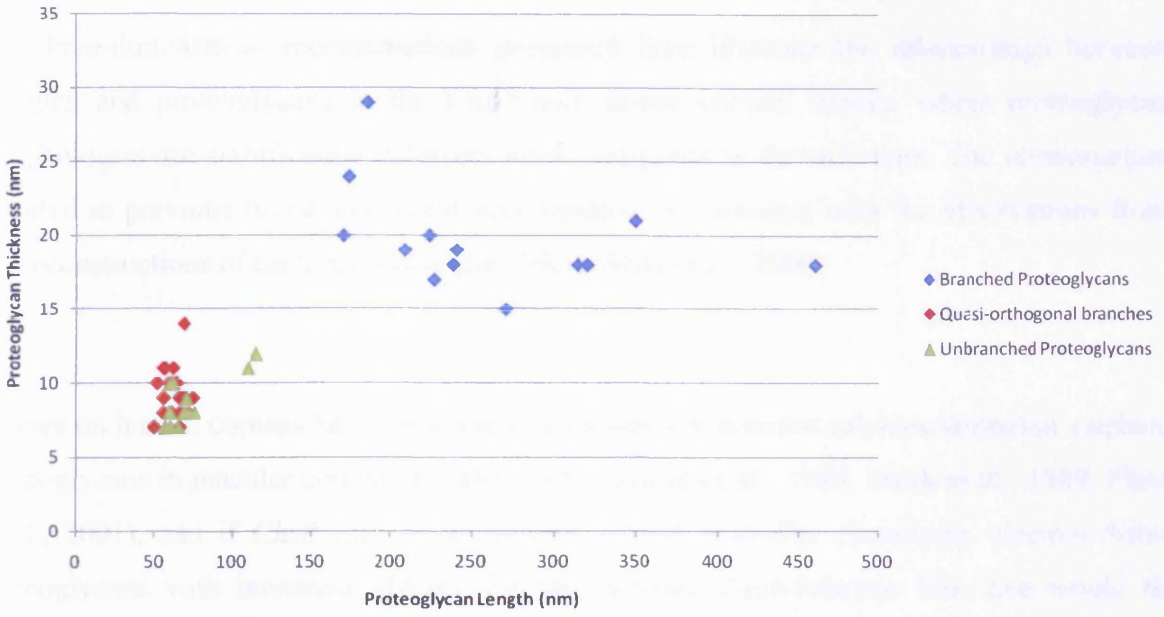

Fig. 4.4. Scatter plot of proteoglycan dimensions in the *Chst*5-null mouse cornea stroma. Measurements were limited to those proteoglycans that exhibit complete morphologies in the three-dimensional reconstruction. Branched proteoglycans = 260 ± 83nm (length); 20 ± 4nm (thickness in diameter). Orthogonal branches = 64 ± 7nm (length); 9 ± 2nm (thickness in diameter). Unbranched proteoglycans = 71 ± 17nm (length); 9 ± 2nm (thickness in diameter). Average distance between quasi-orthogonal branches = 46 ± 10nm.

Collagen fibril organisation in the *Chst*5-null appears to have developed with similar uniformity as in the wild-type tissue (Fig. 4.2(a) and 2(b)). However, in some regions of the mutant tissue collagen fibrils appear to pack tightly to the main body of the enlarged Cupromeronic blue-enhanced glycosaminoglycan filaments (Fig. 4.3(b) and 4.3(d), yellow arrowhead). Proteoglycans of the mutant corneas show no appreciable ordered arrangement around collagen fibrils three-dimensionally, as is the case in the wild-type mouse cornea. Also, the three distinct stromal regions (anterior, mid and posterior stroma) do not appear to differ significantly in their proteoglycan composition (Fig. 4.3).

4.5 Discussion

The three-dimensional reconstructions presented here illustrate the relationships between collagen and proteoglycans in the *Chst5*-null mouse corneal stroma, where proteoglycan morphologies are significantly enlarged when compared to the wild-type. The ultrastructure reported in previous two-dimensional investigation is consistent with the observations from the reconstructions of each stromal region (Hayashida et al., 2006).

Studies on human corneas have shown oversulphated chondroitin sulphate/dermatan sulphate proteoglycans in macular corneal dystrophy (Nakazawa et al., 1984, Meek et al., 1989, Plaas et al., 2001), and if *Chst5*-null mice corneas exhibit a similar phenotype, electron-dense proteoglycans with increased affinity for the cationic Cupromeronic blue dye would be expected on electron microscopy investigation. Indeed, this is the case and the three-dimensional images of enlarged proteoglycan filaments in the *Chst5*-null mouse cornea are striking. Previous research has shown that, through chondroitinase ABC digestion, the oversized proteoglycans are of the chondroitin sulphate/dermatan sulphate hybrid proteoglycan type (Hayashida et al., 2006). In this light, the observations made from the *Chst5*-null mouse cornea reconstructions suggest an important role for glycosaminoglycan sulphation in the packing and self-association of glycosaminoglycans and therefore, the determination of proteoglycan morphology.

Observations on proteoglycans from the *Chst5*-null three-dimensional reconstructions (fig. 4.3) suggest that many more chondroitin sulphate/dermatan sulphate chains have the ability to pack together compared to those in wild-type mouse corneas. The extension of chondroitin sulphate/dermatan sulphate proteoglycans in the *Chst5*-null mouse cornea, in some cases by over 500nm, could occur as a result of end-to-end aggregation or by elongation of single glycosaminoglycans, a process which is coupled with disaccharide sulphation at synthesis (Malstrom et al., 1975), or possibly both. In addition, lateral aggregation seems to take place since the size of ions used in staining (~1nm), and the width of individual glycan chains (<0.5nm) are insufficient (Scott, 1992) to account for the proteoglycan thicknesses observed, where enlarged proteoglycans display comparable diameters to collagen fibrils (Fig. 4.3(f), orange arrowhead; up to 29nm in thickness Fig. 4.4). This strongly implies that individual

proteoglycans pack into complexes in the *Chst5*-null mouse cornea. In normal physiology, the aggregation potential of proteoglycans must therefore be limited in order to regulate proteoglycan dimensions throughout the stroma, which are relatively uniform (Parfitt et al., 2010 - (Chapter Three)). Variations in the distribution of sulphation and the subsequent charge density appear to be the primary cause of increased proteoglycan aggregation in the *Chst5*-null mouse cornea, and so it is probable that the positioning of sulphate esters regulates proteoglycan self-association in the wild-type cornea.

Synchrotron X-ray fibre diffraction experiments have indicated that the average spacing of collagen fibrils in the *Chst5*-null cornea is not that dissimilar from the value in wild-type mice, though the lattice-like arrangement is disturbed (Hayashida et al., 2006). It is likely that an imbalance of the average negative charge on the proteoglycans would have an effect on their ability to attract water molecules and therefore, of regulating interfibrillar distances by osmotic swelling. Thus, the overall balance of electrostatic charge in the *Chst5*-null mouse cornea seems to be maintained despite the complete removal of keratan sulphate proteoglycan sulphation. This further supports the hypothesis of a compensatory mechanism which results in an increased sulphation of the chondroitin sulphate/dermatan sulphate chains in the absence of sulphated keratan sulphate. Therefore, the oversulphation of chondroitin sulphate/dermatan sulphate glycosaminoglycans appears to facilitate further packing and self-association of their chains, probably by the formation of more salt bridges with counter-ions. This idea is supported by the fact that self-association of dermatan sulphate has been shown to be promoted by the presence of Na+ ions (Fransson and Coster, 1979), so an increase in the charge density of proteoglycans would presumably lead to a greater influx and localisation of counter-ions, promoting further proteoglycan aggregation. Keratan sulphate, although non-sulphated, is still likely to be present (lumican core protein is detected in the *Chst5*-null mouse cornea (Hayashida et al., 2006)) and would be able to contribute to the regulation of interfibrillar spacing by drawing fibrils closer together through thermal motion (Knupp et al., 2009, Lewis et al., 2010). As well as a decrease in keratan sulphate proteoglycan hydration and the subsequent local osmotic swelling, self-association between non-sulphated keratan sulphate proteoglycans would still be expected if mediated by hydrogen bonds and/or hydrophobic forces. In conclusion, both types of proteoglycans could still maintain the ability to dynamically influence interfibrillar spacing and corneal fibril architecture necessary for tissue transparency despite their altered sulphation distribution.

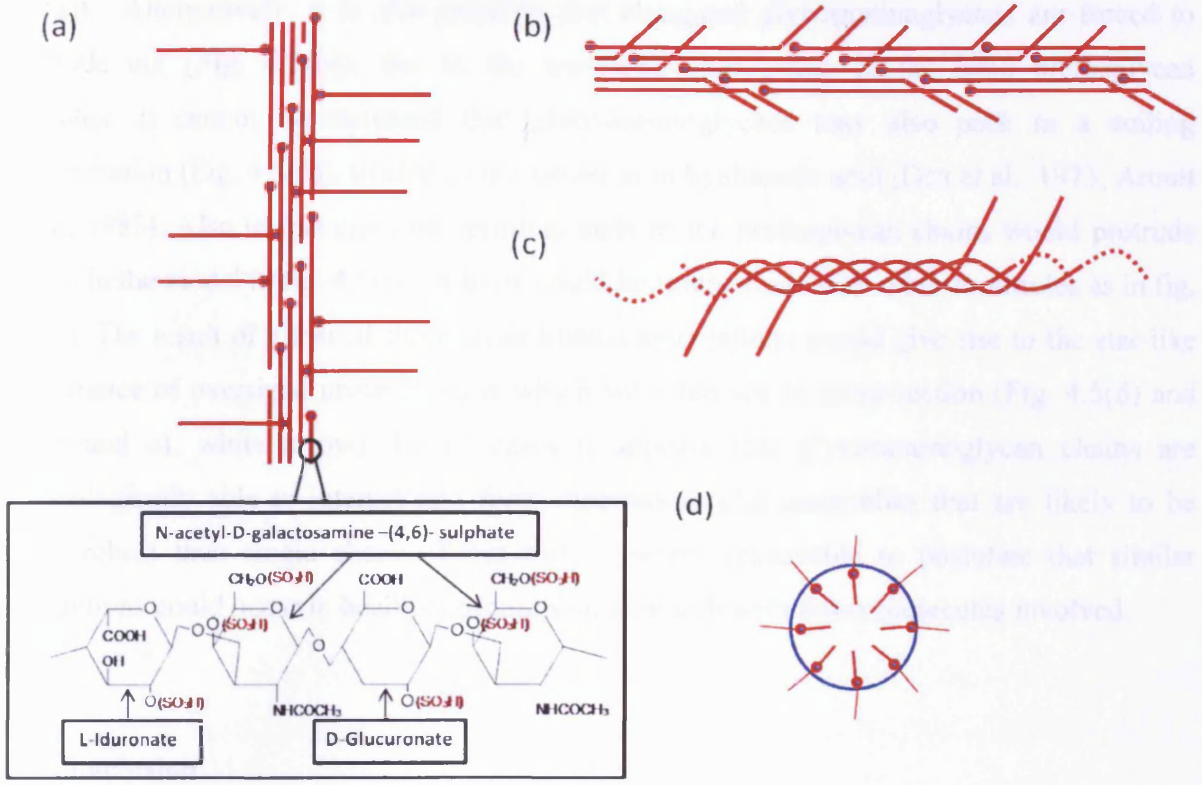

Fig. 4.5. (a and b) Schematic of proposed periodic aggregation of chondroitin sulphate/dermatan sulphate proteoglycans in the *Chst5*-null mouse corneal stroma and the disaccharide constituents, (a) orthogonal binding with protein cores and (b) without. The near regular distances of orthogonal glycosaminoglycans in the reconstructions suggest periodic lateral aggregation of proteoglycans in the main body. (c) Potential helical associations between glycosaminoglycans. (d) Cross-section of oversized proteoglycan with regular protruding glycosaminoglycan branches.

The regular branching of proteoglycans in the mutant corneas with chondroitin sulphate/dermatan sulphate off-shoots indicates that periodicity likely exists in the aggregation of the chondroitin sulphate/dermatan sulphate proteoglycan main body (Fig. 4.5(a) and (b)). It is currently unknown what molecules are involved in forming the branches to the main body of the stained proteoglycan filaments. The average distance between neighbouring quasi-orthogonal branches calculated here (46 ± 10nm) may not take into account the likelihood that not all binding sites may be occupied. Models can be envisaged, however, to explain the appearance of the proteoglycans in the reconstructions. For example, smaller chondroitin sulphate/dermatan sulphate proteoglycans, or other molecules could bind periodically and orthogonally along the chondroitin sulphate/dermatan sulphate body (Fig.

4.5(a)). Alternatively, it is also possible that elongated glycosaminoglycans are forced to protrude out (Fig. 4.5(b)), due to the increased aggregation in the main proteoglycan complex. It cannot be excluded that glycosaminoglycans may also pack in a coiling conformation (Fig. 4.5(c)), similar to the situation in hyaluronic acid (Dea et al., 1973, Arnott et al., 1983). Also in this case, the terminal ends of the proteoglycan chains would protrude out as in the model in fig. 4.5(b), or there could be interactions with other molecules as in fig. 4.5(a). The result of either of these co-ordinated associations would give rise to the star-like appearance of oversized proteoglycans which we often see in cross-section (Fig. 4.5(d) and 4.1(b and c), white arrow). In all cases it appears that glycosaminoglycan chains are physiologically able to interact and form macromolecular assemblies that are likely to be more robust than single chains. From this, it seems reasonable to postulate that similar interactions could occur in healthy corneas too, although with fewer molecules involved.

4.6 Conclusion

In conclusion, proteoglycans present in both the wild-type C57BL/6 and C*hst*5-null mouse corneas show no specific ordered arrangement around collagen fibrils. The removal of the 6-0-acetylglucosamine sulphotransferase enzyme responsible for transferring sulphate esters to keratan sulphate, results in chondroitin sulphate/dermatan sulphate proteoglycans with altered morphologies, which are significantly increased in both thickness and length. We suggest that altered sulphate ester distribution, and possibly disaccharide sequence differences, result in more favourable aggregation conditions that cause elongation as well as lateral and orthogonal aggregation of chondroitin sulphate/dermatan sulphate proteoglycans. The regular quasi-orthogonal glycosaminoglycan associations could be accounted for by periodic glycosaminoglycan aggregation. Sulphation, which influences both glycosaminoglycan elongation, epimerisation and the interactions with counter-ions and other glycosaminoglycans, is likely to be essential to the regulation of proteoglycan aggregation and therefore, the maintenance of corneal collagen fibril architecture

Chapter Five - Proteoglycans are dynamic regulators of both collagen fibril diameter and interfibrillar distance in the cornea: evidence from electron tomography of lumican-null mouse corneas.

5.1 Introduction to chapter

The transparent cornea exhibits a remarkable degree of organisation in its array of collagen fibrils when compared with other connective tissues. This ordered fibrillar arrangement is thought to be a consequence of dynamic regulation by sulphated proteoglycan macromolecules, as proposed in Chapters Three and Four.

To understand the importance of proteoglycans in corneal homeostasis, and specifically the major proteoglycan lumican, with its keratan sulphate glycosaminoglycan side-chains, the corneas of homozygous lumican-null juvenile mice were imaged in a transmission electron microscope and the three-dimensional arrangement of proteoglycans and collagen fibrils was reconstructed by electron tomography. From this, it was apparent that lumican impacts upon the regulation of normal collagen fibril assembly, and the presence of merged fibrils in the lumican-null mouse cornea indicates that these keratan sulphate proteoglycans contribute to the spatial regulation of neighbouring fibrils, most likely through their constituent glycosaminoglycan side-chains. Therefore, proteoglycans influence corneal transparency by maintaining a regular spatial distribution of collagen fibrils and thus, have an essential functional role in vision. Based on this, we propose a model to explain how proteoglycans regulate the ultrastructure of collagen fibrils in the cornea.

5.2 Introduction

Lumican is the major keratan sulphate proteoglycan in the corneal stroma and, along with decorin and biglycan, has been shown to limit collagen fibrillogenesis *in vitro,* as discussed in Chapter One. Similar to the other keratan sulphate proteoglycans in the cornea, lumican has 2-3 glycosaminoglycan extensions of approximately 10-15kDa each, and a core protein of about 51kDa (Hassell et al., 1979, Midura and Hascall, 1989). Homozygous lumican-null

mice have demonstrated the importance of lumican in the maintenance of the intricate collagen fibril architecture in the wild-type mouse cornea (Chakravarti et al., 1998), where lumican protein is present in an ascending gradient from anterior to posterior stroma (Chakravarti et al., 2000). As a consequence of the different distribution, fibril defects in lumican-null mutant corneas are prevalent in the posterior regions of the cornea. Moreover, keratan sulphate content in the lumican mutants decreases by 25% when compared to the wild-type mouse cornea (Chakravarti et al., 2000). The expression of keratocan is dependent on lumican (Carlson et al., 2005, Liu et al., 2010) and thus, lumican-null mice may also exhibit altered expression in other proteoglycan types. Even though chondroitin sulphate/dermatan sulphate proteoglycans account for the bulk of the mouse cornea's proteoglycan content, removal of lumican proteoglycans diminishes corneal transparency marginally. Therefore, observations made from lumican-null mouse corneas may reveal the modes of regulation that proteoglycans, through their glycosaminoglycan extensions, exert in order to maintain the short range order of collagen fibrils in the cornea.

In this investigation, we obtained three-dimensional reconstructions, at high magnification, of the homozygous lumican-null mouse corneal stroma to achieve a greater understanding as to the role of lumican, and proteoglycans in general, in regulating collagen interfibrillar spacing and fibril diameters, which are the two essential parameters in the development and maintenance of corneal transparency.

5.3 Materials and Methods

5.3.1 Sample Preparation for Electron Microscopy

Young adult (3 months old), wild-type (C57BL/6) and homozygous lumican-null mouse corneas were removed within 5 minutes post-mortem. Animals were treated under the ARVO Statement for the Use of Animals in Ophthalmic and Vision Research and local regulations at all times. Corneas were cut into halves and subjected to fixation in 2.5% glutaraldehyde in 25mM sodium acetate (pH 5.7) with 0.05% Cuprolinic blue dye (wt/vol). Cuprolinic blue, a cationic dye utilised here at a critical electrolyte concentration of 0.1M $MgCl_2$, complexes

with proteoglycans by interacting with anionic charges on both sulphate and carboxylate residues of the glycosaminoglycan chains. The specimens were next immersed in a 0.5% sodium tungstate solution to enhance the contrast of proteoglycans in the electron microscope. Samples were then subjected to ethanol washes increasing in concentration from 70-100% to dehydrate the tissue and embedded in Araldite resin, through propylene oxide, for sectioning.

5.3.2 Enzyme Digestion

To determine the presence of specific proteoglycans in the lumican-null mouse corneas, certain glycosaminoglycan-cleaving enzymes were used. Corneas dissected in quarters were prefixed with 1% paraformaldehyde and washed with 1 unit/ml tris/sodium acetate buffer (pH 8), with one cornea remaining in the buffer as a control. To remove hybrid chondroitin sulphate/dermatan sulphate proteoglycans, one cornea was incubated in 2.5 unit/ml chondroitinase ABC (Sigma Aldrich) for 4h at 37°C, whereas keratan sulphate proteoglycans were degraded by treating another cornea with 1 unit/ml keratanase II (Sigma Aldrich), also for 4h at 37°C. To remove both types of proteoglycans, a combination of both enzymes was used. Samples were then fixed, proteoglycan-stained and embedded according to the protocol outlined above.

5.3.3 Electron Tomography

Embedded corneal tissue was cut into sections approximately 100nm in thickness (gold interference) using a Reichert UCE ultra-microtome. Sections were collected on copper grids coated with a 0.38% polyetherimide support film, stained with 1% phosphotungstic acid for 2 minutes followed by saturated uranyl acetate for 12 minutes and treated with colloidal gold solution (BBI, Cardiff, UK) on both faces of the grid. Single axis tilt series, -60° to +60°, of stromal lamellae in both longitudinal and transverse sections, and of each stromal region (anterior, mid and posterior stroma) were captured at 20kx magnification, in one degree increments, on a JEOL 1010 transmission electron microscope (80Kv) equipped with a Gatan ORIUS SC1000 CCD camera. Each 121 image set was aligned using IMOD (Kremer et al., 1996), and with reference to the position of gold fiducial markers (10nm gold particles) on

each image. A back-projected reconstruction was generated using EM3D (Ress et al., 2004), and its segmentation was performed through manual selection of contours in a region of interest, also carried out using EM3D.

5.3.4 Measurement of Fibril Diameters

Collagen fibril diameters were measured using imageJ software (Abramoff, 2004) with the 65nm collagen D-period used for internal calibration. Measurements were taken from fibrils (n=750) for each stromal region (anterior, mid, posterior).

5.4 Results

Electron microscopic investigations showed that the corneas of homozygous lumican-null mice are characterised by the presence of enlarged and irregularly shaped collagen fibrils in the posterior stroma (Fig. 5.1. and Chakravarti et al., 2000). These abnormal fibrils are relatively rare, and although they vary in size and shape, their irregular appearance is consistent with them being the result of neighbouring collagen fibrils that have fused laterally (Figs. 5.1(c) and 5.2.).

In some cases, multiple fibrils seem to fuse to give the appearance of a single fibril with an irregular contour (Fig. 5.2.). These merged fibrils are not apparent in the anterior stroma and their incidence increases towards the posterior region, in line with the findings of Chakravarti et al., 2000.

To identify the proteoglycans seen in the lumican-null mouse cornea, enzyme digestion using keratanase II (which cleaves keratan sulphate) and chondroitinase ABC (which removes chondroitin sulphate/dermatan sulphate glycosaminoglycans) was carried out (Fig. 5.3). Keratanase II treatment of both the lumican mutant (Fig. 5.3(b)) and C57BL/6 wild-type (Fig. 5.3(f)) mouse cornea does not show any appreciable difference in proteoglycan density and morphology, indicative of a low population of keratan sulphate associated proteoglycans in

the mouse cornea (Young et al., 2005, Hayashida et al., 2006). However, chondroitinase ABC treatment removes all apparent Cuprolinic blue stained proteoglycans in the lumican knockout mice (Fig. 5.3(c)), demonstrating the absence of sulphated keratan sulphate proteoglycans. In the wild-type mouse cornea, chondroitinase ABC digestion leaves a minimal amount of fine, fibril associated proteoglycans likely to be of the keratan sulphate variety (Fig. 5.3(g)). Digestion with both enzyme types results in the complete removal of Cuprolinic blue-stained proteoglycans in both the wild-type (Fig. 5.3(d)) and lumican-null mouse cornea (Fig. 5.3(h)).

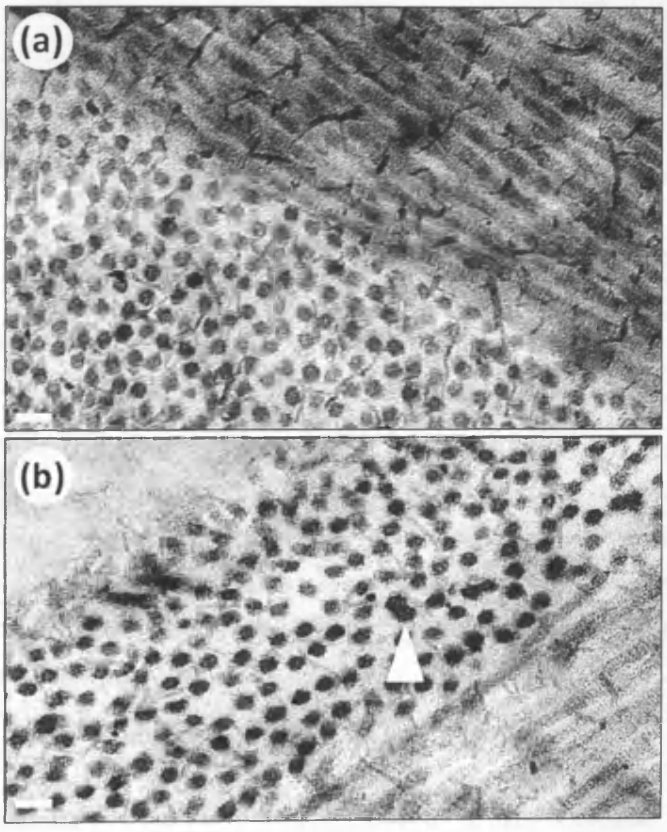

Fig. 5.1. Electron micrograph of (a) wild-type mouse (C57BL/6) corneal stroma and (b) posterior stroma of lum -/- mouse cornea. Lumican knockout corneas are characterised by the presence of oversized fibrils in the posterior stroma ((b) white arrowhead). Scale Bars = 100nm

Three-dimensional reconstructions of the C57BL/6 wild-type mouse cornea reveal an apparent random proteoglycan organisation, where there is a non-specific rotational order

around collagen fibrils with proteoglycans of differing dimensions seen to inter-connect neighbouring, and in some cases, next-nearest neighbour fibrils. Small interfibrillar (Fig. 5.4(b), red arrowhead), and more curved proteoglycans (Fig. 5.4(b), green arrowhead) link nearest neighbours whereas next-nearest neighbour fibrils may be attached via an elongated third type of proteoglycan (Fig. 5.4(b), white arrowhead). The appearance of the collagen fibril arrangement in transverse section is characteristic of the cornea, with a lattice-like array comprised of fibrils with uniform spatial distribution and diameter.

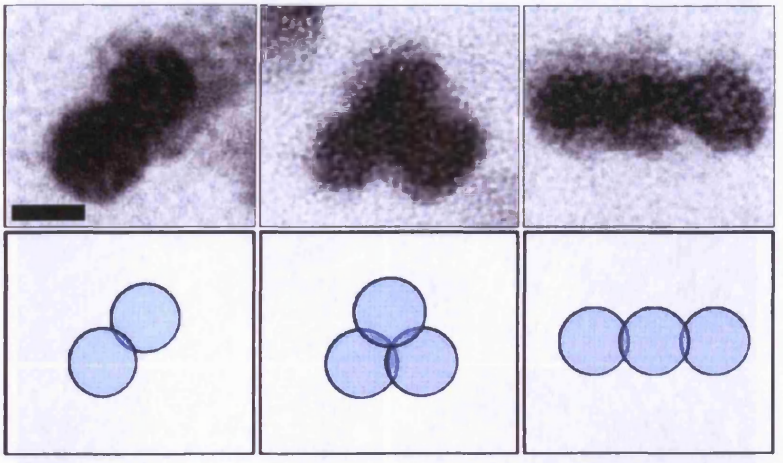

Fig. 5.2. (top panels) Electron micrographs of collagen fibrils in transverse section in the posterior stroma of a lumican knockout mouse cornea. The contours of these fibrils suggest that they arise from the fusion of regularly sized fibrils that have merged in the absence of lumican proteoglycans. (bottom panels) A schematic representation of collagen fibrils (blue circles) coming together to form the aggregates seen in the top panels. Scale Bar = 20nm

Upon measurement of fibril diameters in the lumican mutant mouse corneal stroma, it is apparent that the fibril irregularities are confined to the posterior and mid-stromal regions, with a greater incidence occurring posteriorly. In the posterior region, collagen fibrils with diameters in the range of 55-65nm are relatively frequent which could possibly be accounted for by the presence of two or more laterally fused fibrils with diameters in the "normal" range of 25-35nm. This increase in fibril size is also apparent in the mid-stroma but on a lesser scale. The anterior stroma also has a larger distribution of fibril diameters compared to the wild-type mouse cornea, although no highly enlarged fibrils over 40nm were seen. In the mid stroma, the frequency plot (Fig. 5.5(c)) shows a less prominent bi-modal distribution than in

the posterior stroma, although irregularly sized fibrils are present. The wider distribution in fibril diameters, and the fact that the distribution clearly appears to be bi-modal, is likely to explain the diminished transparency and increase in backscattered light in the posterior corneal stroma.

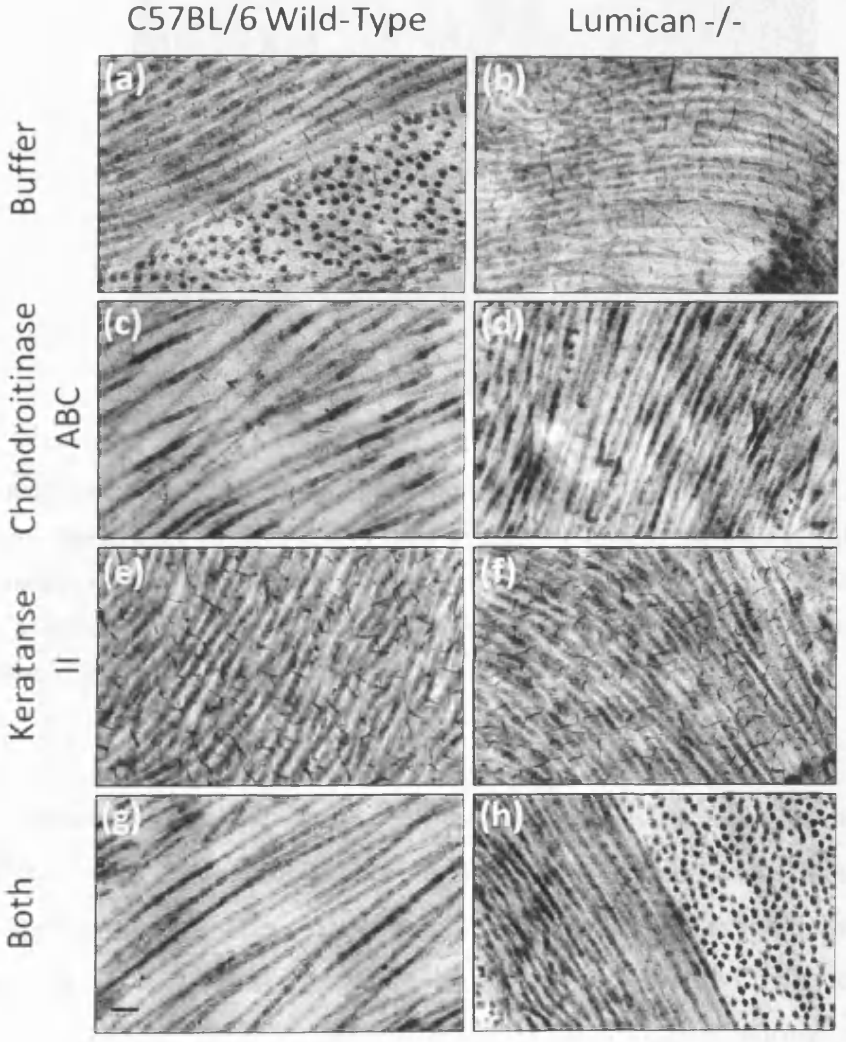

Fig. 5.3. Electron micrographs of wild-type (left column) and homozygous lumican-null (right column) mouse corneal stromas showing Cuprolinic blue stained proteoglycans after incubation in buffer (a and b), chondroitinase ABC (c and d), keratanase II (e and f) and both keratanase and chondroitinase ABC (g and h). Keratanase treatment shows the abundance of chondroitin sulphate/dermatan sulphate proteoglycans in both wild-type (e) and lumican-null corneas (f). Chondroitinase ABC digestion leaves a minimal amount of small filamentous proteoglycans in the wild-type (c), although none are seen in the mutant corneas (d) because of the lack of the major keratan sulphate proteoglycan, lumican. Enzyme digestion with both keratanase and chondroitinase ABC leaves no detectable proteoglycan component. Scale bar = 100nm

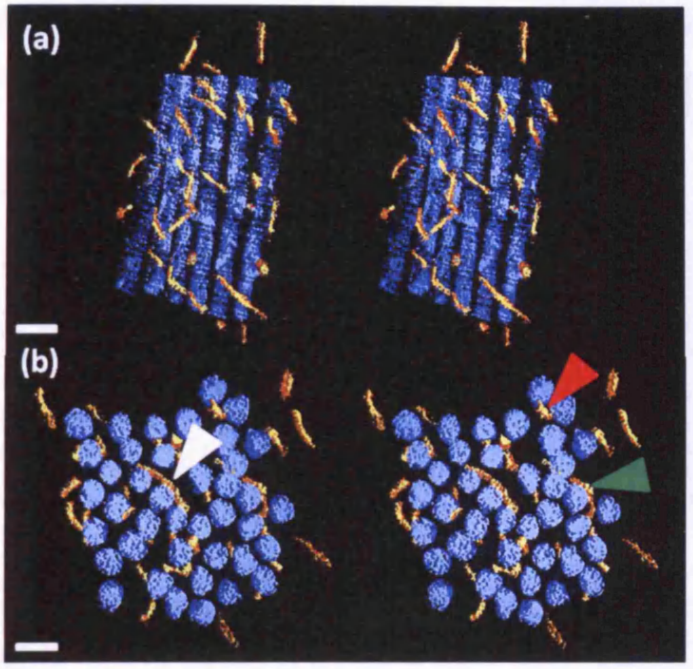

Fig. 5.4. Tomograms of collagen (blue) and proteoglycans (yellow) in the C57BL/6 wild-type mouse corneal stroma. Stereo-pairs of three-dimensional reconstructions in (a) longitudinal and (b) transverse section. Proteoglycans do not exhibit any rotational order around collagen fibrils and are seen to interconnect neighbouring fibrils (red arrowhead) as well as next-nearest neighbours (white arrowhead). Scale bar = 50nm

The three-dimensional reconstructions of the lumican-null mouse cornea show grossly enlarged fibrils with irregular contours in both the posterior and mid-stroma transverse sections, although their occurrence seems to be more frequent posteriorly (Fig. 5.6 and Chakravarti et al., 2000). These enlarged fibrils were not evident in the anterior lumican-null stroma. In longitudinal section, most collagen fibrils appear normal (Fig. 5.6(a,c,e)). However, some regions of the reconstructions reveal enlarged fibrils with evidence of an axially localised fusion of regularly sized fibrils. Interestingly, the collagen banding of each merging fibril appears to be in register (Fig. 5.7 red and green arrowheads). The merging of fibrils is not widespread, probably owing to the abundance of chondroitin sulphate/dermatan sulphate proteoglycans that are located between fibrils and which impede them from coming into contact and fusing. Proteoglycans, similar to what is observed in wild-type mouse corneas, do not exhibit any rotationally ordered arrangement. In addition, there appears to be a lack of the small interfibrillar proteoglycans which are likely to be of the keratan sulphate

variety, as suggested by our enzyme digestion data (Fig. 5.3(c)). As a result, many next-nearest fibrils appear to be inter-connected by the larger chondroitin sulphate/dermatan sulphate filaments.

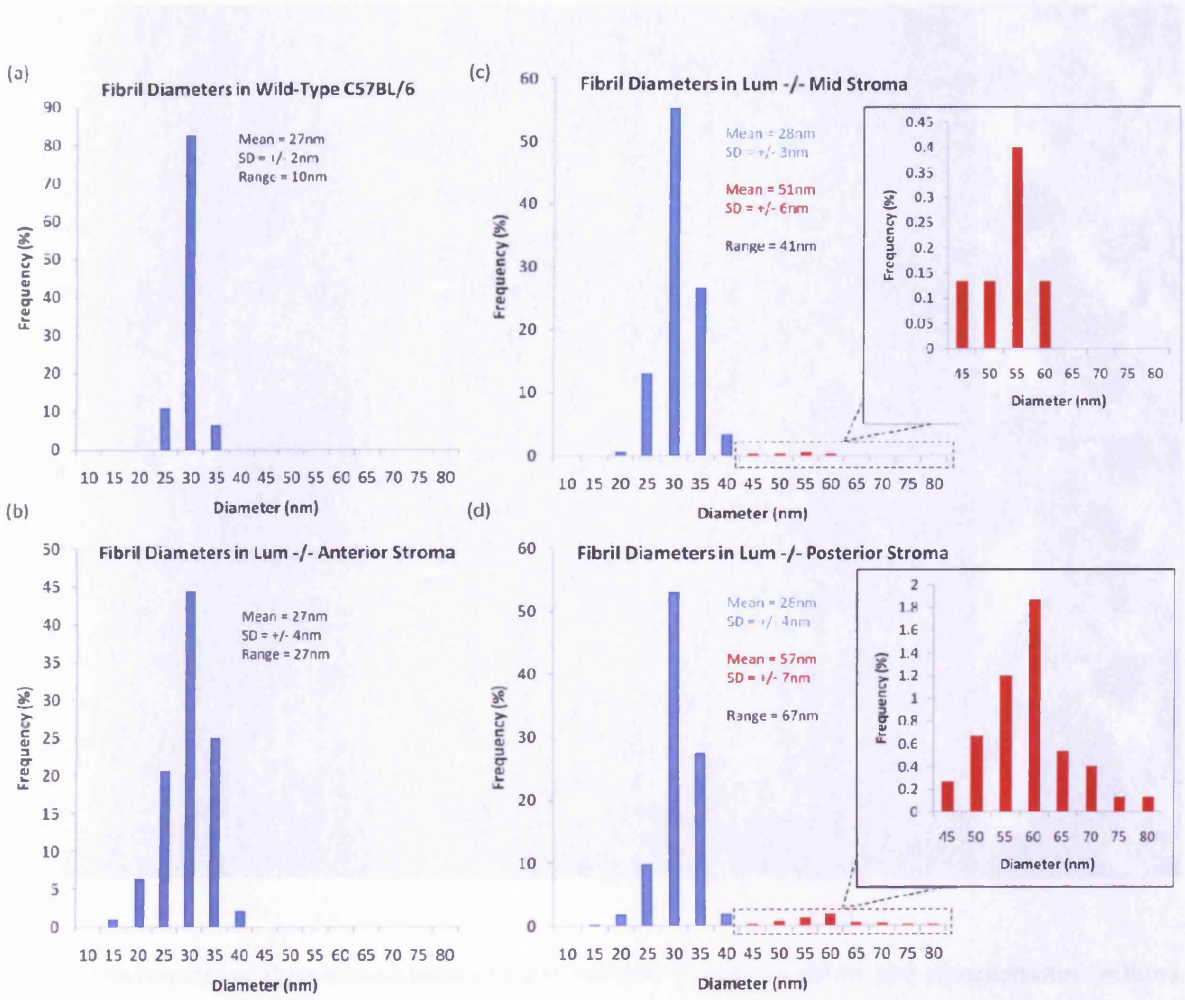

Fig. 5.5. Frequency plots of collagen fibril diameters from (a) C57BL/6 wild-type mouse corneal stroma; (b) Anterior Lum -/- mouse corneal stroma; (c) Mid-stroma Lum -/- mouse corneal stroma; (d) Posterior Lum -/- mouse corneal stroma. As the mid and posterior stroma exhibit a bi-modal distribution for fibril diameter, the mean is calculated for each mode; regular (blue) and irregular (red) sized fibrils.

5.5 Discussion

Using electron tomography we have visualised, in three-dimensions, the collagen-proteoglycan interactions in the homozygous lumican-null mouse corneal stroma. The proteoglycans of the lumican mutant cornea exhibit no rotational order around collagen

fibrils, as is the case in other mammalian corneas (Lewis et al., 2010, Parfitt et al., 2010 - (Chapter Three)).

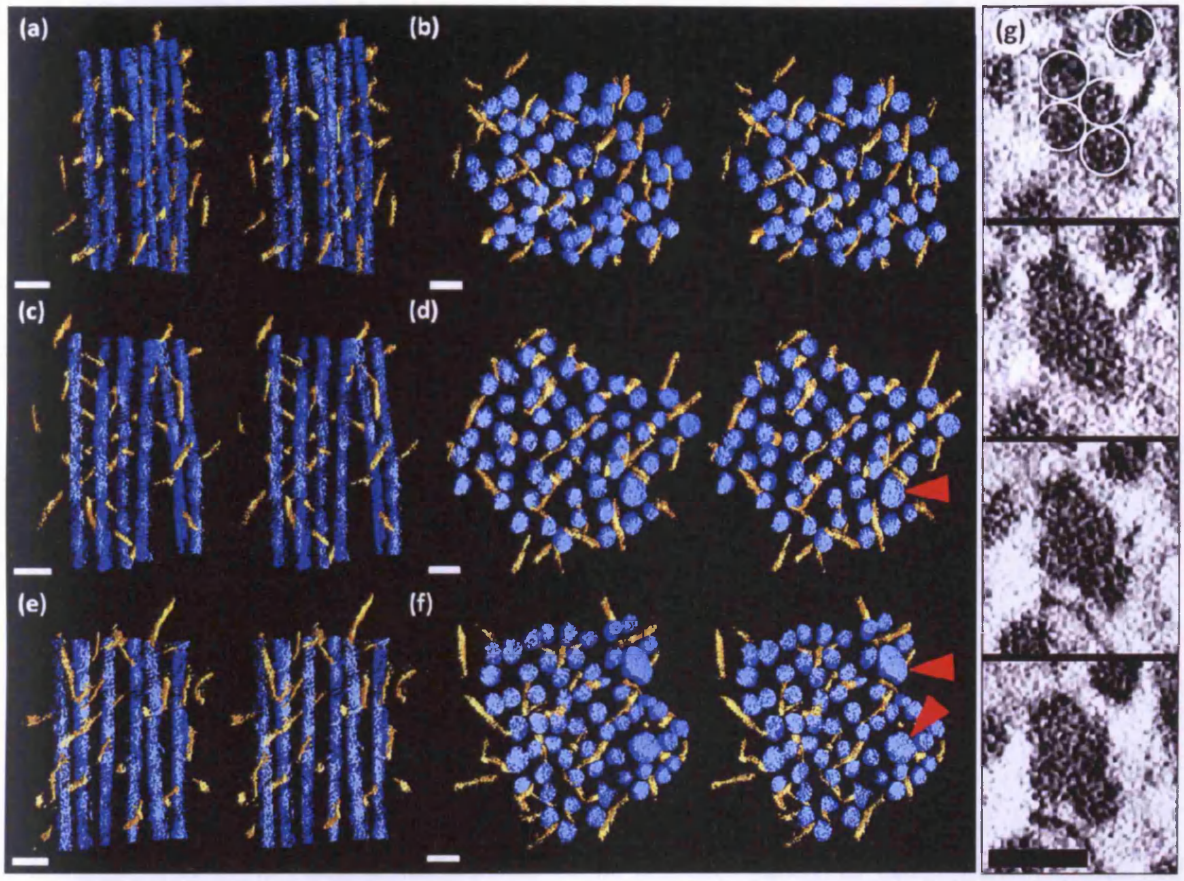

Fig. 5.6. Stereo-pairs of three-dimensional reconstructions of collagen (blue) and proteoglycans (yellow) in the lumican -/- mouse (a and b) anterior, (c and d) mid and (e and f) posterior corneal stroma. Longitudinal (a,c,e) and transverse (b,d,f) sections illustrate the fibril defects of the posterior and mid stroma, where oversized fibrils exist (red arrowheads). (c) Successive slices through a tomogram of an oversized fibril in the posterior lumican-null mouse corneal stroma show four fibrils (bottom panel) merging to form a single fibril with irregular contours (Top panel). Scale bar = 50nm

In the absence of the major keratan sulphate proteoglycan lumican, neighbouring collagen fibrils in the mid and posterior stroma in the lumican-null mouse are seen occasionally fusing together to form enlarged fibrils with irregular contours. There is evidence, from studies of lumican-null mice which are older (7 months old) than those used in this investigation, of further enlargement and lateral fusion of fibrils in the mid and posterior stroma as time

progresses. In 7.5 month old mice, the fused fibrils appear more abundant and exhibit more 'cauliflower'-like morphologies with much larger diameters than those measured in this study, although this is expected as lumican expression is greater in the older mice (Chakravarti et al., 2000). It has been postulated that, even though mouse cornea is not as populated with sulphated keratan sulphate proteoglycans as other mammalian corneas (Scott and Bosworth, 1990, Young et al., 2005), the dominance of the structural change in the posterior stroma is due to keratan sulphate proteoglycans exhibiting more structural influence in the deep stroma. Moreover, lumican removal is likely to affect the expression and distribution of other keratan sulphate proteoglycans (Carlson et al., 2005, Liu et al., 2010), as indicated by the lack of proteoglycans in the lumican-null mouse cornea when treated with chondroitinase ABC.

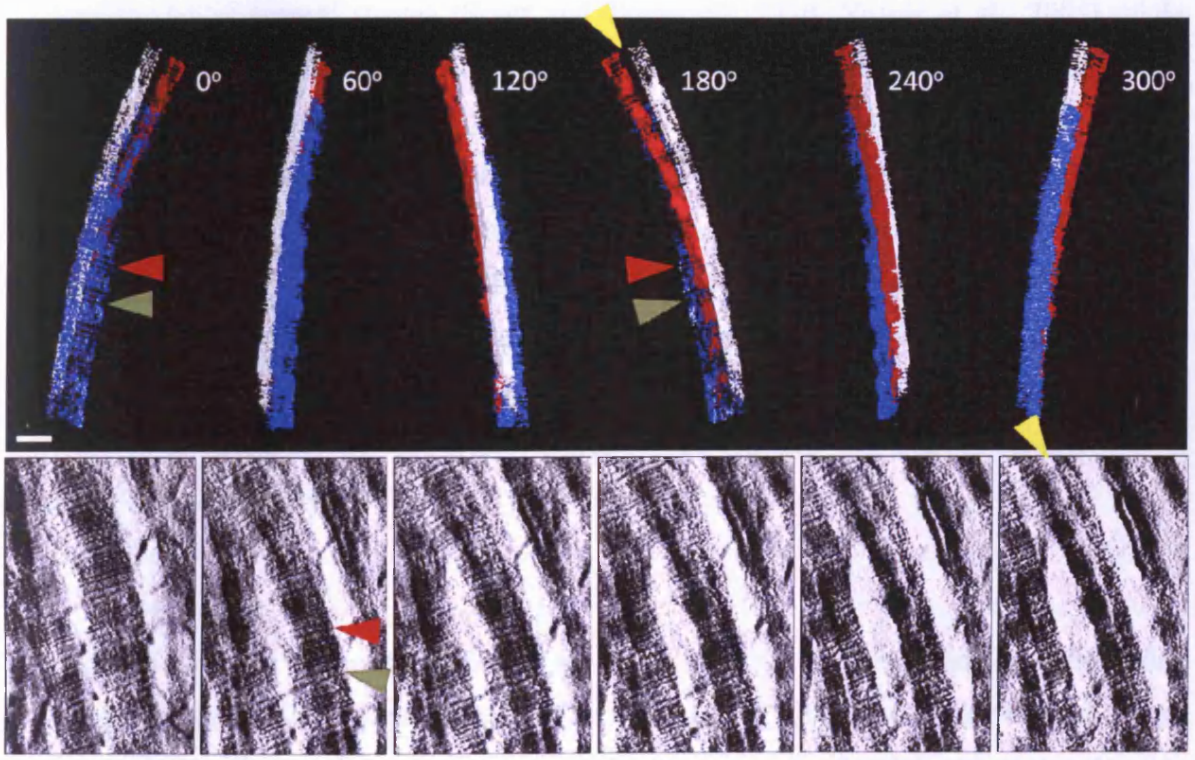

Fig. 5.7. Three-dimensional reconstruction of an irregularly sized fibril in longitudinal section of the lumican-null mouse posterior corneal stroma. Three collagen fibrils fuse locally to give the appearance of an enlarged fibril. In places (yellow arrow), the fibrils are distinct and separate, suggesting that fibrils merge first at localised regions. Collagen banding correlation between the fibrils suggests that fibril fusion is possibly according to specific sites normally occupied by the proteoglycans. Scale bar = 50nm

Chapter Five - Proteoglycans are dynamic regulators of both collagen fibril diameter and interfibrillar distance in the cornea: evidence from electron tomography of lumican-null mouse corneas.

Proteoglycans contribute to the regulation of uniform collagen architecture in the cornea, restricting fibril diameters by preventing fibril fusion and by influencing interfibrillar spacing through opposing osmotic and thermal forces (Fig. 8). Type V collagen initiates and regulates the assembly of the fibrils themselves prior to deposition in the extra-cellular matrix by keratocytes (Hassell and Birk, 2010, Birk, 2001, Birk et al., 1990). Longitudinal reconstructions, where no appreciable defects are seen along the length of the fibril, suggest that enlargement of fibrils may occur, at least initially, at localised points, where neighbouring fibrils possibly coalesce at a single region and not extended axial regions spanning the fibril length. This view is supported by the reconstructed tissue volume that clearly shows three normal diameter fibrils merging into one. It is worth considering the possibility that the low concentration of lumican and other keratan sulphate proteoglycans in the healthy mouse corneal stroma (Scott and Bosworth, 1990, Young et al., 2005) might explain the low prevalence of oversized fibrils in the lumican deficient stroma, where a role in preventing fibril fusion is likely to be assumed by the more abundantly expressed chondroitin sulphate/dermatan sulphate proteoglycans. The enlarged, fused fibrils are irregularly scattered throughout the mid and posterior stroma in the lumican-null mouse cornea and the resultant anisotropy in fibril distribution and size caused by fusion affects light interference within the cornea. Assessment, by *in vivo* confocal microscopy, of backscattered light as an indicator of corneal transparency in lumican-null corneas, has disclosed that more light scattering occurs in the posterior stroma (Chakravarti et al., 2000), indicative of a reduction in transparency.

In consideration of the previously proposed model for the dynamic regulation of interfibrillar spacing (Knupp et al., 2009, Lewis et al., 2010, Parfitt et al., 2010 - (Chapter Three)), a loss of localised osmotic swelling pressure through the removal of sulphated proteoglycans, proposed to push fibrils apart to regulate their distribution in normal physiology, would be expected to allow for neighbouring fibrils to move closer and potentially come into contact with each other. Also, as there would be no lumican protein cores on the fibril, not only a potential source of steric hindrance would be removed, but potential sites for further lateral aggregation of fibrils may become available. This view is also supported by *In vitro* studies that have shown that protein cores, even without a glycosaminoglycan extension, are capable of limiting collagen fibrillogenesis (Rada et al., 1993), supporting the idea that protein core

occupancy of collagen banding restricts lateral fusion. Moreover, the collagen banding of the merged fibrils appears to be in register along the length of the fibril, presumably allowing the forces that keep the collagen molecules together within a fibril to also act between separate fibrils. Although, it is unclear whether the fibrils are required to be register in order for fusion to occur. The removal of lumican is, therefore, likely to result in reduced osmotic pressure, the removal of a source of steric hindrance and also in the freeing of attachment sites on the collagen fibrils, all of which are possible factors in fibril fusion and enlargement, as seen in the posterior regions of the homozygous lumican-null mouse cornea.

The proteoglycans that remain in the lumican-null mouse corneas are likely to be mostly of the chondroitin sulphate/dermatan sulphate variety and are seen to frequently inter-connect more than two fibrils in a non-specific arrangement, maintaining collagen fibril spacing in the mutant cornea. With regards to the model proposed, if the abundant and more sulphated chondroitin sulphate/dermatan sulphate type of proteoglycans were to be removed, and consequently the osmotic pressure they generate, we predict a much greater incidence of lateral fusion would occur; primarily because of their prevalence and their proposed function, not dissimilar from keratan sulphate. This is indeed what is observed in the compound decorin/biglycan double-knockout mouse cornea (Zhang et al., 2009). No fused fibrils are observed in the corneas of *Chst5*-null mice however (Parfitt et al., 2011 - (Chapter Four)), and so it is likely that physical attachment of proteoglycans to fibrils is paramount to fibril separation and the prevention of fusion, whilst sulphation of glycosaminoglycans dictates the extent of localised osmotic pressure and the organised spatial distribution of fibrils. Therefore, our model is capable of explaining how proteoglycans can mediate the intricate corneal collagen fibril architecture by simultaneously regulating interfibrillar distances and fibril diameter to allow for fibril spatial flexibility and corneal transparency.

5.6 Conclusion

Three-dimensional reconstructions of collagen-proteoglycan interactions in the lumican-null mouse cornea imply that keratan sulphate proteoglycans regulate both fibril diameter and interfibrillar spacing by maintaining the separation between neighbouring fibrils. This is

consistent with the view that proteoglycans are dynamic mediators of both fibril diameter and interfibrillar distance. It is possible that chondroitin sulphate/dermatan sulphate regulates collagen fibril architecture with the same mechanisms, and the removal of these proteoglycans, as seen in the studies of decorin-biglycan knockouts, results in a severe phenotype in mouse cornea due to their abundance and ability to connect numerous fibrils in the mouse corneal stroma.

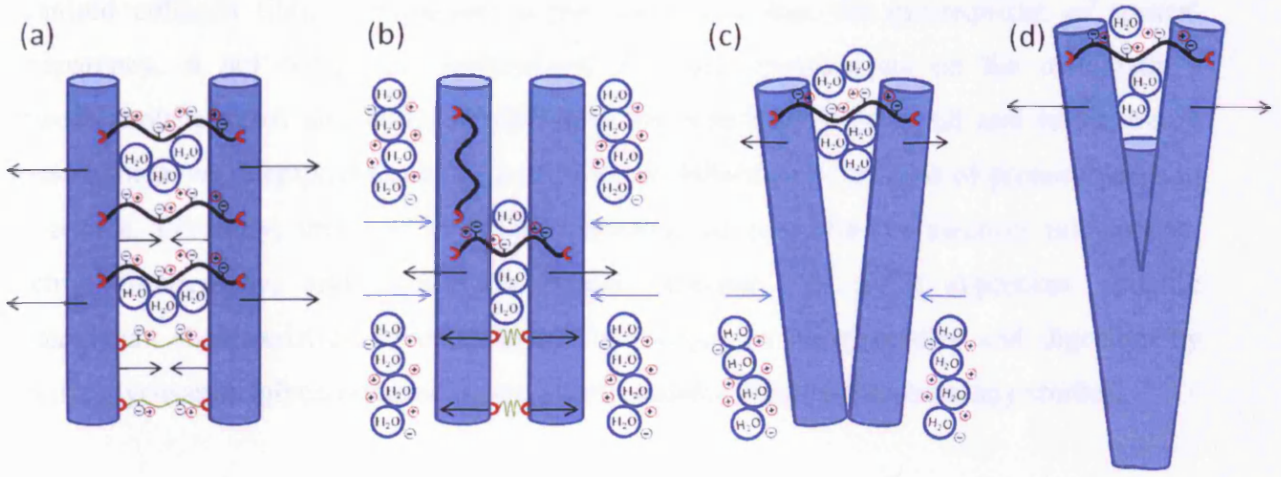

Fig. 5.8. Schematic representation of the proposed role of lumican in regulating collagen fibril diameter, maintaining interfibrillar spacing and preventing fibrils from fusing. (a) In healthy corneas, proteoglycans maintain fibril separation mainly via a combination of the Donnan effect and thermal motion. The proteoglycan's highly anionic charge density attracts positively charged ions, which in turn attract water molecules that cause an increase in local osmotic pressure and which "pushes" adjacent fibrils apart. At the same time, thermal motion of the glycosaminoglycan chains causes a retraction of their terminal ends which are bound, via a protein core, to collagen fibrils. An attractive force thus arises, the tendency of which is to bring fibrils closer together. The combination of attractive and repulsive forces (black arrows) keep the fibrils at optimal separations. (b) Proteoglycan motion is likely to cause movement of protein cores which are held in place by non-covalent interactions with fibrils. This is suggested by the presence of proteoglycans that lie along the fibril axis or display skewed angles, along with a general lack of any rotational symmetry of the proteoglycans around the collagen fibrils. Movement of water, ions and nutrients through the tissue (blue arrows) and in-between fibrils cause the fibrils to move from their average position and at times they get closer together. Fibrils are prevented from fusing laterally by the compressive resistance of proteoglycans imbibed with water and by the steric hindrance caused by their protein cores and glycosaminoglycan chains. (c and d) Localised removal of interfibrillar proteoglycans prevents dynamic mediation of interfibrillar spacing and allows fibrils to come into contact and potentially fuse, most likely keeping their collagen banding in register as the three-dimensional reconstruction of a fused fibril suggests (Fig. 7).

Chapter Six - Concluding Discussion

6.1 Introduction

The main aim of this project was to further our understanding of proteoglycan structure and function in the corneal stroma using the mouse cornea as a model system. By using mouse corneas, we have the opportunity of being able to analyse genetically manipulated specimens, alongside the advantage of using readily available tissue. Proteoglycan regulation of the organised collagen fibril architecture in the corneal stroma, the pre-requisite of corneal transparency, is not completely understood. Through observations on the relationships between proteoglycans and collagen fibrils in the wild-type, *Chst5*-null and lumican-null mouse cornea, we attempted to obtain a more clear definition of the role of proteoglycans in the cornea. Primarily, this was done by conventional transmission electron microscopy, electron tomography, and subsequent image analysis. To fully appreciate specific proteoglycan characteristics, investigation of proteoglycan morphometry and digestion by specific glycosaminoglycan-degrading enzymes complemented our microscopy studies.

A recent histological investigation into the mouse cornea (Young et al., 2005), outlaid the atypical ultrastructure of the mouse corneal stroma and suggested that further analysis would be required to fully understand the proteoglycan-knockout mice that are becoming common place in studies of proteoglycan function. Utilising electron tomography, we were able to visualise proteoglycan-collagen interactions three-dimensionally in the wild-type mouse cornea, which enabled us to propose a model of how collagen fibrils are spatially distributed with a remarkable degree of uniformity by the proteoglycans (Chapter Three). Three-dimensional reconstruction of *Chst5*-null mouse corneas, which exhibit proteoglycans with abnormal morphologies as a result of defective sulphate transfer, gave insights into proteoglycan packing and the flexibility of proteoglycan complexes (Chapter Four). Using the dynamic proteoglycan regulatory model proposed for the wild-type mouse cornea as a basis, we also analysed genetically modified mouse corneas (Lumican-null - Chapter Five) to help compound the idea that proteoglycans regulate both collagen fibril assembly and spatial distribution in the cornea. From this work, possible future avenues of research may include applying electron tomography to human corneas and even diseased corneas (i.e. keratoconus and macular corneal dystrophies) to test fully the hypothesis of dynamic proteoglycan-collagen architecture regulation, as put forward in this thesis. Further investigations using

electron tomography may also include the characterisation of keratocytes, the interface between orthogonal lamellae, and also different developmental stages of the corneal extracellular matrix.

6.2 Discussion

Although much is understood about collagen fibril architecture in the cornea, and the implications of its regularity on the tissue's transparency (Maurice, 1957, Hart and Farrell, 1969, Benedek, 1971, Farrell et al., 1973), little is known about how the fibrils are maintained in an ordered pseudo-hexagonal array that can cope with external stresses as well as the movement of water and nutrients through the stroma. Proteoglycans have been shown to be essential to controlling fibril assembly (Rada et al., 1993) and with the creation of proteoglycan-knockout mice, it has been observed, through electron microscopy (Chakravarti et al., 2000), and x-ray diffraction (Quantock et al., 2001, Meek et al., 2003), that proteoglycans contribute to the regulation of collagen fibril distribution and size. The exact modes of control that proteoglycans exert over the organised collagen fibril framework are still to be fully elucidated. However, electron tomography enables three-dimensional visualisation of macromolecular structures at relatively high resolution, allowing for a more clear interpretation as to proteoglycan interactions with collagen fibrils.

Our initial study was to determine proteoglycan dimensions and their organisation throughout the wild-type mouse cornea using electron tomography, as well as calculating the degree of collagen fibril order in the stroma through computing fibril radial distribution functions. From this, a simple model was proposed to explain how proteoglycans could effectively modulate the intricate collagen fibril organisation in the corneal stroma. Comparative analysis of the wild-type mouse cornea and reconstructions generated from genetically modified mice, granted further insights into proteoglycan structure and function.

6.2.1 Radial Distribution Functions/Proteoglycan dimensions

Corneal collagen fibrils, in a variety of species (Connon et al., 2000, Connon et al., 2004), maintain a short range order that is likely to be paramount to the tissue's transparency, as

elucidated by calculating the radial distribution function of fibrils from electron micrographs. Radial distribution functions specify the probability of locating a fibril centre at a given distance, with respect to any reference fibril, and it can show whether or not fibrillar order extends over a long range. Several studies on mammalian corneas have reported a first peak within the 40 - 55nm range (Hart and Farrell, 1969, Cox et al., 1970, Freund et al., 1995), suggesting that neighbouring fibrils are positioned with remarkable regularity, whereas second peaks arise with a lower amplitude and over a greater range, indicating that order frequently diminishes after next-nearest neighbour fibrils. The less prominent second peak is a common occurrence in analysis of collagen fibril radial distributions and fibril order rarely appears to extend past 120nm (Hart and Farrell, 1969, Freund et al., 1995, Connon et al., 2000, Cooper et al., 2006). There always appears to be short range ordering of collagen fibrils in the corneal stroma. This short range order is likely to be essential for the mutual interference of light entering the cornea as it is under half the wavelength of visible light. A significant increase in interfibrillar spacing, and the consequent decrease in fibril order, has been shown to have detrimental effects on corneal transparency and the formation of corneal haze (Meek et al., 2003, Bredrup et al., 2005, Beecher et al., 2006).

	Mouse	Cow	Human	Rabbit
	(nm)			
Corneal Thickness	**120**	**1000**	**550**	**450**
Fibril Diameter	**39.7**	**38.2**	**30.8**	**38.8**
Interfibrillar Distance	64.6 ±6.5	56.8 ±4.5	55.3 ±4.0	58.8 ±4.5
RDF 1st peak	44	N/A	41.2	46.9
Keratan sulphate Population of Total Polyanion	18%	45%	N/A	42%
*Taken from Scott and Bosworth (1990), Meek and Leonard (1993) and Freund et al (1995)				

Table 6.1. Comparison of fibril and proteoglycan characteristics in mammalian corneas.

In the mouse corneal stroma, collagen fibril order does not appear to extend beyond next-nearest neighbours, defined by a diffuse second peak at ~90nm, whereas at ~44nm there is a distinct possibility of locating a neighbouring fibril, indicated by the first prominent peak. As a result, proteoglycans in the wild-type mouse cornea would probably physically connect

both neighbouring and next-nearest neighbour collagen fibrils to be able to accurately define their spatial order. As the second peak is less prominent, the probability of locating a fibril at this distance (~90nm) is lower than finding neighbouring fibrils at a 44nm separation.

Conventional electron microscopy of mouse corneal ultrastructure hinted to two distinct proteoglycan populations with different morphologies (Young et al., 2005, Hayashida et al., 2006, Parfitt et al., 2010 - (Chapter Three)). However, analysis of proteoglycan morphology using two-dimensional images may give rise to possible inaccuracies, as detailed in an earlier study (Scott, 1992). From our measurements of proteoglycan dimensions using three-dimensional reconstructions of the mouse corneal stroma, next-nearest neighbour fibrils are interconnected infrequently by large proteoglycans approximately 122nm in length, whereas neighbouring fibrils are regularly interconnected axially by short interfibrillar proteoglycans (~31 +/- 4nm in length) and also by longer proteoglycans (~65 +/- 4nm in length) that can vary considerably in thickness (6 to 13nm in diameter). Young et al (2005) showed that the longer, sinuous proteoglycans are of the chondroitin sulphate/dermatan sulphate type whereas the small, interfibrillar proteoglycans are most likely keratan sulphate associated. The observed variation in thickness and length of the proteoglycans strongly implies that they may self-associate laterally or end-to-end to form complexes, likely to be more robust than single glycosaminoglycan chains. Also, there does not appear to be any qualitative differences in the distribution of these various proteoglycan types in the three distinct regions (anterior, mid and posterior) of the central corneal stroma.

6.2.2 Proteoglycan Self-association

Self-association of proteoglycans was first illustrated by Fransson et al (1970) and was shown to be facilitated by the sequence of disaccharides in the glycosaminoglycan chain; complementary, alternating disaccharides are more prone to aggregation, which can be also promoted by the presence of Na^+, the degree of sulphation of the glycosaminoglycan backbone and iduronate-rich sequences (Fransson and Coster, 1979). Scott (2003) furthered this study by elucidating which proteoglycan types are more susceptible to aggregation and their relative individual elasticity, as well as postulating that anti-parallel associations may be possible through hydrogen or hydrophobic bonds.

Chapter Six - Concluding Discussion

The radius of ions used in the staining of proteoglycans (i.e. Cu^{+} and WO_4^{2-}) are no more than 1nm in radius, and the width of an individual glycan chain is also likely to exceed no more than 0.5nm (Scott, 1992). Thus, the stain coating is unlikely to explain the thickness of proteoglycans observed in the wild-type mouse corneal stroma, which may frequently exceed 10nm. The variation in proteoglycan thickness and length, as well as the known thickness contribution from cationic stains, strongly implies that proteoglycans form complexes as opposed to single glycosaminoglycan chains connecting fibrils. It is possible that other bio-molecules may facilitate the formation of proteoglycan complexes, although this is unclear as of yet. In order to understand whether proteoglycan self-association occurs in a co-ordinated manner, or whether artefacts are responsible for the measured thicknesses, an investigation of proteoglycan morphology in conditions of altered aggregation was required.

The existence of a mouse model for macular corneal dystrophy, where a gene (*Chst5)* that encodes a N-acetylglucosamine 6-O sulphotransferase enzyme responsible for transferring sulphate esters to synthesising keratan sulphate is removed, allowed for the analysis of proteoglycan morphology in conditions of altered sulphation. As a consequence of keratan sulphate undersulphation, a compensatory oversulphation of chondroitin sulphate/dermatan sulphate proteoglycans is likely to have occurred. The resultant phenotype of *Chst5* removal is abnormal chondroitin sulphate/dermatan sulphate proteoglycan morphology; proteoglycans increase dramatically in both thickness and length, and near-periodic radial off-shoots are present. Irregular proteoglycans up to 4x longer (~480nm in length) and twice as thick (~29nm in diameter) as the largest proteoglycan type prevalent in the wild-type mouse cornea are evident. This increase in magnitude is strongly indicative of furthered lateral and end-to-end aggregation, as well as orthogonal self-association (shown to be all of the chondroitin sulphate/dermatan sulphate variety (Hayashida et al., 2006)). The regularity of the orthogonal branches suggests that these proteoglycans may have aggregated in a co-ordinated manner, where specific regions are able to exhibit off-shoots, although not all sites may be occupied. It is therefore postulated that proteoglycan complex formation, most likely in a co-ordinated fashion, is a key aspect of normal proteoglycan functionality in the wild-type mouse cornea that occurs to a lesser and more controlled extent than the oversized proteoglycans in the *Chst5*-null mouse cornea.

Chapter Six - Concluding Discussion

As glycosaminoglycan sulphation occurs concomitantly with chain elongation and epimerisation, any disruption at proteoglycan biosynthesis could potentially affect the length of the glycosaminoglycan and the distribution of disaccharides within the side-chain. It has been reported that (Malstrom et al., 1975, Fransson and Coster, 1979) sulphation at synthesis has a bearing on the sequence of disaccharides and the ratio of iduronate:glucuronate through epimerisation of glucuronate. Any alterations in the sequence of disaccharides could therefore lead to favourable aggregation conditions and potentially the increased self-association observed in the *Chst5*-null mouse corneas. We hypothesise that proteoglycan oversulphation and the subsequent increase in counter-ion attraction, as well as potential disaccharide sequence differences, leads to increased self-association as opposed to heightened mutual repulsion which may be expected from the increased negative charge density.

In physiological conditions, proteoglycan aggregation must therefore be regulated in order to produce discrete complexes that are relatively uniform in their dimensions and distribution throughout the stroma, as depicted in the wild-type morphometry studies (Chapter 3), with *Chst5*-null corneas highlighting the importance of sulphation in the determination of proteoglycan morphology. Interestingly, the enlarged proteoglycans in the *Chst5*-null mouse cornea also exhibit remarkable flexibility, with the ability to bend around fibrils in many cases and although they are extremely oversized and oversulphated, the fibril distribution is not greatly affected as the overall hydrophilic charge within the stroma is likely to be maintained.

6.2.3 Proteoglycan Organisation

In the three-dimensional reconstructions of wild-type, *Chst5*-null and lumican-null mouse corneas, it is apparent that the proteoglycans show no specific ordered, symmetrical arrangement around collagen fibrils - supporting the idea that proteoglycans have a dynamic influence on the maintenance of collagen fibril architecture. This is also apparent in bovine corneas (Lewis et al., 2010). In both mouse and cow, proteoglycans often display skewed angles and in some cases lie along the fibril axis, whilst some interconnect neighbouring fibrils as interfibrillar bridges at regular axial positions, in a "ladder-like" manner. This is in disagreement with previous models which postulate that proteoglycans exist in a six-fold

symmetrical arrangement (Farrell and Hart, 1969, Muller et al., 2004), connecting next-nearest neighbours to hold fibrils in a near-perfect lattice-like configuration; even though a precise lattice is not required for corneal transparency. Our findings point to a more "fluid" system whereby fibril positions are not fixed and possibly, neither are proteoglycan self-associations and proteoglycan-collagen fibril interaction.

X-ray diffraction analysis reveals that a crystalline lattice is not a requirement for transparency (Goodfellow et al., 1978) and although it is unclear as to the effects of electron microscopy preparation on the preservation of the proteoglycans' native state; a dynamic, adaptable system would be expected to be more conducive to fibril flexibility in the corneal stroma, where water, ions and nutrients could circulate without affecting the tissue's biophysical properties; namely transparency and corneal curvature. A dynamic system would also limit structural damage from external stresses and allow for cell migratory processes and the transport of important bio-molecules.

6.2.4 Dynamic Proteoglycan Regulation of Collagen Fibril Architecture

From our electron tomography study of lumican-null mouse corneas, it is apparent that proteoglycans, particularly lumican, are responsible for the separation, and consequently the prevention of fusion, of neighbouring fibrils through their interconnection at regular axial intervals. As lumican is not as abundant as chondroitin sulphate/dermatan sulphate associated proteoglycans in the mouse cornea, only few fused fibrils are observed in the lumican-null mouse cornea, although other research (Chakravarti et al., 2000) suggests the prevalence of fibril defects may increase with age. The dramatic increase in fibril aggregates in decorin/biglycan knockout mouse corneas (Zhang et al., 2009) further supports a role for proteoglycans in the prevention of fibril fusion and the maintenance of neighbouring fibril separation. Moreover, when proteoglycans are introduced *in vitro* to collagen type I fibrils, lateral association of fibrils is limited (Rada et al., 1993). Here, we propose a model to explain how proteoglycans maintain the organised fibril assembly in the cornea based on our findings from the wild-type and homozygous lumican null mouse cornea (Chapter 5).

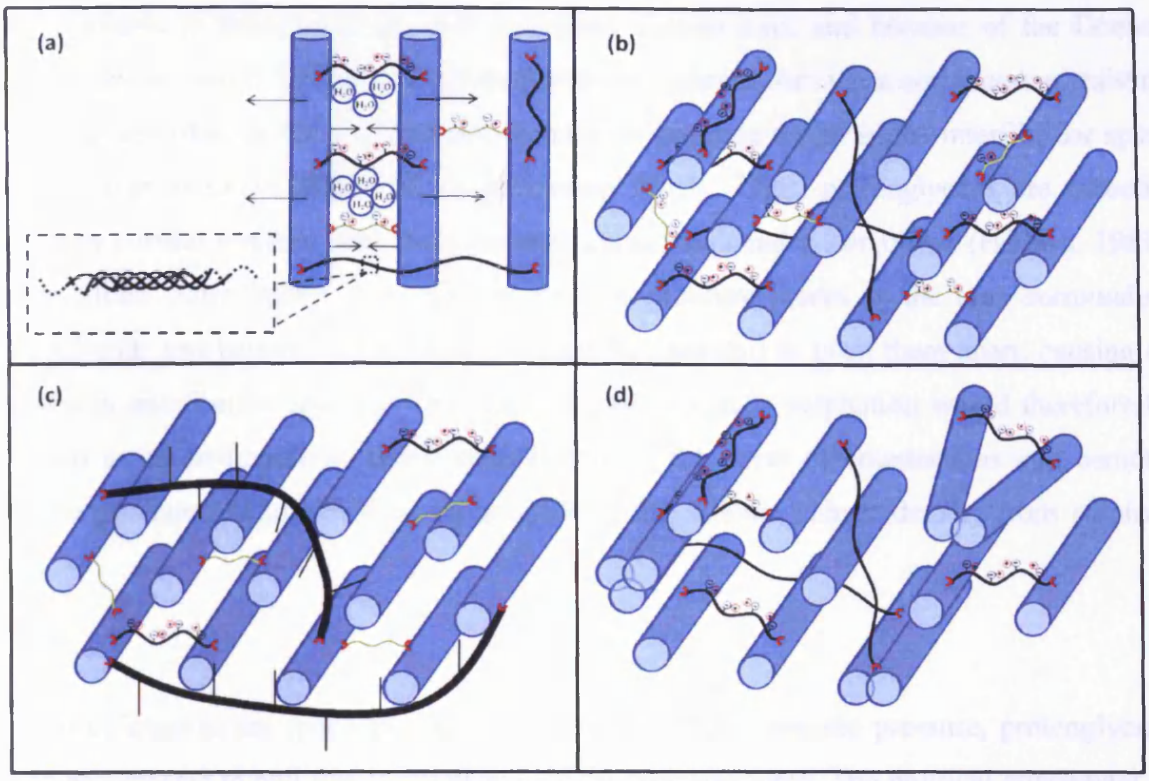

Table. 6.2. The role of proteoglycans in the regulation of corneal collagen fibril architecture and the effects of altered proteoglycan biosynthesis. (a) Proteoglycans (keratan sulphate = green, chondroitin sulphate/dermatan sulphate = black), considered to pack as complexes in an anti-parallel, co-ordinated fashion, regulate interfibrillar spacing through a balance of opposing forces (black arrows). In some cases, proteoglycans lie along the fibril axis which suggests that they have the ability to move according to the requirements of the tissue and to maintain dynamic regulation of fibril organisation. (b) In the wild-type mouse cornea, fibrils are positioned in a pseudo-hexagonal lattice that allows for light transmission through the cornea. Corneal proteoglycans do not exhibit any rotational symmetry around collagen fibrils and are able to interconnect neighbouring and less frequently, next-nearest neighbour fibrils. (c) Upon defective sulphate transfer to keratan sulphate glycosaminoglycans, chondroitin sulphate/dermatan sulphate proteoglycans become oversulphated and exhibit irregular morphologies in the *Chst5*-null mouse cornea. Smaller chondroitin sulphate/dermatan sulphate proteoglycans bind periodically and orthogonally along the enlarged chondroitin sulphate/dermatan sulphate body or possibly, elongated glycosaminoglycans are forced to protrude out due to the increased aggregation in the main proteoglycan complex. Glycosaminoglycans may also pack in a coiling conformation, as suggested for the normal proteoglycans in (a) and similar to the case of hyaluronan (Arnott et al., 1983). Collagen organisation remains relatively intact as the overall hydrophilic charge likely stays similar to that of the wild-type mouse corneal stroma. (d) When lumican, the major keratan sulphate proteoglycan of the cornea, is removed, collagen fibrils fuse laterally. This suggests that proteoglycans actively separate fibrils to prevent their fusion. Fusion of fibrils, and their subsequent lateral aggregation, would affect fibril diameter and the spatial distribution of collagen in the cornea, in turn this would affect the transparency of the cornea.

Chapter Six - Concluding Discussion

Highly anionic proteoglycans are able to attract counter-ions, and because of the Donnan effect, water molecules hydrate the proteoglycan complexes forming a compression resistant bio-gel. Water entering the stroma leads to osmotic pressure/turgor in the interfibrillar space and give rise to forces that repel neighbouring fibrils. Thus, proteoglycans are essential players in corneal swelling and their removal causes reduced water influx (Hedbys, 1961). The localised water intake gives rise to osmotic pressure forces in the area surrounding proteoglycans and between fibrils which would be expected to push them apart, causing an increase in interfibrillar spacing. The extent of proteoglycan sulphation would therefore be expected to be an important factor contributing to the level of counter-ions and osmotic pressure generated within an area, as a result of the anionic charge density from sulphate esters.

To restrict interfibrillar space expanding excessively from osmotic pressure, proteoglycans would be expected to pull fibrils together with an opposite force. The physical attachment of protein cores to fibrils would be expected to prevent fibrils from being positioned too far apart and from coming into immediate proximity to each other, maintaining fibrils at a given distance according to glycosaminoglycan chain length. Furthermore, thermal motion of glycosaminoglycans would retract the terminal ends of the proteoglycans, which are non-covalently bound to collagen fibrils through their protein constituent, and therefore, attached fibrils would experience an attractive force as a result. Constant bombardment of glycosaminoglycans by molecules and ions would be expected to also facilitate the retraction of the proteoglycan terminal ends. As a result of this, fibrils would be expected to constantly move from their average position and potentially come closer together. Therefore, proteoglycans prevent the fibrils from coming into contact through a balance of these forces and the attachment of protein cores to specific binding sites on fibrils, and thus, fibril fusion is prevented and average positions are maintained, enabling light transmission through the cornea.

The extent to which either force is exerted, and whether fibrils are pushed apart or pulled closer together, would be dependent on a variety of factors that affect proteoglycan characteristics. These could include disaccharide sequence, sulphation patterns and the consequent charge density, relative content of iduronate:glucuronate, chain length, and also

the extent of self-association (chain width). The glycosaminoglycan chain length and extent of aggregation, shown previously to be reliant on the degree of disaccharide sulphation, would likely determine fibril separation distances and the robustness of attachment. The amount of each of the different proteoglycans in the stroma, and also the counter-ions present, affect the drawing and retention of water in the stroma (Hedbys, 1961), and so it is likely that the concentrations of individual proteoglycan types are regulated in homeostasis to achieve optimal control of fibril assembly and architecture. This is supported by the compensatory mechanisms that occur when proteoglycans are altered at the genetic level (Carlson et al., 2005), and also the varying proteoglycan compositions observed in corneas from different species that exhibit varying degrees of thickness (Scott and Bosworth, 1990).

Appendices

CB	Cuprolinic Blue
CCD	Charged Coupled Device
CS	Chondroitin Sulphate
DS	Dermatan Sulphate
ECM	Extra-cellular Matrix
g	Gram
GAG	Glycosaminoglycan
KS	Keratan Sulphate
Mg	Milligram
$MgCl_2$	Magnesium Chloride
ml	Millilitre
nm	Nanometre
PEI	Polyetherimide
PG	Proteoglycan
TEM	Transmission Electron Microscope
µm	Micrometre

Appendices

Materials	Supplier
Araldite Monomer CY212	Agar Scientific
BDMA Accelerator	Agar Scientific
Chloroform	Sigma-Aldrich
10nm Colloidal Gold	BBInternational
0.05% Cuprolinic Blue (0.01g)	BDH
DDSA Hardener	Agar Scientific
EM slot grids (2mm x 1mm)	TAAB
EMKMR2 Glass-cutter	Leica
Ethanol (50%, 70%, 90%, 100%)	Sigma-Aldrich
Ethylene Dichloride (1,2 – Dicholoroethane)	Sigma-Aldrich
Glass	Leica
2.5% Glutaraldehyde (2ml)	Agar Scientific
JEM1010 TEM	Jeol
Kodak MegaPlus 1.4/digital CCD camera	Gatan
0.1M Magnesium Chloride	TAAB
Microscope Slides	TAAB
1% Phospho-tungstate Acid	TAAB
Polyetherimide granules	Goodfellow
Propylene Oxide	Agar Scientific
25mM Sodium Acetate (20ml, pH5.7)	Aldrich

Appendices

0.5% Sodium Tungstate (Aq.)	TAAB
Ultracut Microtome	Reichart-Jung
2% Uranyl Acetate	BDH

Appendices

Appendix One

Measurement of proteoglycan dimensions and collagen fibril diameter and distribution in the mouse corneal stroma.

Collagen fibril diameter and interfibrillar distance were calculated from transverse section micrographs with a known pixel size of 0.33nm. The collagen fibril D-period (~65nm in cornea) and gold fiducial markers (10nm) were used for internal calibration. All measurements were made using ImageJ software.

Anterior Mouse Corneal Stroma			
Collagen Fibril Diameters		Interfibrillar Spacing	
Pixels	Diameter (nm)	Pixels	IF Distance (nm)
	AVG = 30.8 ± 1.9		AVG = 48.8 ± 4.5
90	29.7	141	46.53
93	30.69	174	57.42
99	32.67	126	41.58
94	31.02	141	46.53
99	32.67	146	48.18
93	30.69	162	53.46
87	28.71	153	50.49
90	29.7	127	41.91
90	29.7	144	47.52
99	32.67	150	49.5
84	27.72	132	43.56
99	32.67	150	49.5
90	29.7	144	47.52
87	28.71	162	53.46
105	34.65	150	49.5
90	29.7	141	46.53
84	27.72	154	50.82
87	28.71	144	47.52
102	33.66	144	47.52
96	31.68	174	57.42
96	31.68	150	49.5
84	27.72	162	53.46
94	31.02	150	49.5
84	27.72	132	43.56
90	29.7	141	46.53
93	30.69	126	41.58
93	30.69	174	57.42
99	32.67	154	50.82
96	31.68	141	46.53
96	31.68	132	43.56

87	28.71	144	47.52
84	27.72	162	53.46
99	32.67	153	50.49
96	31.68	144	47.52
94	31.02	174	57.42
93	30.69	171	56.43
99	32.67	147	48.51
102	33.66	154	50.82
105	34.65	162	53.46
90	29.7	132	43.56
96	31.68	144	47.52
94	31.02	150	49.5
90	29.7	141	46.53

Mid Mouse Corneal Stroma			
Collagen Fibril Diameters		Interfibrillar Spacing	
Pixels	Diameter (nm)	Pixels	IF Distance (nm)
	AVG = 32.0 ± 2.8		AVG = 49.1 ± 3.9
104	34.32	120	39.6
88	29.04	136	44.88
100	33	170	56.1
100	33	145	47.85
112	36.96	150	49.5
84	27.72	140	46.2
88	29.04	162	53.46
112	36.96	132	43.56
112	36.96	154	50.82
108	35.64	144	47.52
88	29.04	141	46.53
96	31.68	160	52.8
92	30.36	141	46.53
88	29.04	156	51.48
96	31.68	152	50.16
88	29.04	148	48.84
100	33	141	46.53
112	36.96	126	41.58
102	33.66	144	47.52
100	33	156	51.48
112	36.96	178	58.74
116	38.28	134	44.22
92	30.36	144	47.52
91	30.03	141	46.53
94	31.02	144	47.52

Appendices

100	33	150	49.5
92	30.36	132	43.56
93	30.69	138	45.54
98	32.34	165	54.45
100	33	144	47.52
92	30.36	153	50.49
96	31.68	131	43.23
99	32.67	133	43.89
92	30.36	145	47.85
88	29.04	148	48.84
101	33.33	160	52.8
86	28.38	172	56.76
102	33.66	156	51.48
84	27.72	142	46.86
92	30.36	144	47.52
86	28.38	156	51.48
106	34.98	141	46.53
105	34.65	152	50.16
91	30.03	157	51.81
96	31.68	153	50.49
98	32.34	148	48.84
100	33	166	54.78
92	30.36	145	47.85
88	29.04	165	54.45
86	28.38	150	49.5
100	33	144	47.52

Posterior Mouse Corneal Stroma			
Collagen Fibril Diameters		Interfibrillar Spacing	
Pixels	Diameter (nm)	Pixels	IF Distance (nm)
	AVG = 28.9 ± 1.6		AVG = 51.9 ± 5.7
84	27.72	150	49.5
90	29.7	136	44.88
82	27.06	144	47.52
88	29.04	153	50.49
92	30.36	138	45.54
88	29.04	134	44.22
82	27.06	120	39.6
77	25.41	186	61.38
82	27.06	178	58.74
83	27.39	156	51.48
83	27.39	152	50.16
93	30.69	140	46.2

90	29.7	144	47.52
82	27.06	162	53.46
86	28.38	158	52.14
92	30.36	158	52.14
88	29.04	142	46.86
94	31.02	184	60.72
96	31.68	168	55.44
82	27.06	129	42.57
88	29.04	180	59.4
92	30.36	177	58.41
90	29.7	127	41.91
96	31.68	176	58.08
88	29.04	183	60.39
84	27.72	172	56.76
85	28.05	142	46.86
85	28.05	154	50.82
82	27.06	162	53.46
92	30.36	140	46.2
94	31.02	149	49.17
88	29.04	175	57.75
90	29.7	164	54.12
90	29.7	154	50.82
84	27.72	144	47.52
86	28.38	175	57.75
90	29.7	168	55.44
88	29.04	178	58.74
82	27.06	128	42.24
77	25.41	144	47.52
80	26.4	167	55.11
92	30.36	182	60.06
86	28.38	155	51.15
82	27.06	154	50.82
88	29.04	167	55.11
96	31.68	184	60.72
92	30.36	156	51.48
90	29.7	144	47.52
92	30.36	153	50.49
88	29.04	177	58.41
98	32.34	164	54.12

Appendices

Three-dimensional reconstruction of the wild-type mouse corneal stroma

Anterior stroma in longitudinal section

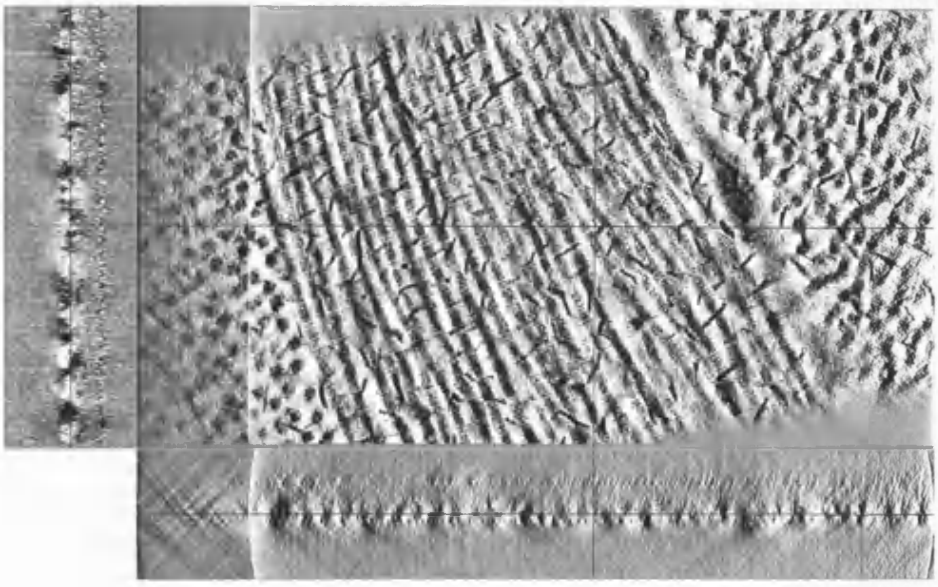

Anterior stroma in transverse section

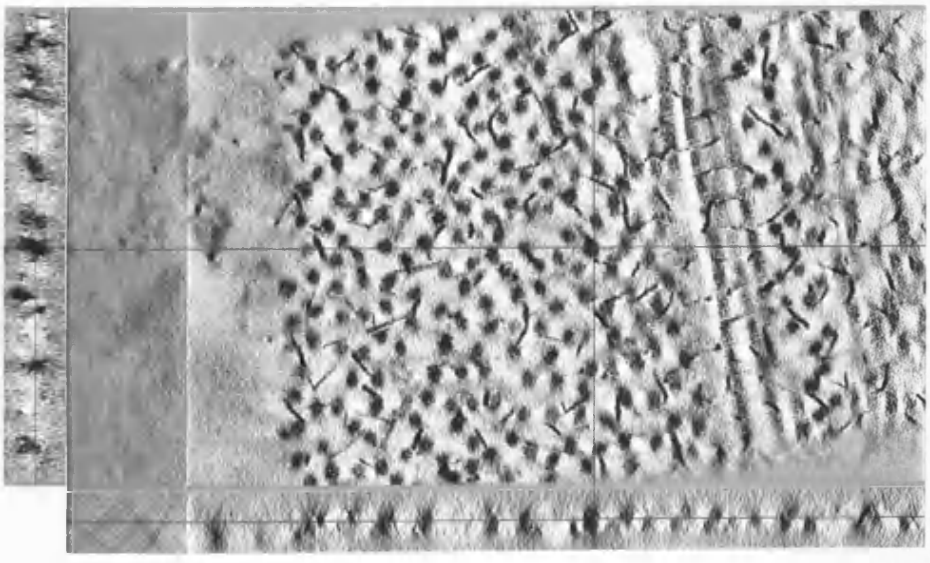

Appendices

Measurement of proteoglycan dimensions

Proteoglycans were only measured if their whole morphology was contained within the reconstruction and also lying in the same plane as the surface of the plastic section. Again, ImageJ was used for measurements.

Anterior Mouse Corneal Stroma			
Proteoglycan Dimensions			
Pixels	Thickness (nm)	Pixels	Length (nm)
20	6.6	210	69.3
32	10.56	197	65.01
18	5.94	192	63.36
28	9.24	202	66.66
32	10.56	200	66
18	5.94	103	33.99
30	9.9	218	71.94
22	7.26	212	69.96
36	11.88	218	71.94
16	5.28	92	30.36
11	3.63	94	31.02
26	8.58	320	105.6
26	8.58	387	127.71
16	5.28	95	31.35
14	4.62	97	32.01
28	9.24	182	60.06
32	10.56	384	126.72
13	4.29	85	28.05
16	5.28	87	28.71

Mid Mouse Corneal Stroma			
Proteoglycan Dimensions			
Pixels	Thickness (nm)	Pixels	Length (nm)
34	11.22	194	64.02
19	6.27	128	42.24
18	5.94	181	59.73
14	4.62	91	30.03
18	5.94	86	28.38
33	10.89	193	63.69
38	12.54	182	60.06
34	11.22	394	130.02

Appendices

13	4.29	85	28.05
12	3.96	96	31.68
15	4.95	91	30.03
28	9.24	184	60.72
33	10.89	198	65.34
21	6.93	115	37.95
16	5.28	89	29.37
30	9.9	185	61.05
18	5.94	98	32.34
24	7.92	194	64.02

Posterior Mouse Corneal Stroma Proteoglycan Dimensions			
Pixels	Thickness (nm)	Pixels	Length (nm)
30	9.9	215	70.95
34	11.22	194	64.02
13	4.29	84	27.72
32	10.56	188	62.04
24	7.92	202	66.66
32	10.56	192	63.36
18	5.94	97	32.01
12	3.96	87	28.71
34	11.22	371	122.43
18	5.94	108	35.64
20	6.6	187	61.71
32	10.56	178	58.74
12	3.96	89	29.37
11	3.63	97	32.01
12	3.96	91	30.03
28	9.24	190	62.7

Radial Distribution Functions were calculated out using in-house software after relative positions of cross-section fibrils were plotted and normalised.

Radial Distribution Function of Collagen Fibrils in the Mouse Corneal Stroma				
	g(r)			
Centre-to-Centre Distance (nm)	Anterior	Mid-Stroma	Posterior	Overall Stroma Average
0	0	0	0	0
2.75	0	0	0	0

5.5	0	0	0	0
8.25	0	0	0	0
11	0	0	0	0
13.75	0	0	0	0
16.5	0	0	0.006154	0.002051
19.25	0.005333	0.013333	0.016	0.011556
22	0.016471	0.028235	0.077647	0.040784
24.75	0.092632	0.088421	0.107368	0.09614
27.5	0.152381	0.19619	0.205714	0.184762
30.25	0.330435	0.37913	0.342609	0.350725
33	0.7456	0.7744	0.6512	0.723733
35.75	1.124444	0.965926	0.811852	0.967407
38.5	1.38069	1.343448	0.855172	1.193103
41.25	1.505806	1.298065	0.814194	1.206022
44	1.669091	1.392727	0.996364	1.352727
46.75	1.389714	1.112	0.835429	1.112381
49.5	1.152432	1.08973	0.851892	1.031351
52.25	0.961026	0.982564	0.785641	0.909744
55	0.900488	0.83122	0.844878	0.858862
57.75	0.773023	0.645581	0.698605	0.705736
60.5	0.801778	0.756444	0.698667	0.752296
63.25	0.773617	0.710638	0.655319	0.713191
66	0.795102	0.737959	0.72898	0.754014
68.75	0.781961	0.75451	0.660392	0.732288
71.5	0.833962	0.798491	0.700377	0.77761
74.25	0.856727	0.84	0.701818	0.799515
77	0.945263	0.89193	0.801404	0.879532
79.75	0.942373	0.834576	0.68	0.818983
82.5	1.028852	0.912787	0.704918	0.882186
85.25	1.012063	0.891429	0.63619	0.846561
88	1.006769	0.954462	0.741538	0.900923
90.75	0.97194	0.896119	0.727164	0.865075
93.5	1.018551	0.936232	0.710725	0.888502
96.25	0.953239	0.851831	0.699718	0.83493
99	0.966027	0.90137	0.730959	0.866119
101.75	0.931733	0.8176	0.7232	0.824178
104.5	0.895584	0.812987	0.710649	0.806407
107.25	0.921519	0.827342	0.761013	0.836624
110	0.840494	0.840988	0.731358	0.80428
112.75	0.906024	0.765301	0.70506	0.792129
115.5	0.889412	0.864471	0.700706	0.818196
118.25	0.922299	0.825287	0.666667	0.804751
121	0.950562	0.896629	0.716404	0.854532
123.75	0.939341	0.897143	0.720879	0.852454

126.5	0.887312	0.87871	0.687742	0.817921
129.25	0.941474	0.859368	0.647158	0.816
132	0.961237	0.880412	0.760825	0.867491
134.75	0.924444	0.837576	0.731717	0.831246
137.5	0.937426	0.857426	0.732277	0.842376
140.25	0.911068	0.83534	0.699417	0.815275
143	0.944762	0.875048	0.719619	0.846476
145.75	0.866168	0.824299	0.672523	0.787664
148.5	0.93578	0.787523	0.709725	0.811009
151.25	0.904505	0.78018	0.711712	0.798799
154	0.932743	0.838938	0.689204	0.820295
156.75	0.897391	0.804522	0.67687	0.792928
159.5	0.911111	0.874872	0.690598	0.825527
162.25	0.923361	0.814118	0.65916	0.79888

Appendix Two

Measurement of proteoglycan dimensions

Measurement of proteoglycan dimensions in the *Chst5*-null mouse cornea were restricted to those wholly contained and lying in the plane of the plastic section.

Proteoglycan Dimensions in the Anterior *Chst5*-null Mouse Corneal Stroma					
Branched Proteoglycans		Proteoglycan Branches		Unbranched Proteoglycans	
Thickness (nm)	Length (nm)	Thickness (nm)	Length (nm)	Thickness (nm)	Length (nm)
21	349	9	67	10	60
17	226	10	60	7	57
20	170	11	62	8	69
29	184	9	75	8	59
15	270	14	69	9	70
		11	57	12	115
		10	64	8	60
		10	52		
		7	66		
		9	68		
		8	61		

Proteoglycan Dimensions in the Mid *Chst5*-null Mouse Corneal Stroma					
Branched Proteoglycans		Proteoglycan Branches		Unbranched Proteoglycans	
Thickness (nm)	Length (nm)	Thickness (nm)	Length (nm)	Thickness (nm)	Length (nm)
18	320	11	56	8	68
19	208	9	56	7	65

20	223	7	50	8	60
		10	64	10	62
				7	60

Proteoglycan Dimensions in the Posterior *Chst5*-null Mouse Corneal Stroma					
Branched Proteoglycans		Proteoglycan Branches		Unbranched Proteoglycans	
Thickness (nm)	Length (nm)	Thickness (nm)	Length (nm)	Thickness (nm)	Length (nm)
18	238	9	69	8	72
24	173	8	66	8	76
18	460	9	70	9	71
18	314	9	70	11	110
19	240	8	56		
		8	72		
		9	66		
		8	72		

Three-dimensional reconstruction of the *Chst5*-null mouse corneal stroma

Posterior stroma in longitudinal section

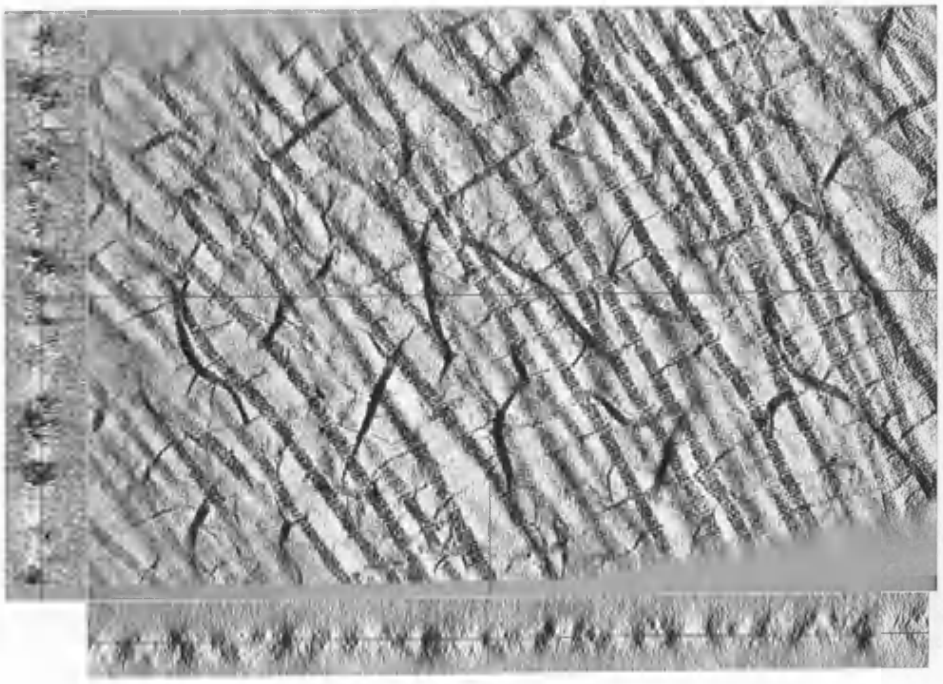

Posterior stroma in transverse section

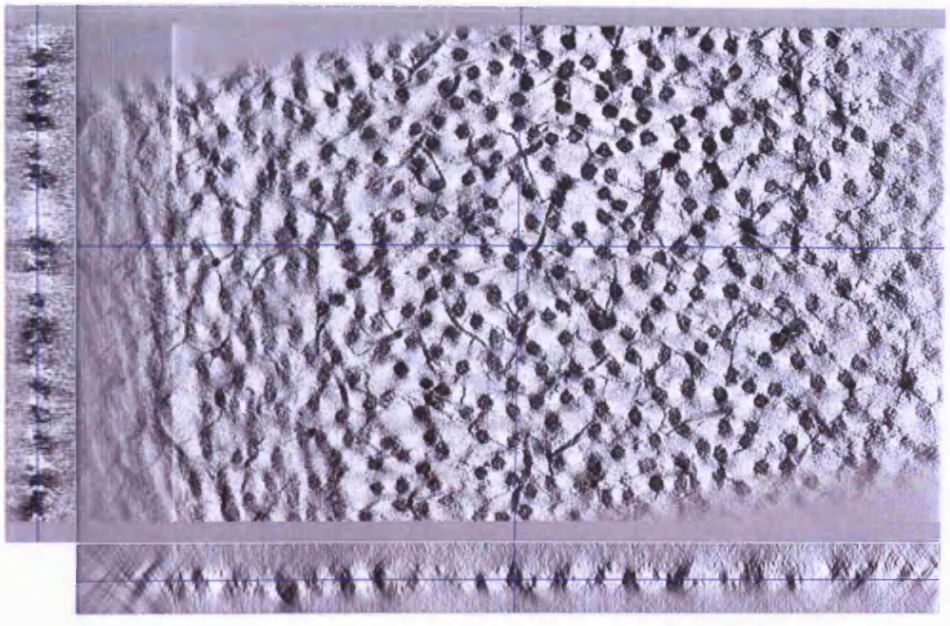

Appendix Three

Three-dimensional reconstruction of the lumican-null mouse corneal stroma

Posterior stroma in longitudinal section

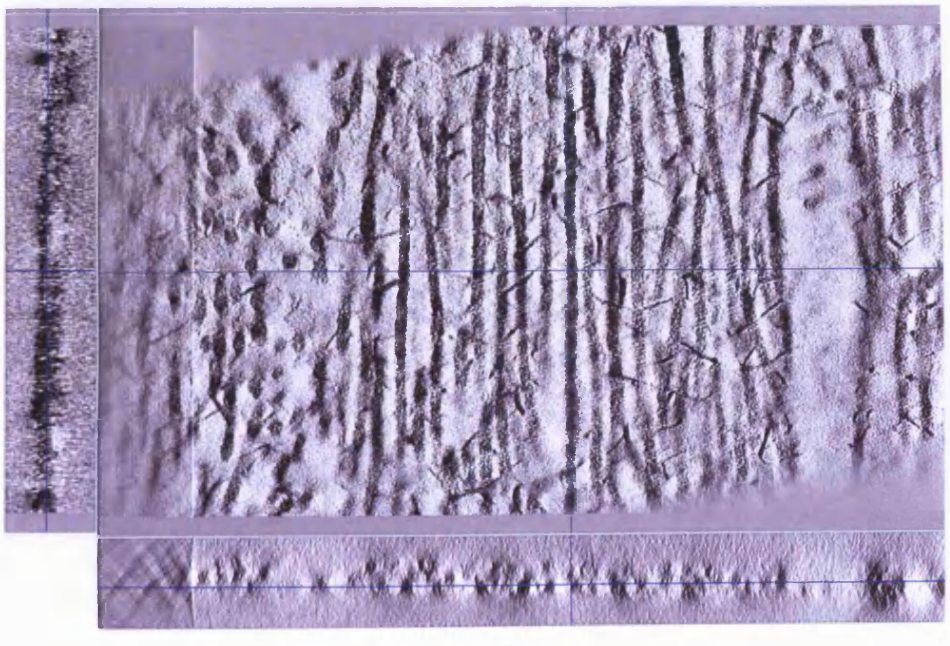

Appendices

Posterior stroma in transverse section

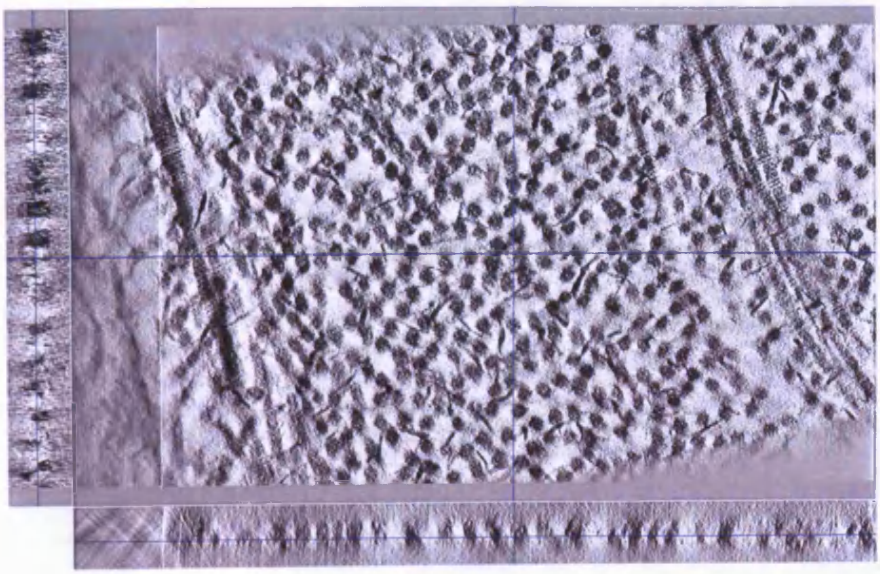

irregular fused fibril in the posterior stroma of the lumican-null mouse corneal stroma

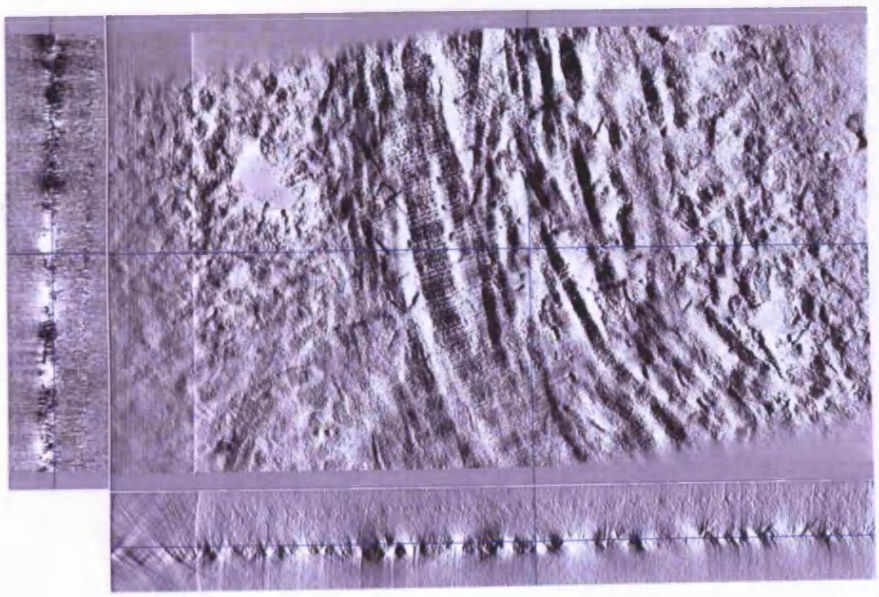

Appendices

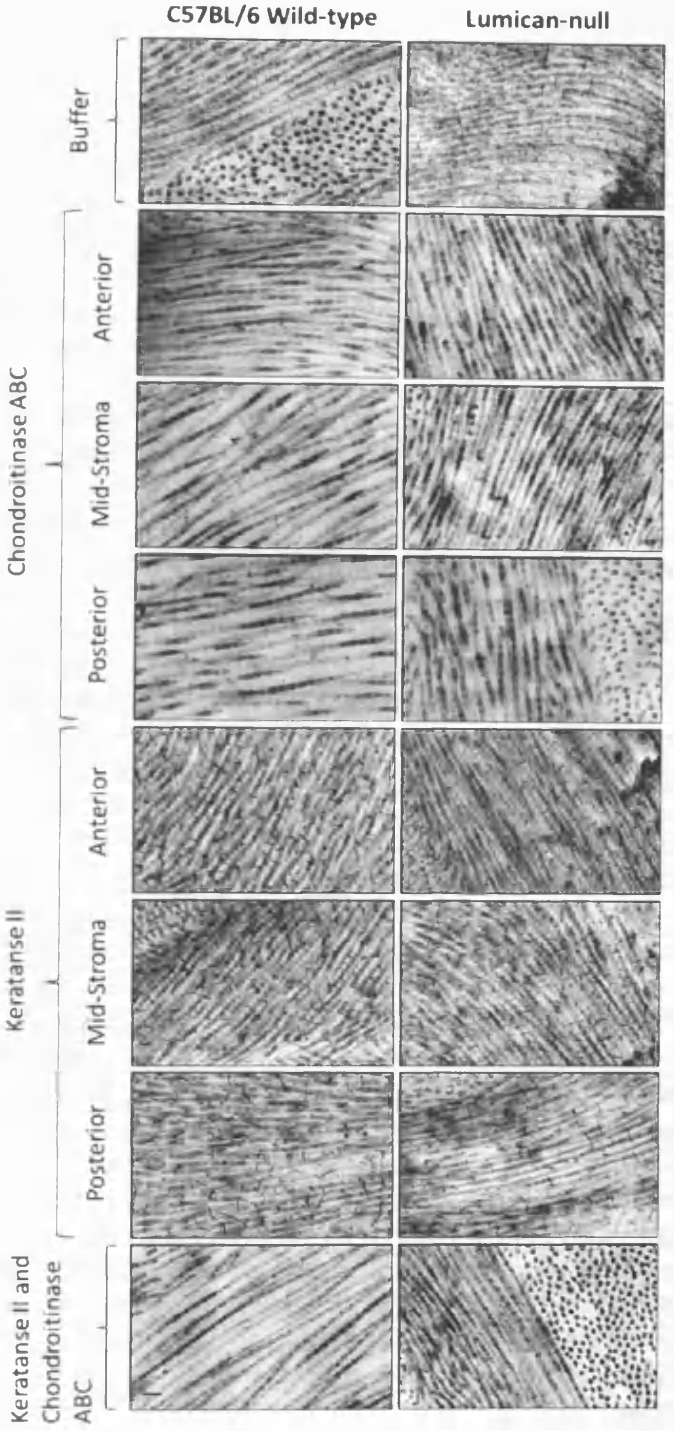

Enzymatic digestion through the stroma of (left panel) the wild-type mouse cornea and (right panel) lumican-null mouse cornea.

No obvious qualitative differences were observed through the stroma and in the different stromal regions and so only the mid-stroma was used (Chapter Five).

References

ABRAMOFF, M. D., MAGELHAES, P.J., RAM, S.J. 2004. Image Processing with ImageJ. *Biophotonics International,* 11, 36-42.

AGHAMOHAMMADZADEH, H., NEWTON, R. H. & MEEK, K. M. 2004. X-ray scattering used to map the preferred collagen orientation in the human cornea and limbus. *Structure,* 12, 249-56.

AKAMA, T. O., NISHIDA, K., NAKAYAMA, J., WATANABE, H., OZAKI, K., NAKAMURA, T., DOTA, A., KAWASAKI, S., INOUE, Y., MAEDA, N., YAMAMOTO, S., FUJIWARA, T., THONAR, E. J., SHIMOMURA, Y., KINOSHITA, S., TANIGAMI, A. & FUKUDA, M. N. 2000. Macular corneal dystrophy type I and type II are caused by distinct mutations in a new sulphotransferase gene. *Nat Genet,* 26, 237-41.

AKIMOTO, Y., YAMAKAWA, N., FURUKAWA, K., KIMATA, K., KAWAKAMI, H. & HIRANO, H. 2002. Changes in distribution of the long form of type XII collagen during chicken corneal development. *J Histochem Cytochem,* 50, 851-62.

ALBERTS, B., JOHNSON, A., LEWIS, J. & RAFF, M. 2002. *Molecular Biology of the Cell,* Garland.

ARNOTT, S., MITRA, A. K. & RAGHUNATHAN, S. 1983. Hyaluronic acid double helix. *J Mol Biol,* 169, 861-72.

BEECHER, N., CARLSON, C., ALLEN, B. R., KIPCHUMBA, R., CONRAD, G. W., MEEK, K. M. & QUANTOCK, A. J. 2005. An x-ray diffraction study of corneal structure in mimecan-deficient mice. *Invest Ophthalmol Vis Sci,* 46, 4046-9.

BEECHER, N., CHAKRAVARTI, S., JOYCE, S., MEEK, K. M. & QUANTOCK, A. J. 2006. Neonatal development of the corneal stroma in wild-type and lumican-null mice. *Invest Ophthalmol Vis Sci,* 47, 146-50.

BENEDEK, G. B. 1971. Theory of transparency of the eye. *Applied Optics.*

BETTELHEIM, F. A. & PLESSY, B. 1975. The hydration of proteoglycans of bovine cornea. *Biochim Biophys Acta,* 381, 203-14.

BEUERMAN, R. & PEDROZA, L. 1996. Ultrastructure of the human cornea. *Microscopy Research and Technique,* 33, 320-335.

BIRK, D. E. 2001. Type V collagen: heterotypic type I/V collagen interactions in the regulation of fibril assembly. *Micron,* 32, 223-37.

BIRK, D. E., FITCH, J. M., BABIARZ, J. P., DOANE, K. J. & LINSENMAYER, T. F. 1990. Collagen fibrillogenesis in vitro: interaction of types I and V collagen regulates fibril diameter. *J Cell Sci,* 95 (Pt 4), 649-57.

BIRK, D. E., FITCH, J. M., BABIARZ, J. P. & LINSENMAYER, T. F. 1988. Collagen type I and type V are present in the same fibril in the avian corneal stroma. *J Cell Biol,* 106, 999-1008.

BIRK, D. E., FITCH, J. M. & LINSENMAYER, T. F. 1986. Organization of collagen types I and V in the embryonic chicken cornea. *Invest Ophthalmol Vis Sci,* 27, 1470-7.

BLOCHBERGER, T. C., VERGNES, J. P., HEMPEL, J. & HASSELL, J. R. 1992. cDNA to chick lumican (corneal keratan sulfate proteoglycan) reveals homology to the small interstitial proteoglycan gene family and expression in muscle and intestine. *J Biol Chem,* 267, 347-52.

BONANNO, J. A. 2003. Identity and regulation of ion transport mechanisms in the corneal endothelium. *Prog Retin Eye Res,* 22, 69-94.

BOOTE, C., DENNIS, S., NEWTON, R. H., PURI, H. & MEEK, K. M. 2003. Collagen fibrils appear more closely packed in the prepupillary cornea: optical and biomechanical implications. *Invest Ophthalmol Vis Sci,* 44, 2941-8.

BORCHERDING, M. S., BLACIK, L. J., SITTIG, R. A., BIZZELL, J. W., BREEN, M. & WEINSTEIN, H. G. 1975. Proteoglycans and collagen fibre organization in human corneoscleral tissue. *Exp Eye Res,* 21, 59-70.

BREDRUP, C., KNAPPSKOG, P. M., MAJEWSKI, J., RODAHL, E. & BOMAN, H. 2005. Congenital stromal dystrophy of the cornea caused by a mutation in the decorin gene. *Invest Ophthalmol Vis Sci,* 46, 420-6.

References

BRON, A. J. 2001. The architecture of the corneal stroma. *Br J Ophthalmol,* 85, 379-81.

CARLSON, E. C., LIU, C. Y., CHIKAMA, T., HAYASHI, Y., KAO, C. W., BIRK, D. E., FUNDERBURGH, J. L., JESTER, J. V. & KAO, W. W. 2005. Keratocan, a cornea-specific keratan sulfate proteoglycan, is regulated by lumican. *J Biol Chem,* 280, 25541-7.

CASPERSSON, T. & ENGSTROM, A. 1949. Corneal Transparency. *Nord. Med,* 30, 1279.

CASTORO, J. A., BETTELHEIM, A. A. & BETTELHEIM, F. A. 1988. Water gradients across bovine cornea. *Invest Ophthalmol Vis Sci,* 29, 963-8.

CHAKRAVARTI, S. & MAGNUSON, T. 1995. Localization of mouse lumican (keratan sulfate proteoglycan) to distal chromosome 10. *Mamm Genome,* 6, 367-8.

CHAKRAVARTI, S., MAGNUSON, T., LASS, J. H., JEPSEN, K. J., LAMANTIA, C. & CARROLL, H. 1998. Lumican regulates collagen fibril assembly: skin fragility and corneal opacity in the absence of lumican. *J Cell Biol,* 141, 1277-86.

CHAKRAVARTI, S., PETROLL, W. M., HASSELL, J. R., JESTER, J. V., LASS, J. H., PAUL, J. & BIRK, D. E. 2000. Corneal opacity in lumican-null mice: defects in collagen fibril structure and packing in the posterior stroma. *Invest Ophthalmol Vis Sci,* 41, 3365-73.

CLARK, C. C. 1982. Asparagine-linked glycosides. *Methods Enzymol,* 82 Pt A, 346-60.

CONNON, C. J., MARSHALL, J., PATMORE, A. L., BRAHMA, A. & MEEK, K. M. 2003. Persistent haze and disorganization of anterior stromal collagen appear unrelated following phototherapeutic keratectomy. *J Refract Surg,* 19, 323-32.

CONNON, C. J., MEEK, K. M., KINOSHITA, S. & QUANTOCK, A. J. 2004. Spatial and temporal alterations in the collagen fibrillar array during the onset of transparency in the avian cornea. *Exp Eye Res,* 78, 909-15.

CONNON, C. J., MEEK, K. M., NEWTON, R. H., KENNEY, M. C., ALBA, S. A. & KARAGEOZIAN, H. 2000. Hyaluronidase treatment, collagen fibril packing, and normal transparency in rabbit corneas. *J Refract Surg,* 16, 448-55.

COOPER, L. J., BENTLEY, A. J., NIEDUSZYNSKI, I. A., TALABANI, S., THOMSON, A., UTANI, A., SHINKAI, H., FULLWOOD, N. J. & BROWN, G. M. 2006. The role of dermatopontin in the stromal organization of the cornea. *Invest Ophthalmol Vis Sci,* 47, 3303-10.

CORNUET, P. K., BLOCHBERGER, T. C. & HASSELL, J. R. 1994. Molecular polymorphism of lumican during corneal development. *Invest Ophthalmol Vis Sci,* 35, 870-7.

COX, J. L., FARRELL, R. A., HART, R. W. & LANGHAM, M. E. 1970. The transparency of the mammalian cornea. *J Physiol,* 210, 601-16.

CRAIG, A. S. & PARRY, D. A. 1981. Collagen fibrils of the vertebrate corneal stroma. *J Ultrastruct Res,* 74, 232-9.

CRAIG, A. S., ROBERTSON, J. G. & PARRY, D. A. 1986. Preservation of corneal collagen fibril structure using low-temperature procedures for electron microscopy. *J Ultrastruct Mol Struct Res,* 96, 172-5.

DANIELSON, K. G., BARIBAULT, H., HOLMES, D. F., GRAHAM, H., KADLER, K. E. & IOZZO, R. V. 1997. Targeted disruption of decorin leads to abnormal collagen fibril morphology and skin fragility. *J Cell Biol,* 136, 729-43.

DEA, I. C., MOORHOUSE, R., REES, D. A., ARNOTT, S., GUSS, J. M. & BALAZS, E. A. 1973. Hyaluronic acid: a novel, double helical molecule. *Science,* 179, 560-2.

DEROSIER, D. J. & KLUG, A. 1968. Reconstruction of three-dimensional structures from electron micrographs. *Nature,* 217.

DOETSCHMAN, T., GREGG, R. G., MAEDA, N., HOOPER, M. L., MELTON, D. W., THOMPSON, S. & SMITHIES, O. 1987. Targetted correction of a mutant HPRT gene in mouse embryonic stem cells. *Nature,* 330, 576-8.

DOUGHTY, M. J. & MAURICE, D. 1988. Bicarbonate sensitivity of rabbit corneal endothelium fluid pump in vitro. *Invest Ophthalmol Vis Sci,* 29, 216-23.

References

DUNLEVY, J. R., NEAME, P. J., VERGNES, J. P. & HASSELL, J. R. 1998. Identification of the N-linked oligosaccharide sites in chick corneal lumican and keratocan that receive keratan sulfate. *J Biol Chem,* 273, 9615-21.

EIKENBERRY, E. F., BRODSKY, B. B., CRAIG, A. S. & PARRY, D. A. D. 1982. Collagen fibril morphology in developing chick metatarsal tendon: 2. Electron microscope studies. *International Journal of Biological Macromolecules,* 4, 393-398.

ELLIOTT, G. F., HODSON, S.A. 1998. Cornea, and the swelling of polyelectrolyte gels of biological interest *Rep. Prog. Phys.,* 61, 1325-1365.

EYRE, D. R., PAZ, M. A. & GALLOP, P. M. 1984. Cross-linking in collagen and elastin. *Annu Rev Biochem,* 53, 717-48.

EZURA, Y., CHAKRAVARTI, S., OLDBERG, A., CHERVONEVA, I. & BIRK, D. E. 2000. Differential expression of lumican and fibromodulin regulate collagen fibrillogenesis in developing mouse tendons. *J Cell Biol,* 151, 779-88.

FARRELL, R. A. 1994. Corneal Transparency. *In:* ALBERT, D. M. A. J., S.A. (ed.) *Principles and Practice of Opthalmology.* Saunders.

FARRELL, R. A. & HART, R. W. 1969. On the theory of the spatial organization of macromolecules in connective tissue. *Bull Math Biophys,* 31, 727-60.

FARRELL, R. A., MCCALLY, R. L. & TATHAM, P. E. 1973. Wave-length dependencies of light scattering in normal and cold swollen rabbit corneas and their structural implications. *J Physiol,* 233, 589-612.

FATT, I. 1978. Measurement of oxygen flux into the cornea by pressing a sensor onto a soft contact lens on the eye. *Am J Optom Physiol Opt,* 55, 294-301.

FITCH, J. M., BIRK, D. E., LINSENMAYER, C. & LINSENMAYER, T. F. 1991. Stromal assemblies containing collagen types IV and VI and fibronectin in the developing embryonic avian cornea. *Dev Biol,* 144, 379-91.

FRANK, J. 2006. *Electron Tomography: Methods for Three-Dimensional Visualization of Structures in the Cell,* Springer.

FRANSSON, L. A. 1976. Interaction between dermatan sulphate chains. I. Affinity chromatography of copolymeric galactosaminioglycans on dermatan sulphate-substituted agarose. *Biochim Biophys Acta,* 437, 106-15.

FRANSSON, L. A. & COSTER, L. 1979. Interaction between dermatan sulphate chains. II. Structural studies on aggregating glycan chains and oligosaccharides with affinity for dermatan sulphate-substituted agarose. *Biochim Biophys Acta,* 582, 132-44.

FRANSSON, L. A. & HAVSMARK, B. 1970. Structure of dermatan sulfate. VII. The copolymeric structure of dermatan sulfate from horse aorta. *J Biol Chem,* 245, 4770-83.

FREUND, D. E., MCCALLY, R. L., FARRELL, R. A., CRISTOL, S. M., L'HERNAULT, N. L. & EDELHAUSER, H. F. 1995. Ultrastructure in anterior and posterior stroma of perfused human and rabbit corneas. Relation to transparency. *Invest Ophthalmol Vis Sci,* 36, 1508-23.

FUNDERBURGH, J. L. 2000. Keratan sulfate: structure, biosynthesis, and function. *Glycobiology,* 10, 951-8.

FUNDERBURGH, J. L., CATERSON, B. & CONRAD, G. W. 1987. Distribution of proteoglycans antigenically related to corneal keratan sulfate proteoglycan. *J Biol Chem,* 262, 11634-40.

FUNDERBURGH, J. L., CORPUZ, L. M., ROTH, M. R., FUNDERBURGH, M. L., TASHEVA, E. S. & CONRAD, G. W. 1997. Mimecan, the 25-kDa corneal keratan sulfate proteoglycan, is a product of the gene producing osteoglycin. *J Biol Chem,* 272, 28089-95.

FUNDERBURGH, J. L., FUNDERBURGH, M. L., HEVELONE, N. D., STECH, M. E., JUSTICE, M. J., LIU, C. Y., KAO, W. W. & CONRAD, G. W. 1995. Sequence, molecular properties, and chromosomal mapping of mouse lumican. *Invest Ophthalmol Vis Sci,* 36, 2296-303.

FUNDERBURGH, J. L., FUNDERBURGH, M. L., MANN, M. M. & CONRAD, G. W. 1991. Physical and biological properties of keratan sulphate proteoglycan. *Biochem Soc Trans,* 19, 871-6.

References

GELSE, K., POSCHL, E. & AIGNER, T. 2003. Collagens--structure, function, and biosynthesis. *Adv Drug Deliv Rev,* 55, 1531-46.

GOLDMAN, J. N. & BENEDEK, G. B. 1967. The relationship between morphology and transparency in the nonswelling corneal stroma of the shark. *Invest Ophthalmol,* 6, 574-600.

GOLDONI, S., OWENS, R. T., MCQUILLAN, D. J., SHRIVER, Z., SASISEKHARAN, R., BIRK, D. E., CAMPBELL, S. & IOZZO, R. V. 2004. Biologically active decorin is a monomer in solution. *J Biol Chem,* 279, 6606-12.

GOODFELLOW, J. M., ELLIOTT, G. F. & WOOLGAR, A. E. 1978. X-ray diffraction studies of the corneal stroma. *J Mol Biol,* 119, 237-52.

GORDON, M. K., FITCH, J. M., FOLEY, J. W., GERECKE, D. R., LINSENMAYER, C., BIRK, D. E. & LINSENMAYER, T. F. 1997. Type XVII collagen (BP 180) in the developing avian cornea. *Invest Ophthalmol Vis Sci,* 38, 153-66.

GORDON, M. K., FOLEY, J. W., BIRK, D. E., FITCH, J. M. & LINSENMAYER, T. F. 1994. Type V collagen and Bowman's membrane. Quantitation of mRNA in corneal epithelium and stroma. *J Biol Chem,* 269, 24959-66.

HART, R. W. & FARRELL, R. A. 1969. Light scattering in the cornea. *J Opt Soc Am,* 59, 766-74.

HASSELL, J. R. & BIRK, D. E. 2010. The molecular basis of corneal transparency. *Exp Eye Res,* 91, 326-35.

HASSELL, J. R., NEWSOME, D. A. & HASCALL, V. C. 1979. Characterization and biosynthesis of proteoglycans of corneal stroma from rhesus monkey. *J Biol Chem,* 254, 12346-54.

HASSELL, J. R., NEWSOME, D. A., KRACHMER, J. H. & RODRIGUES, M. M. 1980. Macular corneal dystrophy: failure to synthesize a mature keratan sulfate proteoglycan. *Proc Natl Acad Sci U S A,* 77, 3705-9.

HAUSTEIN, J. 1983. On the ultrastructure of the developing and adult mouse corneal stroma. *Anat Embryol (Berl),* 168, 291-305.

HAYASHIDA, Y., AKAMA, T. O., BEECHER, N., LEWIS, P., YOUNG, R. D., MEEK, K. M., KERR, B., HUGHES, C. E., CATERSON, B., TANIGAMI, A., NAKAYAMA, J., FUKADA, M. N., TANO, Y., NISHIDA, K. & QUANTOCK, A. J. 2006. Matrix morphogenesis in cornea is mediated by the modification of keratan sulfate by GlcNAc 6-O-sulfotransferase. *Proc Natl Acad Sci U S A,* 103, 13333-8.

HEDBYS, B. O. 1961. The role of polysaccharides in corneal swelling. *Experimental Eye Research,* 1, 81-91.

HEDBYS, B. O., MISHIMA, S. & MAURICE, D. M. 1963. The inbibition pressure of the corneal stroma. *Exp Eye Res,* 2, 99-111.

HOCKING, A. M., SHINOMURA, T. & MCQUILLAN, D. J. 1998. Leucine-rich repeat glycoproteins of the extracellular matrix. *Matrix Biology,* 17, 1-19.

HODGE, A. J. & SCHMITT, F. O. 1960. The Charge Profile of the Tropocollagen Macromolecule and the Packing Arrangement in Native-Type Collagen Fibrils. *Proc Natl Acad Sci U S A,* 46, 186-97.

HODSON, S. & EARLAM, R. 1993. The incorporation of gel pressure into the irreversible thermodynamic equation of fluid flow in order to explain biological tissue swelling. *J Theor Biol,* 163, 173-80.

HOLMES, D. F., GILPIN, C. J., BALDOCK, C., ZIESE, U., KOSTER, A. J. & KADLER, K. E. 2001. Corneal collagen fibril structure in three dimensions: Structural insights into fibril assembly, mechanical properties, and tissue organization. *Proc Natl Acad Sci U S A,* 98, 7307-12.

IOZZO, R. & SCHAEFER, L. 2008. Biological functions of the small leucine-rich Proteoglycans:From genetics to signal transduction. *The Journal of Biological Chemistry,* 283, 21305-21309.

IOZZO, R. V. 1997. The family of the small leucine-rich proteoglycans: key regulators of matrix assembly and cellular growth. *Crit Rev Biochem Mol Biol,* 32, 141-74.

IOZZO, R. V. 1999. The biology of the small leucine-rich proteoglycans. Functional network of interactive proteins. *J Biol Chem,* 274, 18843-6.

References

IOZZO, R. V. & MURDOCH, A. D. 1996. Proteoglycans of the extracellular environment: clues from the gene and protein side offer novel perspectives in molecular diversity and function. *FASEB J,* 10, 598-614.

KADLER, K. E., HOLMES, D. F., TROTTER, J. A. & CHAPMAN, J. A. 1996. Collagen fibril formation. *Biochem J,* 316 (Pt 1), 1-11.

KAO, W. W. & LIU, C. Y. 2002. Roles of lumican and keratocan on corneal transparency. *Glycoconj J,* 19, 275-85.

KATO, T., NAKAYASU, K., KANAI, A., NISHIYAMA, T., IMAMURA, Y. & HAYASHI, T. 2000. Distribution and isoform characterization of type XII collagen in bovine cornea. *Ophthalmic Res,* 32, 215-21.

KITAYAMA, K., HAYASHIDA, Y., NISHIDA, K. & AKAMA, T. O. 2007. Enzymes responsible for synthesis of corneal keratan sulfate glycosaminoglycans. *J Biol Chem,* 282, 30085-96.

KLYCE, S. D. 1977. Enhancing fluid secretion by the corneal epithelium. *Invest Ophthalmol Vis Sci,* 16, 968-73.

KNUPP, C., PINALI, C., LEWIS, P. N., PARFITT, G. J., YOUNG, R. D., MEEK, K. M. & QUANTOCK, A. J. 2009. The Architecture of the Cornea and Structural Basis of Its Transparency. *Adv Protein Chem Struct Biol,* 78C, 25-49.

KOBE, B. & DEISENHOFER, J. 1993. Crystal structure of porcine ribonuclease inhibitor, a protein with leucine-rich repeats. *Nature,* 366, 751-6.

KOBE, B. & KAJAVA, A. V. 2001. The leucine-rich repeat as a protein recognition motif. *Curr Opin Struct Biol,* 11, 725-32.

KOMAI, Y. & USHIKI, T. 1991. The Three-Dimensional Organization of Collagen Fibrils in the Human Cornea and Sclera. *Investigative Opthalmology & Visual Science,* 32, 2244-2258.

KREMER, J. R., MASTRONARDE, D. N. & MCINTOSH, J. R. 1996. Computer visualization of three-dimensional image data using IMOD. *Journal of Structural Biology,* 116, 71-76.

KRESSE, H., LISZIO, C., SCHONHERR, E. & FISHER, L. W. 1997. Critical role of glutamate in a central leucine-rich repeat of decorin for interaction with type I collagen. *J Biol Chem,* 272, 18404-10.

KRUSIUS, T. & RUOSLAHTI, E. 1986. Primary structure of an extracellular matrix proteoglycan core protein deduced from cloned cDNA. *Proc Natl Acad Sci U S A,* 83, 7683-7.

KUANG, K. Y., XU, M., KONIAREK, J. P. & FISCHBARG, J. 1990. Effects of ambient bicarbonate, phosphate and carbonic anhydrase inhibitors on fluid transport across rabbit corneal endothelium. *Exp Eye Res,* 50, 487-93.

LEONARD, D. W. & MEEK, K. M. 1997. Refractive indices of the collagen fibrils and extrafibrillar material of the corneal stroma. *Biophys J,* 72, 1382-7.

LEWIS, P. N., PINALI, C., YOUNG, R. D., MEEK, K. M., QUANTOCK, A. J. & KNUPP, C. 2010. Structural interactions between collagen and proteoglycans are elucidated by three-dimensional electron tomography of bovine cornea. *Structure,* 18, 239-45.

LIND, G. J. & CAVANAGH, H. D. 1995. Identification and subcellular distribution of muscarinic acetylcholine receptor-related proteins in rabbit corneal and Chinese hamster ovary cells. *Invest Ophthalmol Vis Sci,* 36, 1492-507.

LINSENMAYER, T. F., BRUNS, R. R., MENTZER, A. & MAYNE, R. 1986. Type VI collagen: immunohistochemical identification as a filamentous component of the extracellular matrix of the developing avian corneal stroma. *Dev Biol,* 118, 425-31.

LINSENMAYER, T. F., FITCH, J. M., GORDON, M. K., CAI, C. X., IGOE, F., MARCHANT, J. K. & BIRK, D. E. 1998. Development and roles of collagenous matrices in the embryonic avian cornea. *Prog Retin Eye Res,* 17, 231-65.

LIU, C. Y., BIRK, D. E., HASSELL, J. R., KANE, B. & KAO, W. W. 2003. Keratocan-deficient mice display alterations in corneal structure. *J Biol Chem,* 278, 21672-7.

References

LIU, C. Y., SHIRAISHI, A., KAO, C. W., CONVERSE, R. L., FUNDERBURGH, J. L., CORPUZ, L. M., CONRAD, G. W. & KAO, W. W. 1998. The cloning of mouse keratocan cDNA and genomic DNA and the characterization of its expression during eye development. *J Biol Chem,* 273, 22584-8.

LIU, H., ZHANG, J., LIU, C. Y., WANG, I. J., SIEBER, M., CHANG, J., JESTER, J. V. & KAO, W. W. 2010. Cell therapy of congenital corneal diseases with umbilical mesenchymal stem cells: lumican null mice. *PLoS One,* 5, e10707.

LIVELY, G. D., JIANG, B., HEDBERG-BUENZ, A., CHANG, B., PETERSEN, G. E., WANG, K., KUEHN, M. H. & ANDERSON, M. G. 2010. Genetic dependence of central corneal thickness among inbred strains of mice. *Invest Ophthalmol Vis Sci,* 51, 160-71.

LODISH, HARVEY, BERK & ZIPURSKY 1999. *Molecular Cell Biology,* W H FREEMAN.

LONG, C. J., ROTH, M. R., TASHEVA, E. S., FUNDERBURGH, M., SMIT, R., CONRAD, G. W. & FUNDERBURGH, J. L. 2000. Fibroblast growth factor-2 promotes keratan sulfate proteoglycan expression by keratocytes in vitro. *J Biol Chem,* 275, 13918-23.

MADISEN, L., NEUBAUER, M., PLOWMAN, G., ROSEN, D., SEGARINI, P., DASCH, J., THOMPSON, A., ZIMAN, J., BENTZ, H. & PURCHIO, A. F. 1990. Molecular cloning of a novel bone-forming compound: osteoinductive factor. *DNA Cell Biol,* 9, 303-9.

MALIK, N. S., MOSS, S. J., AHMED, N., FURTH, A. J., WALL, R. S. & MEEK, K. M. 1992. Ageing of the human corneal stroma: structural and biochemical changes. *Biochim Biophys Acta,* 1138, 222-8.

MALSTROM, A., CARLSTEDT, I., ABERG, L. & FRANSSON, L. A. 1975. The copolymeric structure of dermatan sulphate produced by cultured human fibroblasts. Different distribution of iduronic acid and glucuronic acid-containing units in soluble and cell-associated glycans. *Biochem J,* 151, 477-89.

MARCHINI, M., MOROCUTTI, M., RUGGERI, A., KOCH, M. H., BIGI, A. & ROVERI, N. 1986. Differences in the fibril structure of corneal and tendon collagen. An electron microscopy and X-ray diffraction investigation. *Connect Tissue Res,* 15, 269-81.

MARSHALL, G. E., KONSTAS, A. G. & LEE, W. R. 1991. Immunogold fine structural localization of extracellular matrix components in aged human cornea. I. Types I-IV collagen and laminin. *Graefes Arch Clin Exp Ophthalmol,* 229, 157-63.

MARSHALL, G. E., KONSTAS, A. G. & LEE, W. R. 1993. Collagens in ocular tissues. *Br J Ophthalmol,* 77, 515-24.

MAURICE, D. M. 1957. The structure and transparency of the cornea. *J Physiol,* 136, 263-86.

MAURICE, D. M. 1962. Clinical physiology of the cornea. *Int Ophthalmol Clin,* 2, 561-72.

MAURICE, D. M. 1972. The location of the fluid pump in the cornea. *J Physiol,* 221, 43-54.

MAURICE, D. M. & GIARDINI, A. A. 1951. Swelling of the cornea in vivo after the destruction of its limiting layers. *Br J Ophthalmol,* 35, 791-7.

MAURICE, D. M. & MONROE, F. 1990. Cohesive strength of corneal lamellae. *Exp Eye Res,* 50, 59-63.

MCCALLY, R. L. & FARRELL, R. A. 1999. Small-angle light scattering and birefringence properties of chick cornea. *J Refract Surg,* 15, 706-10.

MCEWAN, P. A., SCOTT, P. G., BISHOP, P. N. & BELLA, J. 2006. Structural correlations in the family of small leucine-rich repeat proteins and proteoglycans. *J Struct Biol,* 155, 294-305.

MEEK, K. M., BLAMIRES, T., ELLIOTT, G. F., GYI, T. J. & NAVE, C. 1987. The organisation of collagen fibrils in the human corneal stroma: a synchrotron X-ray diffraction study. *Curr Eye Res,* 6, 841-6.

MEEK, K. M. & BOOTE, C. 2004. The organization of collagen in the corneal stroma. *Exp Eye Res,* 78, 503-12.

MEEK, K. M., ELLIOTT, G. F. & NAVE, C. 1986. A synchrotron X-ray diffraction study of bovine cornea stained with cupromeronic blue. *Coll Relat Res,* 6, 203-18.

MEEK, K. M. & FULLWOOD, N. J. 2001. Corneal and scleral collagens--a microscopist's perspective. *Micron,* 32, 261-72.

References

MEEK, K. M. & LEONARD, D. W. 1993. Ultrastructure of the corneal stroma: a comparative study. *Biophys J,* 64, 273-80.

MEEK, K. M. & QUANTOCK, A. J. 2001. The use of X-ray scattering techniques to determine corneal ultrastructure. *Prog Retin Eye Res,* 20, 95-137.

MEEK, K. M., QUANTOCK, A. J., BOOTE, C., LIU, C. Y. & KAO, W. W. 2003. An X-ray scattering investigation of corneal structure in keratocan-deficient mice. *Matrix Biol,* 22, 467-75.

MEEK, K. M., QUANTOCK, A. J., ELLIOTT, G. F., RIDGWAY, A. E., TULLO, A. B., BRON, A. J. & THONAR, E. J. 1989. Macular corneal dystrophy: the macromolecular structure of the stroma observed using electron microscopy and synchrotron X-ray diffraction. *Exp Eye Res,* 49, 941-58.

MEEK, K. M., TUFT, S. J., HUANG, Y., GILL, P. S., HAYES, S., NEWTON, R. H. & BRON, A. J. 2005. Changes in collagen orientation and distribution in keratoconus corneas. *Invest Ophthalmol Vis Sci,* 46, 1948-56.

MEYER, K., LINKER, A., DAVIDSON, E. A. & WEISSMANN, B. 1953. The mucopolysaccharides of bovine cornea. *J Biol Chem,* 205, 611-6.

MICHELACCI, Y. M. 2003. Collagens and proteoglycans of the corneal extracellular matrix. *Braz J Med Biol Res,* 36, 1037-46.

MIDURA, R. J. & HASCALL, V. C. 1989. Analysis of the proteoglycans synthesized by corneal explants from embryonic chicken. II. Structural characterization of the keratan sulfate and dermatan sulfate proteoglycans from corneal stroma. *J Biol Chem,* 264, 1423-30.

MOLLER-PEDERSEN, T. 2004. Keratocyte reflectivity and corneal haze. *Exp Eye Res,* 78, 553-60.

MORRIS, N. P. & BACHINGER, H. P. 1987. Type XI collagen is a heterotrimer with the composition (1 alpha, 2 alpha, 3 alpha) retaining non-triple-helical domains. *J Biol Chem,* 262, 11345-50.

MULLER, L. J., PELS, E., SCHURMANS, L. R. & VRENSEN, G. F. 2004. A new three-dimensional model of the organization of proteoglycans and collagen fibrils in the human corneal stroma. *Exp Eye Res,* 78, 493-501.

MULLER, L. J., PELS, E. & VRENSEN, G. F. 2001. The specific architecture of the anterior stroma accounts for maintenance of corneal curvature. *Br J Ophthalmol,* 85, 437-43.

NAKAMURA, M., KIMURA, S., KOBAYASHI, M., HIRANO, K., HOSHINO, T. & AWAYA, S. 1997. Type VI collagen bound to collagen fibrils by chondroitin/dermatan sulfate glycosaminoglycan in mouse corneal stroma. *Jpn J Ophthalmol,* 41, 71-6.

NAKAMURA, M., KOBAYASHI, M., HIRANO, K., KOBAYASHI, K., HOSHINO, T. & AWAYA, S. 1992. Assembly of 100 nm periodic fibrils (type VI collagen) in human infant corneal stroma. *Jpn J Ophthalmol,* 36, 458-64.

NAKAZAWA, K., HASSELL, J. R., HASCALL, V. C., LOHMANDER, L. S., NEWSOME, D. A. & KRACHMER, J. 1984. Defective processing of keratan sulfate in macular corneal dystrophy. *J Biol Chem,* 259, 13751-7.

NEWSOME, D. A., GROSS, J. & HASSELL, J. R. 1982. Human corneal stroma contains three distinct collagens. *Invest Ophthalmol Vis Sci,* 22, 376-81.

ORGEL, J. P., EID, A., ANTIPOVA, O., BELLA, J. & SCOTT, J. E. 2009. Decorin core protein (decoron) shape complements collagen fibril surface structure and mediates its binding. *PLoS One,* 4, e7028.

ORGEL, J. P., IRVING, T. C., MILLER, A. & WESS, T. J. 2006. Microfibrillar structure of type I collagen in situ. *Proc Natl Acad Sci U S A,* 103, 9001-5.

OTTANI, V., RASPANTI, M. & RUGGERI, A. 2001. Collagen structure and functional implications. *Micron,* 32, 251-60.

OYSTER, C. 1999. *The Human Eye: Structure and Function,* Sinauer.

PACE, J. M., CORRADO, M., MISSERO, C. & BYERS, P. H. 2003. Identification, characterization and expression analysis of a new fibrillar collagen gene, COL27A1. *Matrix Biol,* 22, 3-14.

PARFITT, G. J., PINALI, C., AKAMA, T. O., YOUNG, R. D., NISHIDA, K., QUANTOCK, A. J. & KNUPP, C. 2011. Electron tomography reveals multiple self-association of chondroitin sulphate/dermatan sulphate proteoglycans in Chst5-null mouse corneas. *J Struct Biol.*

References

PARFITT, G. J., PINALI, C., YOUNG, R. D., QUANTOCK, A. J. & KNUPP, C. 2010. Three-dimensional reconstruction of collagen-proteoglycan interactions in the mouse corneal stroma by electron tomography. *J Struct Biol,* 170, 392-7.

PATEL, S., MARSHALL, J. & FITZKE, F. W., 3RD 1995. Refractive index of the human corneal epithelium and stroma. *J Refract Surg,* 11, 100-5.

PELLEGATA, N. S., DIEGUEZ-LUCENA, J. L., JOENSUU, T., LAU, S., MONTGOMERY, K. T., KRAHE, R., KIVELA, T., KUCHERLAPATI, R., FORSIUS, H. & DE LA CHAPELLE, A. 2000. Mutations in KERA, encoding keratocan, cause cornea plana. *Nat Genet,* 25, 91-5.

PIEZ, K. A. & REDDI, A. H. 1984. Structures of the collagens. *In:* PIEZ, K. A. (ed.) *Extracellular Matrix Biochemistry.* Elsevier.

PLAAS, A. H., WEST, L. A., THONAR, E. J., KARCIOGLU, Z. A., SMITH, C. J., KLINTWORTH, G. K. & HASCALL, V. C. 2001. Altered fine structures of corneal and skeletal keratan sulfate and chondroitin/dermatan sulfate in macular corneal dystrophy. *J Biol Chem,* 276, 39788-96.

PROCKOP, D. J. & KIVIRIKKO, K. I. 1995. Collagens: molecular biology, diseases, and potentials for therapy. *Annu Rev Biochem,* 64, 403-34.

QUANTOCK, A. J., MEEK, K. M. & CHAKRAVARTI, S. 2001. An x-ray diffraction investigation of corneal structure in lumican-deficient mice. *Invest Ophthalmol Vis Sci,* 42, 1750-6.

QUANTOCK, A. J., YOUNG, R. D. & AKAMA, T. O. 2010. Structural and biochemical aspects of keratan sulphate in the cornea. *Cell Mol Life Sci,* 67, 891-906.

RADA, J. A., CORNUET, P. K. & HASSELL, J. R. 1993. Regulation of corneal collagen fibrillogenesis in vitro by corneal proteoglycan (lumican and decorin) core proteins. *Exp Eye Res,* 56, 635-48.

REGINI, J. W., ELLIOTT, G. F. & HODSON, S. A. 2004. The ordering of corneal collagen fibrils with increasing ionic strength. *J Mol Biol,* 336, 179-86.

RESS, D. B., HARLOW, M. L., MARSHALL, R. M. & MCMAHAN, U. J. 2004. Methods for generating high-resolution structural models from electron microscope tomography data. *Structure,* 12, 1763-74.

ROUGHLEY, P. J., RODRIGUEZ, E. & LEE, E. R. 1995. The interactions of 'non-aggregating' proteoglycans. *Osteoarthritis Cartilage,* 3, 239-48.

RUGGIERO, F., BURILLON, C. & GARRONE, R. 1996. Human corneal fibrillogenesis. Collagen V structural analysis and fibrillar assembly by stromal fibroblasts in culture. *Invest Ophthalmol Vis Sci,* 37, 1749-60.

RUHLAND, C., SCHONHERR, E., ROBENEK, H., HANSEN, U., IOZZO, R. V., BRUCKNER, P. & SEIDLER, D. G. 2007. The glycosaminoglycan chain of decorin plays an important role in collagen fibril formation at the early stages of fibrillogenesis. *Febs J,* 274, 4246-55.

SANCHEZ, J. M., LI, Y., RUBASHKIN, A., ISEROVICH, P., WEN, Q., RUBERTI, J. W., SMITH, R. W., RITTENBAND, D., KUANG, K., DIECKE, F. P. & FISCHBARG, J. 2002. Evidence for a central role for electro-osmosis in fluid transport by corneal endothelium. *J Membr Biol,* 187, 37-50.

SANDBERG-LALL, M., HAGG, P. O., WAHLSTROM, I. & PIHLAJANIEMI, T. 2000. Type XIII collagen is widely expressed in the adult and developing human eye and accentuated in the ciliary muscle, the optic nerve and the neural retina. *Exp Eye Res,* 70, 401-10.

SAWADA, H., KONOMI, H. & HIROSAWA, K. 1990. Characterization of the collagen in the hexagonal lattice of Descemet's membrane: its relation to type VIII collagen. *J Cell Biol,* 110, 219-27.

SCOTT, J. E. 1972. Histochemistry of Alcian blue. 3. The molecular biological basis of staining by Alcian blue 8GX and analogous phthalocyanins. *Histochemie,* 32, 191-212.

SCOTT, J. E. 1975. Composition and structure of the pericellular environment. Physiological function and chemical composition of pericellular proteoglycan (an evolutionary view). *Philos Trans R Soc Lond B Biol Sci,* 271, 135-42.

SCOTT, J. E. 1980. Collagen--proteoglycan interactions. Localization of proteoglycans in tendon by electron microscopy. *Biochem J,* 187, 887-91.

SCOTT, J. E. 1988. Proteoglycan-fibrillar collagen interactions. *Biochem J,* 252, 313-23.

References

SCOTT, J. E. 1990. Proteoglycan:collagen interactions and subfibrillar structure in collagen fibrils. Implications in the development and ageing of connective tissues. *J Anat,* 169, 23-35.

SCOTT, J. E. 1991. Proteoglycan: collagen interactions in connective tissues. Ultrastructural, biochemical, functional and evolutionary aspects. *Int J Biol Macromol,* 13, 157-61.

SCOTT, J. E. 1992. Morphometry of cupromeronic blue-stained proteoglycan molecules in animal corneas, versus that of purified proteoglycans stained in vitro, implies that tertiary structures contribute to corneal ultrastructure. *J Anat,* 180 (Pt 1), 155-64.

SCOTT, J. E. 1995. Extracellular matrix, supramolecular organisation and shape. *J Anat,* 187 (Pt 2), 259-69.

SCOTT, J. E. 1996. Proteodermatan and proteokeratan sulfate (decorin, lumican/fibromodulin) proteins are horseshoe shaped. Implications for their interactions with collagen. *Biochemistry,* 35, 8795-9.

SCOTT, J. E. 2001. Structure and function in extracellular matrices depend on interactions between anionic glycosaminoglycans. *Pathologie Biologie,* 49, 284-289.

SCOTT, J. E. 2003. Elasticity in extracellular matrix 'shape modules' of tendon, cartilage, etc. A sliding proteoglycan-filament model. *J Physiol,* 553, 335-43.

SCOTT, J. E. & BOSWORTH, T. R. 1990. A comparative biochemical and ultrastructural study of proteoglycan-collagen interactions in corneal stroma. Functional and metabolic implications. *Biochem J,* 270, 491-7.

SCOTT, J. E., CHEN, Y. & BRASS, A. 1992. Secondary and tertiary structures involving chondroitin and chondroitin sulphates in solution, investigated by rotary shadowing/electron microscopy and computer simulation. *Eur J Biochem,* 209, 675-80.

SCOTT, J. E. & HAIGH, M. 1988a. Identification of specific binding sites for keratan sulphate proteoglycans and chondroitin-dermatan sulphate proteoglycans on collagen fibrils in cornea by the use of cupromeronic blue in 'critical-electrolyte-concentration' techniques. *Biochem J,* 253, 607-10.

SCOTT, J. E. & HAIGH, M. 1988b. Keratan sulphate and the ultrastructure of cornea and cartilage: a 'stand-in' for chondroitin sulphate in conditions of oxygen lack? *J Anat,* 158, 95-108.

SCOTT, J. E. & PARRY, D. A. 1992. Control of collagen fibril diameters in tissues. *Int J Biol Macromol,* 14, 292-3.

SCOTT, J. E. & THOMLINSON, A. M. 1998. The structure of interfibrillar proteoglycan bridges (shape modules') in extracellular matrix of fibrous connective tissues and their stability in various chemical environments. *J Anat,* 192 (Pt 3), 391-405.

SCOTT, P. G., MCEWAN, P. A., DODD, C. M., BERGMANN, E. M., BISHOP, P. N. & BELLA, J. 2004. Crystal structure of the dimeric protein core of decorin, the archetypal small leucine-rich repeat proteoglycan. *Proc Natl Acad Sci U S A,* 101, 15633-8.

SMELSER, G. K. & OZANICS, V. 1959. The effect of vascularization on the metabolism of the sulfated mucopolysaccharides and swelling properties of the cornea. *Am J Ophthalmol,* 48(5)Pt 2, 418-26.

SMITH, J. W. & FRAME, J. 1969. Observations on the collagen and proteinpolysaccharide complex of rabbit cornea stroma. *J Cell Sci,* 4, 421-36.

SODERHALL, C., MARENHOLZ, I., KERSCHER, T., RUSCHENDORF, F., ESPARZA-GORDILLO, J., WORM, M., GRUBER, C., MAYR, G., ALBRECHT, M., ROHDE, K., SCHULZ, H., WAHN, U., HUBNER, N. & LEE, Y. A. 2007. Variants in a novel epidermal collagen gene (COL29A1) are associated with atopic dermatitis. *PLoS Biol,* 5, e242.

STOCKWELL, R. A. & SCOTT, J. E. 1965. Observations on the acid glycosaminoglycan (mucopolysaccharide) content of the matrix of aging cartilage. *Ann Rheum Dis,* 24, 341-50.

SVENSSON, L., OLDBERG, A. & HEINEGARD, D. 2001. Collagen binding proteins. *Osteoarthritis Cartilage,* 9 Suppl A, S23-8.

References

TASHEVA, E. S., CORPUZ, L. M., FUNDERBURGH, J. L. & CONRAD, G. W. 1997. Differential splicing and alternative polyadenylation generate multiple mimecan mRNA transcripts. *J Biol Chem,* 272, 32551-6.

TASHEVA, E. S., KOESTER, A., PAULSEN, A. Q., GARRETT, A. S., BOYLE, D. L., DAVIDSON, H. J., SONG, M., FOX, N. & CONRAD, G. W. 2002. Mimecan/osteoglycin-deficient mice have collagen fibril abnormalities. *Mol Vis,* 8, 407-15.

THOMAS, K. R. & CAPECCHI, M. R. 1987. Site-directed mutagenesis by gene targeting in mouse embryo-derived stem cells. *Cell,* 51, 503-12.

TURSS, R., FRIEND, J. & DOHLMAN, C. H. 1970. Effect of a corneal fluid barrier on the nutrition of the epithelium. *Exp Eye Res,* 9, 254-9.

VARKI, A. & CUMMINGS, R. 2008. *Essentials of glycobiology*, CSH Press.

VOGEL, K. G., PAULSSON, M. & HEINEGARD, D. 1984. Specific inhibition of type I and type II collagen fibrillogenesis by the small proteoglycan of tendon. *Biochem J,* 223, 587-97.

WALKENBACH, R. J. & CHAO, W. T. 1985. Adenosine regulation of cyclic AMP in corneal endothelium. *J Ocul Pharmacol,* 1, 337-42.

WARD, N. P., SCOTT, J. E. & COSTER, L. 1987. Dermatan sulphate proteoglycans from sclera examined by rotary shadowing and electron microscopy. *Biochem J,* 242, 761-6.

WARING, G. O., 3RD 1989. Making sense of keratospeak II: Proposed conventional terminology for corneal topography. *Refract Corneal Surg,* 5, 362-7.

WESS, T. J., HAMMERSLEY, A. P., WESS, L. & MILLER, A. 1998. Molecular packing of type I collagen in tendon. *J Mol Biol,* 275, 255-67.

WESSEL, H., ANDERSON, S., FITE, D., HALVAS, E., HEMPEL, J. & SUNDARRAJ, N. 1997. Type XII collagen contributes to diversities in human corneal and limbal extracellular matrices. *Invest Ophthalmol Vis Sci,* 38, 2408-22.

WILSON, S. E. & HONG, J. W. 2000. Bowman's layer structure and function: critical or dispensable to corneal function? A hypothesis. *Cornea,* 19, 417-20.

WINNEMOLLER, M., SCHON, P., VISCHER, P. & KRESSE, H. 1992. Interactions between thrombospondin and the small proteoglycan decorin: interference with cell attachment. *Eur J Cell Biol,* 59, 47-55.

WU, J. J. & EYRE, D. R. 1995. Structural analysis of cross-linking domains in cartilage type XI collagen. Insights on polymeric assembly. *J Biol Chem,* 270, 18865-70.

YAMAGUCHI, Y., MANN, D. M. & RUOSLAHTI, E. 1990. Negative regulation of transforming growth factor-beta by the proteoglycan decorin. *Nature,* 346, 281-4.

YING, S., SHIRAISHI, A., KAO, C. W., CONVERSE, R. L., FUNDERBURGH, J. L., SWIERGIEL, J., ROTH, M. R., CONRAD, G. W. & KAO, W. W. 1997. Characterization and expression of the mouse lumican gene. *J Biol Chem,* 272, 30306-13.

YOUNG, R. D., TUDOR, D., HAYES, A. J., KERR, B., HAYASHIDA, Y., NISHIDA, K., MEEK, K. M., CATERSON, B. & QUANTOCK, A. J. 2005. Atypical composition and ultrastructure of proteoglycans in the mouse corneal stroma. *Invest Ophthalmol Vis Sci,* 46, 1973-8.

ZHANG, G., CHEN, S., GOLDONI, S., CALDER, B. W., SIMPSON, H. C., OWENS, R. T., MCQUILLAN, D. J., YOUNG, M. F., IOZZO, R. V. & BIRK, D. E. 2009. Genetic evidence for the coordinated regulation of collagen fibrillogenesis in the cornea by decorin and biglycan. *J Biol Chem,* 284, 8888-97.

ZIMMERMANN, D. R., TRUEB, B., WINTERHALTER, K. H., WITMER, R. & FISCHER, R. W. 1986. Type VI collagen is a major component of the human cornea. *FEBS Lett,* 197, 55-8.